

2003

A rapid performance test for Superpave HMA mixtures

Il-Seok Oh

Iowa State University

Follow this and additional works at: <https://lib.dr.iastate.edu/rtd>



Part of the [Civil Engineering Commons](#)

Recommended Citation

Oh, Il-Seok, "A rapid performance test for Superpave HMA mixtures " (2003). *Retrospective Theses and Dissertations*. 609.
<https://lib.dr.iastate.edu/rtd/609>

This Dissertation is brought to you for free and open access by the Iowa State University Capstones, Theses and Dissertations at Iowa State University Digital Repository. It has been accepted for inclusion in Retrospective Theses and Dissertations by an authorized administrator of Iowa State University Digital Repository. For more information, please contact digirep@iastate.edu.

A rapid performance test for SUPERPAVE HMA mixtures

by

Il-Seok Oh

A dissertation submitted to the graduate faculty
in partial fulfillment of the requirements for the degree of

DOCTOR OF PHILOSOPHY

Major: Civil Engineering (Civil Engineering Materials)

Program of Study Committee:
Brian Coree, Major Professor
Kejin Wang
David White
James Cable
Thomas Rudolphi

Iowa State University

Ames, Iowa

2003

UMI Number: 3085934

UMI[®]

UMI Microform 3085934

Copyright 2003 by ProQuest Information and Learning Company.
All rights reserved. This microform edition is protected against
unauthorized copying under Title 17, United States Code.

ProQuest Information and Learning Company
300 North Zeeb Road
P.O. Box 1346
Ann Arbor, MI 48106-1346

Graduate College
Iowa State University

This is to certify that the doctoral dissertation of

Il-Seok Oh

has met the dissertation requirements of Iowa State University

Signature was redacted for privacy.

Major Professor

Signature was redacted for privacy.

For the Major Program

TABLE OF CONTENTS

LIST OF FIGURES	v
LIST OF TABLES	vii
ABSTRACT	ix
1. INTRODUCTION	1
1.1 Study Objectives	3
2. LITERATURE REVIEW	5
2.1 The Historical Development of the SGC	5
2.2 Use of Gyrotory Compactors	8
2.3 Summary	15
3. A PRELIMINARY STUDY	16
3.1 A Proposed Rapid Performance Test	17
3.2 A Pilot Test and Discussion	24
3.3 Summary	35
4. DESIGN OF EXPERIMENT	37
4.1 Material Properties	38
4.2 Optimum Binder Contents	42
4.3 Tests	43
5. ANALYSIS OF TEST RESULTS AND DISCUSSION	50
5.1 The RPT on Laboratory-Fabricated Samples	51
5.2 The NAT on Laboratory-Fabricated Samples	58
5.3 The RPT on Plant-Mixed Samples	62
6. CONCLUSIONS AND RECOMMENDATIONS	66
6.1 Conclusions	67
6.2 Discussion	67
6.2 Recommendations	73
APPENDIX A. DETERMINATION OF OPTIMUM BINDER CONTENTS	74
APPENDIX B - 1. DATA SUMMARY: The RPT at p = 87psi	85

APPENDIX B - 2. DATA SUMMARY: The RPT at $p = 100\text{psi}$	102
APPENDIX C. DATA SUMMARY: Nottingham Asphalt Tester (NAT)	112
REFERENCES	117
ACKNOWLEDGMENTS	125

LIST OF FIGURES

Figure 1.	Unit weights and GTM indices vs. asphalt content (26)	9
Figure 2.	Compaction energy index and traffic densification index (32)	12
Figure 3.	Temperature – Viscosity relationships of the asphalt binder (Data from Koch Materials Company, Dubuque, Iowa)	19
Figure 4.	The SGC compaction protocol	20
Figure 5.	The compaction curve of the Superpave mix design	21
Figure 6.	The proposed RPT	23
Figure 7.	The SGC, Troxler 4140-B (a) and the indenter (b)	23
Figure 8.	Aggregate gradations used in the preliminary study	25
Figure 9.	D/P _{bo} /58(left) and D/P _{b+} /58(right) after subjected to 300 gyrations	28
Figure 10.	% ϵ vs. N curves showing temperature effect	28
Figure 11.	% ϵ vs. N curves showing asphalt content effect	28
Figure 12.	% ϵ vs. N curves showing aggregate gradation effect	29
Figure 13.	Trends of the responses (N for % ϵ =2) on the main effects	30
Figure 14.	The Nottingham Asphalt Tester, Cooper Research Technology Ltd.	32
Figure 15.	The permanent deformations of nine mixtures from the NAT	34
Figure 16.	The NAT (micro strain) versus the RPT (%strain)	35
Figure 17.	Fine, Dense, and Coarse gradations used in the study	41
Figure 18.	Effect of confining stress on the deformations of identical mixtures	47
Figure 19.	JMF gradations of field samples provided by Iowa DOT	48
Figure 20.	Repeatability of the proposed RPT	51
Figure 21.	% ϵ vs. N curves of FG mixes	52
Figure 22.	% ϵ vs. N curves of DG mixes	52

Figure 23.	% ϵ vs. N curves of CG mixes	52
Figure 24.	Observed vs. predicted percent strain at N=100	57
Figure 25.	Percent strains of nine ($N_d=100$) mixes from the NAT	59
Figure 26.	% ϵ (at N=100) of field samples compared with laboratory mixes	65
Figure 27.	Simplified schematic illustration of the rationale behind the RPT	68
Figure 28.	Possible shapes of the indenter	69
Figure 29.	% ϵ vs. % $\dot{\epsilon}$ rate (% $\dot{\epsilon}$)	70
Figure 30.	The concepts of N' and N_{RPT}	72

LIST OF TABLES

Table 1.	The volumetrics of three mixtures for $N_{\text{design}}=109$	26
Table 2.	Notations for 27 treatment combinations	27
Table 3.	Number of gyrations causing 2% vertical strain	29
Table 4.	ANOVA for number of gyrations causing 2% vertical strain	31
Table 5.	Test conditions for the repeated load axial test	33
Table 6.	Comparison of the results from two test methods	34
Table 7.	Notations for twenty seven mixtures	38
Table 8.	Aggregate gradations recently used for asphalt surface course in Iowa	40
Table 9.	The properties of nine aggregate blends	41
Table 10.	Fine aggregate angularities of three aggregate blends	41
Table 11.	Optimum asphalt binder contents ($P_{b(\text{opt})}$) and the number of gyration required to achieve 7% air voids	43
Table 12.	Volumetrics and other properties of twenty seven mixes at $P_{b(\text{opt})}$	44
Table 13.	The randomized testing order	45
Table 14.	Test conditions for the confined repeated load axial test	46
Table 15.	The properties of field samples from JMFs	48
Table 16.	Percent strains ($\% \epsilon$) of twenty seven mixes	53
Table 17.	ANOVA for percent strains ($\% \epsilon$) from the RPT at $N = 100$	55
Table 18.	Mean percent strains for each factor at $N = 100$	56
Table 19.	Regression results for $\% \epsilon$	58
Table 20.	Comparison of the results (the NAT vs. the RPT)	60
Table 21.	ANOVA for percent strains ($\% \epsilon$) from the NAT at $N = 10000$	60
Table 22.	Mean percent strains for each factor at $N = 10000$	61

Table 23.	p – values of t – test ($\alpha = 0.05$)	62
Table 24.	The pooled average $\% \varepsilon$ from the RPT after 100 gyrations	63
Table 25.	The responses of eight field samples to the RPT	64

ABSTRACT

Permanent deformation and shear instability of Hot-Mix Asphalt (HMA) have been major concerns in the asphalt paving industry for a long time because permanent deformation failure, e.g., rutting and shoving, significantly reduces the ride quality of asphalt pavements and may even cause hazardous hydroplaning of vehicles. Furthermore, the fact that truck tire pressures are increasing and most of rutting occurs in the top 3 ~ 4 inches of the HMA layer requires the production of more rut-resistant and stable mixtures.

HMA mix design has escaped from its empirical stage and become more rational with the advent of the Superpave system. Superpave Level-I mix design, however, entirely depends on the volumetric properties of the mixture, without evaluating the potential performance of mixtures. In order to cope with the increasing demand for a simple performance test, extensive research has been conducted recently across the U.S. and new test methods and/or testing equipment have been introduced. Unfortunately the equipment is expensive, and the test procedures and sample preparations are rather complicated.

This study sought to develop a performance test that is rapid and easy to perform so that it can be routinely used during mix design and during construction to differentiate stable from unstable or rut-susceptible mixtures. In order to be cost-effective, the Rapid Performance Test (RPT) presented in this study utilizes the existing Superpave Gyrotory Compactor (SGC), without the need for new, elaborate or sophisticated equipment.

However, it has been recognized that the behavior of HMA mixtures observed during

the conventional compaction procedure cannot properly represent the performance of the mixture due to the unrealistically elevated compaction temperatures used in testing, and the confined movements of the mixture inside the rigid mold. Therefore the indenter of 4"-diameter is inserted between the SGC loading platen and the mixture in order to allow plastic flow or lateral/upward movements of the mixture. Also, the RPT is performed at in-service temperatures to better capture realistic shear strength of HMA mixtures.

Extensive experiments were conducted on Iowa mixes and the RPT was evaluated by the dynamic creep test using the Nottingham Asphalt Tester (NAT).

1. INTRODUCTION

The behavior of Hot-Mix Asphalt (HMA) mixtures under repeated trafficking and various environmental conditions is quite complicated. As a unique distress mode of asphalt pavements, permanent deformation, i.e., rutting and shoving, has been accounted for by the load-temperature related viscoelastic properties of the HMA, responding to diverse in-situ states of stress and/or strain. Even though it has been known that permanent deformation is primarily caused by shear (q) rather than the mean normal stress (p), it is not a simple matter of selecting appropriate stress states representing the variation of ' q ' near the surface of asphalt pavements for laboratory testing (1). Besides, the characterization of the permanent deformation response of HMA mixtures to loading requires that complex analytical models be determined through extensive laboratory testing and field validation. For instance, the generalized permanent-deformation law proposed by Sousa et al. as follows (2):

$$\Delta \varepsilon_{pij} = f(\bar{\varepsilon}_{pij}, \sigma_{ij}, \varepsilon_{ij}, T, \omega, C) \quad (1)$$

In equation (1), the increment in the generalized state of permanent deformation per load cycle is a function of the states of stress and strain (σ, ε), temperature (T), loading condition (ω) and the properties of the mixture (C).

Since this type of performance failure, which often occurs in the early service years, significantly reduces the serviceability and even causes hazardous hydroplaning of vehicles, the permanent deformation characteristics of HMA have been a major concern to asphalt paving technologists for a long time. Furthermore, the fact that truck tire pressures are increasing and that most rutting observed in trench cuts occurs in the top

3 ~ 4 inches of the HMA layer requires the production of more rut-resistant and stable mixtures (3, 4, 5, 6, 7).

With the advent of the Superpave system, HMA mix design has become more rational, and the selection of materials and the volumetric properties of the mixture have been emphasized to ensure satisfactory performance. The Superpave Level-1 mix design, however, entirely depends for its success on the volumetrics of the mixture. Accordingly, mix design without evaluating the performance potential of the mixture still makes paving technologists uncomfortable and gives less confidence on their products. In this context, it is not surprising that the Association of Asphalt Paving Technologists (AAPT) adopted “Physical Tests for Mixture Evaluation Using Gyratory compacted Specimens” as the subject of a symposium at their 2002 annual meeting. Also, there have been extensive studies pertaining to performance testing under the National Cooperative Highway Research Program: NCHRP project 9-19 “Superpave Support and Performance Models Management”, 9-16 “Relationship Between Superpave Gyratory Compaction Properties and Permanent Deformation of Pavements in Service”, and 9-29 “Simple Performance Testers for Superpave Mix Design”.

It is necessary to note that a recent study conducted at the National Center for Asphalt Technology (NCAT), “Performance Tests for Hot Mix Asphalt”, was initiated to compare available tests and select the best test for immediate adoption because it has been clear that volumetric mixture design alone is not sufficient to ensure quality products (8). Test methods with potential to evaluate the permanent deformation susceptibility of HMA mixtures were classified into six types: a) Diametral tests, b) Uniaxial tests, c) Triaxial tests, d) Shear tests, e) Empirical tests, and f) Simulative tests. Also, each type of test was sub-classified by loading modes. Based on their

comparison criteria including available performance data of a test, simulative tests (wheel tracking tests) such as Asphalt Pavement Analyzer, Hamburg Wheel-Tracking Device, and French Rutting Tester were recommended. Another extensive study by Witczak et al., NCHRP 9-29, reported not only the best candidate simple performance tests (SPT), but also HMA mixture responses obtained from the candidates that are highly correlated to pavement distress (9, 10). With respect to rutting, the recommended SPT method - response parameter combinations were a) the dynamic complex modulus, $E^*/\sin\phi$, determined from the triaxial dynamic modulus tests, b) the flow time, F_t , determined from the triaxial static creep test, and c) the flow number, F_n , determined from the triaxial repeated load test.

As seen in the literature, to date, numerous test methods and testing equipment have been proposed to predict and/or identify the permanent deformation characteristics of HMA mixtures, and some of them seem to work well. However, due to the cost of the test equipment and complicated sample preparation and procedures for testing, from a practical point of view, the use of currently available tests appears to be limited to "research tools". Moreover, since end-result specifications (QC/QA type) tend to move forward on Performance-Related Specifications (PRS), contractors need to have more confidence in their final product and to take the responsibility for the quality (or performance) of mixtures (11, 12). Therefore, the need to develop a simple performance test is increasing as a compliment to the volumetric mix design.

1.1 Study Objectives

The objective of this study is to develop a rapid performance test for Superpave mixtures. A new test should be practical enough so that it can be routinely used during

mix design and during construction to differentiate a potentially stable mixture from a potentially unstable HMA mixture. Accordingly, the major considerations emphasized in the development of performance testing are as follows:

- a) the cost of test equipment,
- b) time required to complete a test,
- c) the feasibility of testing, and
- d) the quality of test results.

In order to meet these, the test equipment and procedure need to be familiar to paving technologists, and most importantly for the cost effectiveness, it is preferred to use equipment already available. This brought the Superpave Gyrotory Compactor (SGC) into consideration. The SGC to some extent shears the mixture during compaction and thus, many attempts have been made to utilize the SGC for characterizing HMA mixtures. Also, this equipment has now been used in paving industry for almost a decade, and contractors are therefore familiar with it.

Specific objectives that this study seeks to accomplish are as follows:

1. to review the proposed uses of the SGC
2. to establish a test protocol of a rapid performance test (RPT) for Superpave mixtures using the SGC
3. to examine the potential of the RPT and analyze the responses of HMA mixtures to the RPT through a pilot test
4. to establish criteria and a practical guide for the RPT by conducting extensive laboratory testing

2. LITERATURE REVIEW

The Superpave Gyratory Compactor (SGC) has been introduced by the Strategic Highway Research Program (SHRP) researchers as a standard device to compact hot-mix asphalt (HMA) specimens in a new mix design method, *Superior Performing Asphalt Pavements*, known as Superpave. This device has been recognized as one of the most outstanding products of the SHRP asphalt research program, which distinguishes Superpave from other methods, together with a new asphalt binder specification, the Performance Grading (PG) system. In this chapter, the historical development of the SGC and its use for characterizing the HMA mixture are reviewed.

2.1 The Historical Development of the SGC

Basically, the equipment and the operating protocol of the SGC originated from the Texas gyratory compactor and French Laboratoire Central des Ponts et Chaussées (LCPC) gyratory compactor (13). However, the SHRP researchers spent significant time and effort in tuning the compaction parameters (gyratory angle, speed of rotation, and vertical pressure) and preparing the N_{design} table. The major basis for selection of the gyratory compactor over the others, such as the kneading compactor and the Marshall hammer, was the fact that it produces test specimens that duplicate, as nearly as possible, the compacted mix as it exists in an actual pavement layer (14, 15, 16). This conclusion was drawn from extensive studies on the comparison of the laboratory specimens compacted by various methods and samples cored from pavements, in terms of their densities and other physical properties.

The difference between mold compaction in the laboratory and roller or pneumatic-

tired compaction in the field, as Endersby and Vallergera pointed out, is that the particles, adjacent to the roller or tire, can move laterally or longitudinally, or even vertically with considerable freedom (17). Also, the arrangements of aggregate particles, which have a significant effect on the deformation resistance of HMA mixtures, vary depending upon the compaction method used. Hence the compaction method used would be vital in the matter of particle arrangements, and the field compaction (roller compaction and trafficking) should be simulated during mold compaction.

The gyratory mode of compaction was brought into the paving industry as early as 1950s by the engineers at Texas Highway Department and U.S. Army Engineer COE Waterways Experiment Station. Ortolani and Sandberg Jr. presented the Gyratory Molding Machine and the procedure for molding asphaltic concrete specimens as a standard method adopted by Texas Highway Department (18). In their research, large amount of data accumulated were correlated with field performance and the densities obtained from this method of molding were compared with core densities from roads. They also considered the breakdown of aggregates under field compaction so that the molding method approximates the aggregate degradation expected under field conditions.

In the late 1950s, McRae and Foster introduced their version of gyratory compactor (19, 20). The study was initiated by recognizing that pavement densities obtained under high-pressure-tire traffic of heavy military airplanes are in excess of those obtained by impact compaction, e.g., the Marshall hammer, and increasing the number of impact blows is infeasible due to the excessive degradation of the aggregate. Based on the results from the accelerated traffic test, it was proved that the densities and stability values of specimens compacted by the gyratory compactor agree much better with those

of field cores than those of specimens compacted by impact method. Furthermore, they showed the possible use of the machine to select optimum binder content and to measure plastic properties of the bituminous paving mixture. Those were possible because the machine was equipped with an apparatus recording the variable gyratory angle, which is referred to as the gyratory motions band. The recorded band first shows a slight decrease in the width, indicating a slight increase in stability, and then as gyrations continue and the mixture continues to densify, the band eventually starts to spread. It is believed this spread occurs because the mix starts to flush and to lose strength. This concept, coupled with the principle of Proctor compaction in soil engineering was proposed as a mix design method (21). Later, this machine was further modernized, referred to as the Gyratory Testing Machine (GTM) and adopted as one of the standard test methods by ASTM (22).

After those early attempts, the gyratory compactor did not attract noteworthy public attention until the SHRP researchers revisited it as a part of the SHRP asphalt research program for the development of the Superpave mix design system.

During the early 1990s, significant efforts, including the SHRP research, were made to find the most suitable laboratory compaction methods for HMA mixtures. Most of the work performed at that time, was devoted to evaluating several laboratory compaction methods and their effects on the properties of mixes (23, 24, 25). The major types of compaction device compared were gyratory compactor (Texas), kneading compactor, rolling wheel compactor and Marshall hammer. After the SHRP researchers reviewed the related literature and performed extensive experiments, they concluded that the gyratory compactor reasonably simulates field compaction and that the compaction characteristics represented by C_x ($\%G_{mm}$ at X numbers of gyration) and K (slope of the

compaction curve) can be used for field verification of mix properties and field control of the mix during construction (15, 16). It was since SHRP reported their findings mentioned above and selected the SGC for the Superpave that the use of the gyratory compactor other than for just compacting HMA mixtures has been studied intensively in the United States.

2.2 Use of Gyratory Compactors

It should be recognized here that there are definite differences between the SHRP (or Superpave) gyratory compactor, referred to as the SGC and the U.S. Army Corps of Engineers gyratory compactor, referred to as the GTM, with respect to the way of applying gyration angle and the data obtained during or after compaction. Hence, it is more appropriate to review the uses of those gyratory compactors separately.

The GTM, unlike the SGC, records the variation of gyratory angle or the force required to maintain the angle constant during compaction process. Since the inclined angle and force are related to the properties of the mix, there have been several studies to correlate these with the performance potential of HMA mixtures.

After the early studies of 1950s, Kumar and Goetz demonstrated the potential of the GTM as a design tool and as an instrument for bituminous mixture evaluation (26). In their study, the tentative ASTM testing method using the GTM, which evolved into ASTM D3387, was followed (22). Using aggregates and gradations common in Indiana, specimens were prepared at five levels of asphalt content with 0.5 percent increments, and then subjected to testing in the GTM. In order to select the design asphalt content, the GTM indices were calculated based on sample weight and height, asphalt content, gyratory angle, and gyrograph band width. As seen in Figure 1, for instance, the gravel

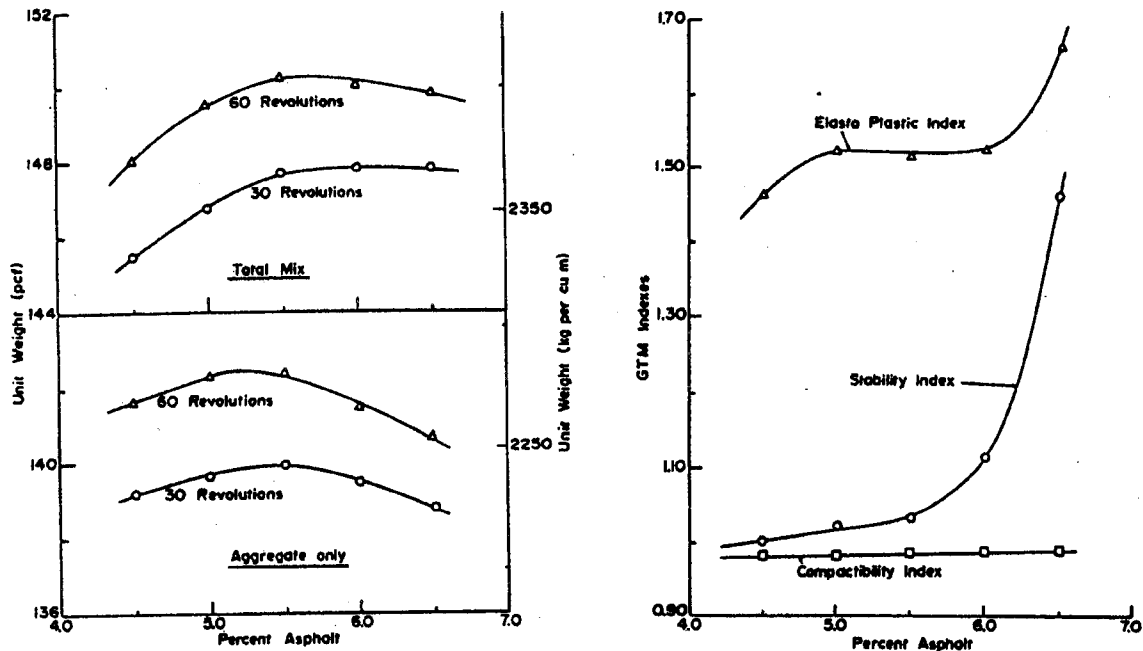


Figure 1. Unit weights and GTM indices vs. asphalt content (26)

mixture showed significant loss in stability at about 5.5%. Since their approach to the optimum asphalt content was to select the maximum asphalt content at which a bitumen-aggregate combination is as durable as possible and yet is stable, the design asphalt content of 5.0 percent was selected for the gravel mixture.

Bonnot at Laboratoire Central des Ponts et Chaussées (LCPC), France, introduced French gyratory shear compacting press (PCG) which was referred to for the development of the SGC by the SHRP researchers (27). French PCG can be categorized with the GTM because it records the force required to keep the gyration angle constant at 1 degree. It is important to note that, when Bonnot presented the PCG and French mix design technology, he clearly mentioned that the PCG was devised to study the “compacting performance” or “compacting characteristics” of bituminous mixes as a

measure of workability, by continuously evaluating measurements of the sample height and the inclination force. The performance of the mix was examined using the LPC wheel-tracking rutting-test machine, bending fatigue test machine and shear fatigue test machine.

Sigurjonsson and Ruth used the GTM in their study to evaluate the effect of aggregate characteristics on asphalt paving mix properties (28). They pointed out that the deficiencies in mix design (Marshall) are primarily associated with the characteristics of the aggregates and the gradation. Thus, it was suggested that aggregate blends which exhibit low sensitivity to changes in asphalt content should be selected. Any mixture giving a substantial reduction in shear resistance measured by the GTM at 60°C, with asphalt content 0.5 percent over design should be considered as highly sensitive. Based on the GTM test results on mixtures of known performance, they concluded that shear responses obtained from the GTM can be used to evaluate the adequacy of asphalt mixtures and to design a high-quality mix which is not sensitive to reasonable changes in binder content, gradation, and mineral filler content.

Cabrera at the University of Leeds emphasized that thoroughness of compaction is the single most important factor necessary to achieve adequate performance of bituminous mixtures in road pavements, therefore, for the design of bituminous mixtures, workability should be considered as one of the main requirements (29). The workability index (WI) proposed as a parameter to quantify the workability of bituminous mixtures was defined as the inverse of the intercept of the densification curve obtained by the GTM. He explained the GTM process bears some resemblance to the mode of compaction energy applied in the field and the machine allows application of an axial static pressure at the same time that the specimen is subjected to a dynamic

kneading by a gyratory motion of a steel mold. He also mentioned that by measuring the WI using the GTM at the design stage it is possible to detect the influence of filler type, filler morphology, binder content and temperature on the workability of bituminous mixtures.

In the middle of 1990s, after the SHRP asphalt research program, the SGC became the dominant compaction device for HMA mixtures and, therefore, several research projects were conducted to evaluate the performance or behavior of HMA mixtures using the SGC. It needs to be noted that, during the compaction process, the only data obtained from the SGC is the continuous reduction of sample height. Using the measured specific gravity of the compacted specimen (G_{mb}) and theoretical maximum density (G_{mm}) of the mix, the void contents and the volumetrics of the mix at any number of gyrations (N) may be back-calculated and plotted in, the so-called, compaction curve or the densification curve ($\%G_{mm}$ vs. $\log(N)$). This compaction curve represents the entire compaction history of the mix, and compaction characteristics, like C_x and K , are calculated from that linearized compaction curve.

In the study performed by Anderson et al., the SGC was utilized for field quality control testing. The results indicated that the compaction curves or compaction characteristics of the specimen compacted by the SGC are sensitive to changes in material components such as, asphalt content and filler to binder ratio (30). Hence they concluded that the SGC could be used for quality control and quality management in the field, which confirmed the findings of the SHRP study.

Harman et al did similar studies and they demonstrated the use of the SGC as a tool to examine the conformity of field mixes to the Job Mix Formula (JMF) prepared in the laboratory because the SGC is capable of detecting variations in the materials by

comparing volumetric properties of the mixes, such as air voids, and voids in mineral aggregate (31).

Bahia et al. attempted to optimize the densification characteristics of HMA mixtures under construction and traffic, using the SGC compaction curve (32). They proposed the compaction energy index (CEI) and the traffic densification index (TDI), which are the areas under the densification curve drawn using the SGC data, as measures to relate to performance of mixtures and as criteria to select mixtures that are workable enough during construction and strong enough to resist densification under traffic. In order to calculate the CEI and TDI, the densification curve is fitted into a power-law equation and then the areas are calculated by integrating the equation under the curve between selected reference points, related to the field construction and in-service conditions, like N_{initial} , N at $92\%G_{\text{mm}}$, N_{design} , and N at $98\%G_{\text{mm}}$ (Figure 2). These areas were believed to represent the work required to achieve the change in density.

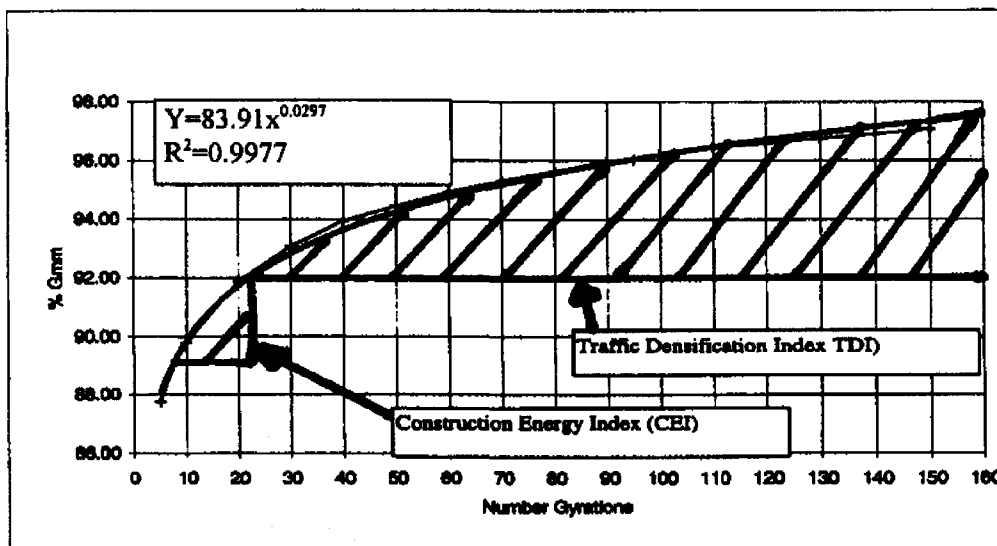


Figure 2. Compaction energy index and traffic densification index (32)

The hypothesis made was that a weak mixture will dissipate less energy during the gyratory compaction, and more energy will be available for the vertical densification. Therefore a lower number of gyrations will be required to make the same change in density and the area under the densification curve will be smaller for the same change in %G_{mm} or air voids, compared to a strong mixture.

Mallick concluded that the ratio of the number of gyrations required to compact a mix to 2 percent air voids and 5 percent air voids, called the gyratory ratio, can be used to identify inferior mixes (33). The basis of his method was that, in the case of the stable mix, the mix gains in strength with densification and retains it through further compaction and ultimately resists lowering of voids below a particular value, whereas in the case of an unstable mix, the mix initially gains in strength but loses it beyond a certain densification point and becomes susceptible to shear failure. Air voids of 5 percent and 2 percent were considered as two critical points where the strength of the mix should be evaluated. By comparing the GTM test results and the field rutting performance of the mixes with their gyratory ratios, a gyratory ratio of 4 was recommended as a threshold criterion between unstable and stable mixes. A mix with the gyratory ratio less than 4 is expected to be unstable.

Even though several researchers showed the possible use of the SGC to characterize HMA mixtures as mentioned above, in the late 1990s, some studies revealed that 1) the compaction characteristics of the mixture obtained from the SGC during compaction are not good indicators of the strength of the mixture, 2) there is no correlation between the SGC data and the results of simulative tests (e.g., Asphalt Pavement Analyzer), and 3) mixtures generating similar SGC compaction characteristics can exhibit considerably different rutting performances in field tests (34, 35, 36). Hence, recent studies have

focused on modifying the SGC to measure the shear properties of the HMA mixture.

Butcher introduced the second Australian gyratory compactor, the Servopac, modifying the first gyratory compactor, the Gyropac, which is more or less similar to the SGC (37). Unlike the Gyropac, the Servopac is capable of measuring the shear resistance of the mixture during gyratory compaction by the installation of pressure transducers in the pressure lines of the three gyratory actuators.

Guler et al. described the development of a gyratory load-cell and plate assembly (GLPA), an accessory that can measure the shear resistance of HMA mixtures (38). The GLPA is inserted on top of the mixture in the SGC compaction mold, and three load cells inside the GLPA allow measurement of the variation in force distribution on top of the sample so that the position of the resultant force can be determined. The effective moment, calculated based on the distribution of the eccentricity of the resultant force, is believed to be a measure of the resistance of HMA mixtures (primarily aggregate structures) to distortion and densification during compaction process, which is related to the resistance of the mixture to rutting under traffic.

Anderson presented a modified SGC with a shear measurement system that produces a ratio of shear stress to normal stress, and suggested that the $N-SR_{max}$, the number of gyrations at the maximum stress ratio, be utilized as a mixture performance-screening tool (39).

It is worth noting that an extensive literature review conducted recently at the National Center for Asphalt Technology (NCAT) as a part of their study under the contract of NCHRP 9-9, well-summarized the issues pertaining to the development and evaluation of the SGC (40).

2.3 Summary

The historical development and uses of the gyratory compactor were reviewed. The SGC, currently specified as a standard compaction method in the Superpave mix design, originated from the Texas gyratory compactor. The protocols are based on that of French gyratory compactor with modifications made by the SHRP researchers.

Two distinct types of gyratory compactor have evolved since 1950s, and those are the GTM of the U.S. Army Corps of Engineers and the SGC of the SHRP. The GTM is capable of measuring the variations of the gyration angle and/or the force necessary to maintain the angle. Using those properties, several attempts were made to characterize the shear resistance of HMA mixtures.

With the advent of the Superpave, the SGC became a standard compactor for the HMA mixture and now, it is the most common equipment to state agencies and asphalt industry in the U.S. As earlier studies indicated, the SGC compaction characteristics of the mixture appeared to be useful for the quality management in the field. In spite of some efforts made to utilize the SGC data for evaluating the performance potential of the mixture, it has been shown that there is no clear correlation between the SGC data and the simulative tests or the field performance of the mix. Recent studies, however, demonstrated the possible use of the SGC to characterize the HMA mixture by installing additional device measuring the shear resistance of the mix during compaction.

3. A PRELIMINARY STUDY

In this chapter, the background of this study is briefly mentioned. This chapter is dedicated particularly to describing the approach to the development of a rapid performance test (RPT) for Superpave HMA mixtures. Test results of the pilot test performed to examine the potential of the proposed RPT by analyzing the responses of HMA mixtures are also presented.

The literature search presented in the previous chapters revealed that there is still a lack of a simple performance test to complement the Superpave volumetric mix design. In addition, the reviewed literature indicates that the Superpave Gyrotory Compactor (SGC) developed under the Strategic Highway Research Program (SHRP) has a potential of being used as testing equipment.

This study was conducted to develop a rapid performance test (RPT) for Superpave HMA mixtures which can be routinely used as a practical tool for ensuring the performance of HMA mixtures. It has been emphasized, throughout the study, that the RPT does not have to be a fundamental test by which the stress (or strain) states of the mixture under trafficking and various environmental conditions are exactly reproduced in the laboratory. Therefore, it was hypothesized that a test by which permanent deformation can be measured, by inducing shear failure and/or plastic flow of the HMA mixture, could be a candidate for the RPT. A new RPT, however, should be based on a rational background and provide a reasonable correlation with the results from the fundamental/simulative tests and the field performance of the mixture.

In order to meet the various considerations for developing the RPT, e.g., the cost of

test equipment, time required to complete a test, the feasibility of testing, and the quality of test results, the SGC was selected as the test equipment of choice. As shown through the literature search, the SGC to some limited extent shears the mixture during compaction and many researchers have tried to characterize HMA mixtures using this device. Most importantly, it is the most common equipment in the asphalt paving industry and the users are already quite familiar with it because it has been used in most state agencies and contractors for almost a decade.

3.1 A Proposed Rapid Performance Test

Most attempts made to utilize the SGC in determining the rut susceptibility or the resistance to shear of the HMA mixture require some modifications of equipment because the original SHRP SGC is incapable of quantitatively measuring the shear resistance of the mixture. The only data obtainable from the SGC is the continuous vertical height changes of a mixture as the number of gyrations increases, and the number of gyrations and the vertical pressure are all the flexibility the user has. Hence, the possible versatility of the use of this equipment is limited to compacting loose mixes.

Not only the equipment itself but also the manner in which the SGC is being used conventionally needs to be adjusted to utilize the SGC as testing equipment for differentiating a stable from unstable HMA mixture mainly for the following reasons:

- (a) The compaction temperature at which the viscosity of the binder is $0.28 \pm 0.03 \text{ Pa}\cdot\text{s}$, e.g., 135°C , is unrealistically high for evaluating the potential service performance of a mixture, compared with the actual in-service pavement temperature. It is true that the aggregate skeleton is

the main contributor to rut-resistance of the HMA mixture. However, it should be recognized that 1) the contribution of binders, say, a cohesion term in the Mohr-Coulomb failure criteria ($\tau = c + \sigma \tan\phi$), can be less significant than the friction angle, but, not negligible at in-service temperatures, 2) the friction angle (ϕ) is not a function of the aggregate skeleton alone, and 3) other binder-related properties of the mixture such as, binder content, grade, and film thickness have a considerable effect on the stability of the mixture. Besides, the major disadvantage of using the compaction temperature is that the temperature (e.g., 135°C) is determined as the equi-viscous temperature (0.28 ± 0.03 Pa·s), and therefore all binders will have the same characteristics. Figure 3 shows the typical temperature – viscosity relationship of the asphalt binder. It should be emphasized that the approximate linear relationship is observed when the viscosity is plotted on logarithmic scale. Therefore, the magnitude of the difference of the viscosities of two binders at in-service temperature is not the same as that of two binders at the elevated temperature. In Figure 3, the difference of the viscosity of PG 64 and PG 58 is 0.12 Pa·s at 135°C, but it is 25.4 Pa·s at 70°C – two whole orders of magnitude of difference. The viscoelastic and rheological properties of asphalt binder and HMA mixtures cannot be fully understood by simply considering temperature susceptibility. However, the facts mentioned above explain in part why considerably different rutting performances of five different binders, but generating nearly the same SGC compaction parameters were observed at the Federal

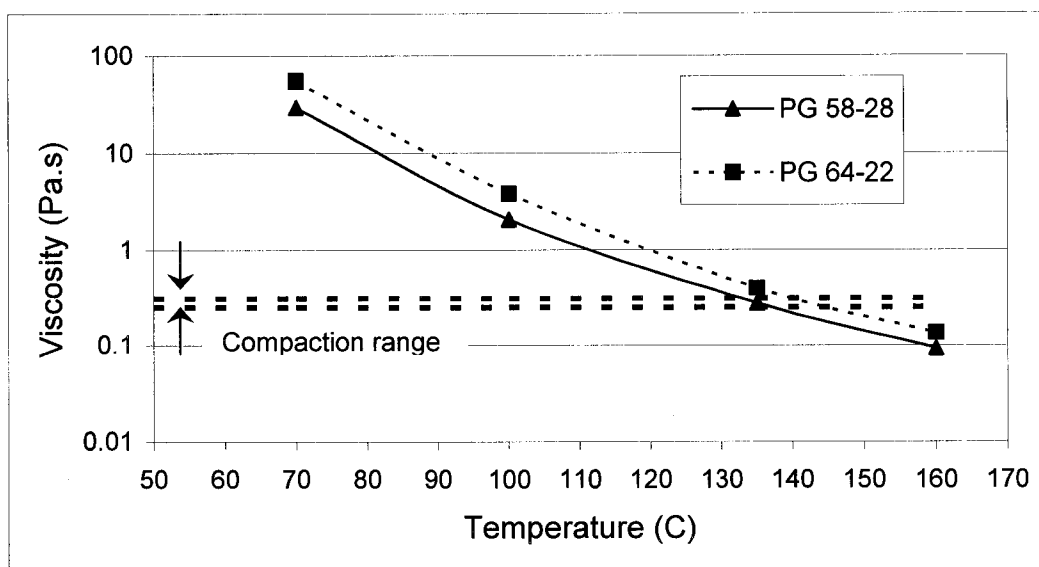


Figure 3. Temperature – Viscosity relationships of the asphalt binder (Data from Koch Materials Company, Dubuque, Iowa)

Highway Administration (FHWA) Accelerated Loading Facility (ALF) experiment (41). Also, a recently conducted study, NCHRP 9-16, revealed that, using standard SGC compaction protocols (Figure 4), none of the SGC compaction properties appear to be capable of identifying differences in mixture performance based on asphalt binder stiffness (39).

- (b) A mixture in the cylindrical SGC mold is surrounded by the top platen affixed to the loading ram and the rigid mold assemblies during compaction. Thus, the plastic flow or lateral movement of the mixture, which is the main mechanism of rutting, cannot be fully developed and is limited to horizontal planes. This strongly holds the truth as percent theoretical maximum specific gravity (%G_{mm}) of the mixture increases during compaction, usually beyond 96 ~ 98%, depending on a mixture.

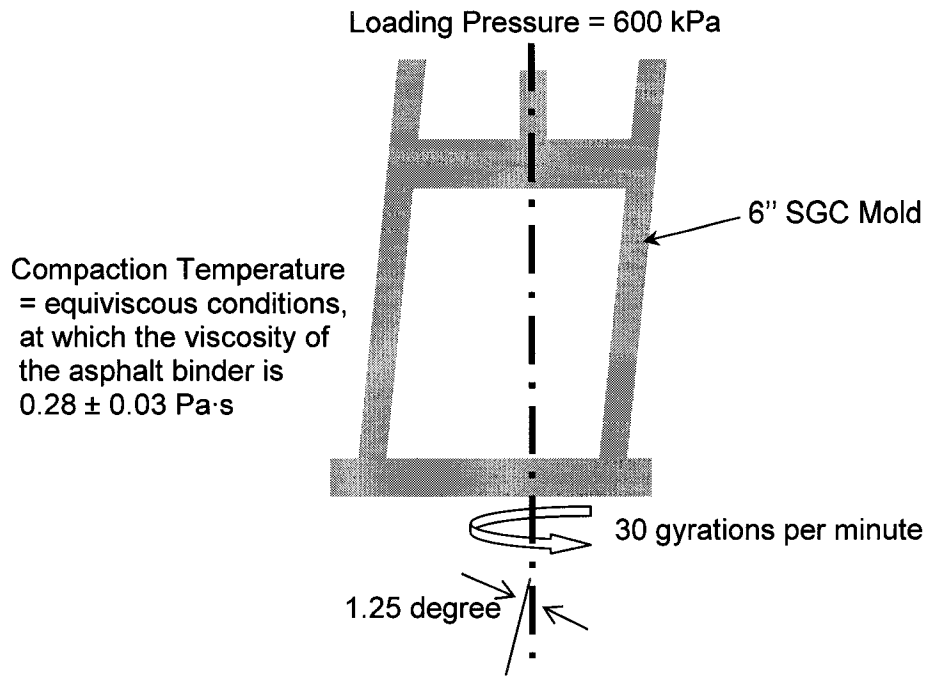


Figure 4. The SGC compaction protocol

- (c) For the appropriate appreciation of the SGC data or the compaction curve used in Superpave mix design, it needs to be separated into two phases; a construction phase and a performance phase. As seen in Figure 5, construction phase is represented by the data from the beginning of compaction to $N_{92\%G_{mm}}$ or $N_{93\%G_{mm}}$, the number of gyrations required to achieve the specified post-construction density (92 ~ 93% G_{mm}), and the second phase, performance phase should start from there, assuming that is the condition at which the field-compacted mixture is opened to the traffic. Further, these two phases should have significantly different temperature regimes.

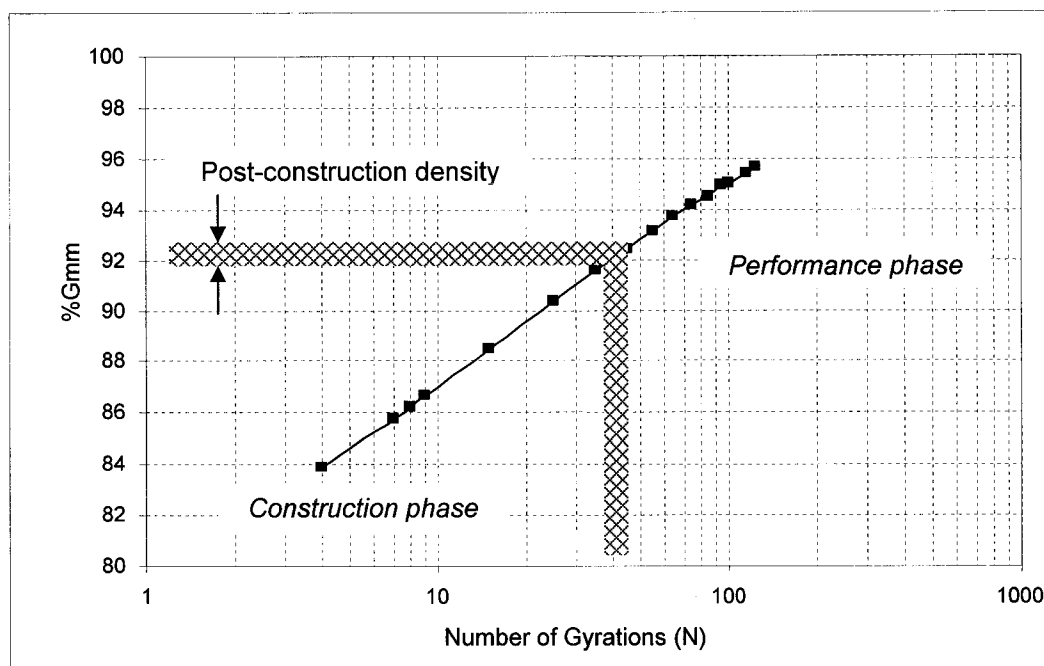


Figure 5. The compaction curve of the Superpave mix design

Since the behavior of the HMA mixture in the performance phase cannot be represented by the conventional laboratory compaction procedure due to the reasons, (a), (b), and (c) above, some modifications are necessary on both of the equipment and the compaction procedure.

In order to cost-effectively utilize the SGC as possible RPT equipment, while overcoming the limitations of the conventional manner in which the SGC has been used, the test protocol of the RPT is proposed as follows (42):

- Step 1. Compact a mixture to the specified level of density, representing the post-construction condition at the conventional compaction temperature. The number of gyrations required to achieve this density is readily available from ordinary Superpave volumetric mix design procedure.

Step 2. Place the mold containing the compacted mixture and the secondary loading platen (the SGC indenter) in an oven set the temperature to the performance temperature and keep them in the oven for a sufficient time to achieve uniform thermal equilibrium throughout the mixture achieved.

Step 3. Re-place the mold containing the mixture into the SGC and insert the SGC indenter on top of the mixture. After adjusting the compaction pressure to a specified value, resume compaction up to a specified number of gyrations.

Using the continuously measured height changes of the mixture, calculate the vertical strains, which are normalized by the height of the mixture at $N = 1$ and plot the strain versus N curve.

During the preliminary study, the post-construction density in Step 1 was assumed to be $92\%G_{mm}$, and the performance temperature in Step 2 was selected as the high temperature of the PG system for the simplicity. The experiments conducted for the mixture conditioning in Step 2 indicated that, after compacting a mixture to the post-construction density, cooling the SGC mold containing the mixture at the ambient ($23^{\circ}\text{C} \sim 25^{\circ}\text{C}$) temperature for one hour, followed by two hours oven-condition is the most efficient way to achieve stabilized performance temperature throughout the specimen. In step 3, the SGC indenter is placed on top of the mixture contained in the mold before resuming the compaction procedure. The proposed RPT test protocol is illustrated in Figure 6.

The SGC and the indenter used in this study are shown in Figure 7. The upper part

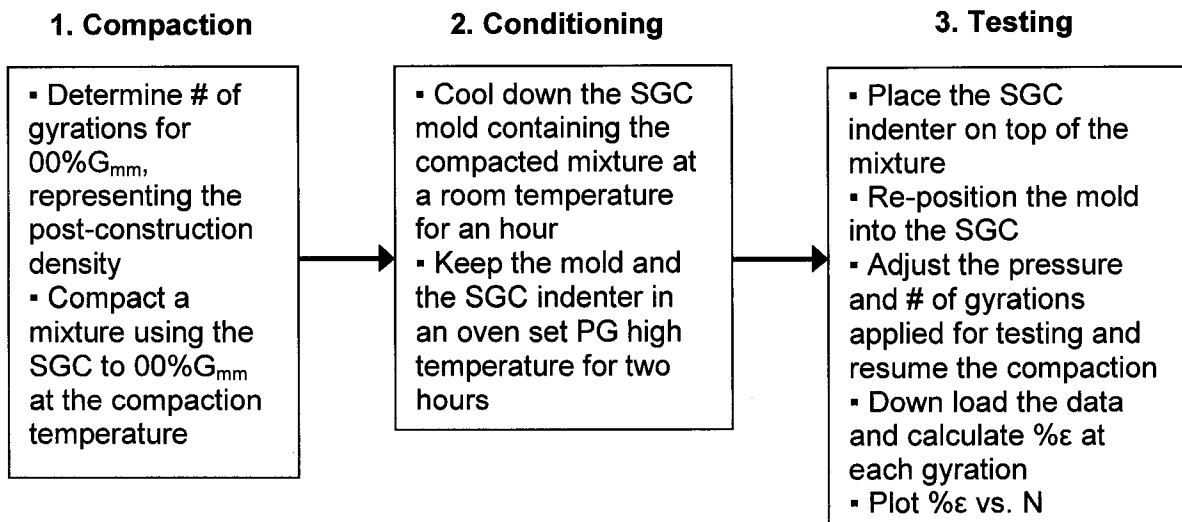


Figure 6. The proposed RPT

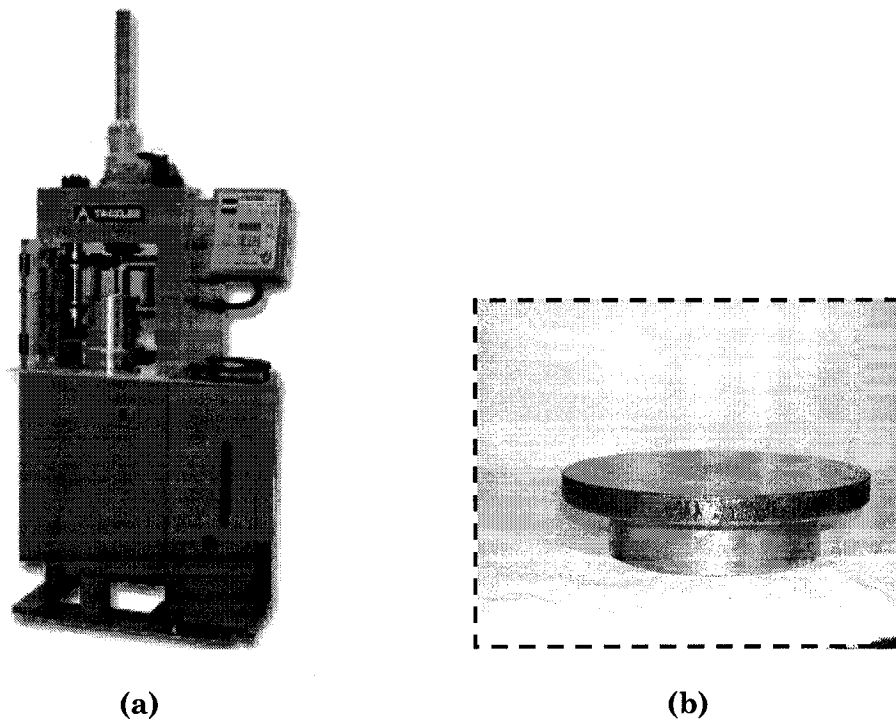


Figure 7. The SGC, Troxler 4140-B (a) and the indenter (b)

of this indenter is 147 mm in diameter, which is slightly smaller than the SGC loading platen and 10-mm thick. The lower part is 100 mm in diameter and 25-mm deep. The SGC indenter can be easily machined at the cost about \$100 ~ \$200. The reduced contact area creates a ring-shaped space that provides room for HMA mixtures to plastically flow or deform during testing.

Since the contact diameter has been reduced to 100 mm, by inserting the indenter, the vertical pressure applied needs to be adjusted to 267 kPa in order to apply 600 kPa (87 psi), which is the normal SGC compaction pressure, or 306/368 kPa can be applied to simulate 689/827 kPa (100/120 psi) tire inflation pressure. Three hundred gyrations ($N = 300$) was applied somewhat arbitrarily as the number of gyrations for testing.

3.2 A Pilot Test and Discussion

Using available materials, limited numbers of mixtures were tested during this preliminary study with the purposes of 1) evaluating the capability of the proposed method, 2) examining the conformity of the test results with the general expectations based on experience, and 3) refining the test protocol, if necessary. Primarily, as an experimental stage, it was necessary to confirm that the results obtained from the proposed RPT show more permanent deformation in less favorable conditions with regard to permanent deformation of the HMA mixture. These 'less favorable conditions' were made by controlling the aggregate properties, binder contents, and test temperature. Different levels of 'less favorable conditions' were generated by fabricating mixtures with three different aggregate gradations mixed with three levels of asphalt binder content, and by testing mixtures at three temperatures. Hence, the experiment was considered as 3^3 factorial design. In exploratory work, the factorial experimentation

is suitable to determine quickly the effects of each of a number of factors (or treatments) over a specified range (43, 44).

A 19-mm nominal size crushed limestone was re-blended to obtain three gradations, designated fine, dense, and coarse, as shown in Figure 8. To maximize the allowable variations of aggregate gradations, the maximum density line was selected for dense gradation, and the smooth curves connecting the upper and lower limits of control points described in the Superpave mix design were selected as fine and coarse gradations, respectively. The restricted zone was ignored throughout the study because it has been recommended to delete the restricted zone in Superpave, based on recent studies indicating that HMA mixtures having gradations passing through the restricted zone do not necessarily have lower rut resistance compared to mixtures having gradations outside the restricted zone (45, 46).

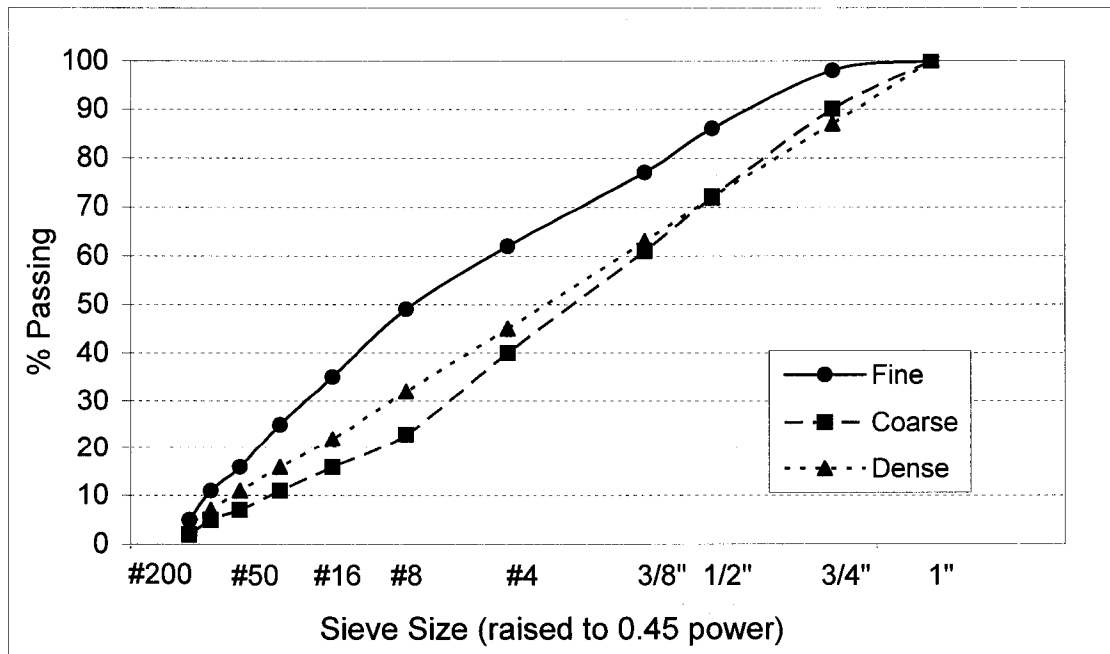


Figure 8. Aggregate gradations used in the preliminary study

As a binder, PG 58-28, which is in common use in Iowa, was used and the optimum asphalt contents ($P_{b(opt)}$) for each of three gradations were determined at which four percent air voids were achieved at $N_{design}=109$. Table 1 summarizes the volumetrics of those mixtures.

Without replications in the 3^3 factorial experiment (three factors at three levels), 27 mixtures fabricated using three levels of aggregate gradation (Fine, Dense, Coarse) with three levels of asphalt binder content ($P_{b(opt)}-0.5\%$, $P_{b(opt)}$, $P_{b(opt)}+0.5\%$) were tested at three levels of test temperature (52°C , 58°C , 64°C), in accordance with the proposed test protocol shown in Figure 5. All 27 notations for treatment combinations are described in Table 2.

After mixing the aggregates with the target amount of asphalt binder, the loose mix was kept in the oven set 135°C for four hours for short term aging. Since the post-construction density of the HMA mixture was assumed to be $92\%G_{mm}$, the short term aged loose mix was then compacted to 8% air voids, and after conditioning the mixture

Table 1. The volumetrics of three mixtures for $N_{design}=109$

Gradation	Surface Area (m ² /kg)	Optimum Binder (%)	%Gmm @N _{ini}	%Gmm @N _{max}	VMA	VFA	D/B	FT
Fine (F)	6.33	5.3	86.8	97.1	11.7	67.6	1.5	5.4
Dense (D)	4.52	4.8	86.0	97.2	11.7	66.8	1.2	7.4
Coarse (C)	3.04	5.2	85.3	97.5	12.5	68.1	0.5	12.1

Table 2. Notations for 27 treatment combinations

Asphalt Binder Content	Aggregate Gradation								
	Fine			Dense			Coarse		
	Testing Temperature (°C)								
	52	58	64	52	58	64	52	58	64
$P_{b(opt)} - 0.5\%$	F/P _b /52	F/P _b /58	F/P _b /64	D/P _b /52	D/P _b /58	D/P _b /64	C/P _b /52	C/P _b /58	C/P _b /64
$P_{b(opt)}$	F/P _{bo} /52	F/P _{bo} /58	F/P _{bo} /64	D/P _{bo} /52	D/P _{bo} /58	D/P _{bo} /64	C/P _{bo} /52	C/P _{bo} /58	C/P _{bo} /64
$P_{b(opt)} + 0.5\%$	F/P _{b+} /52	F/P _{b+} /58	F/P _{b+} /64	D/P _{b+} /52	D/P _{b+} /58	D/P _{b+} /64	C/P _{b+} /52	C/P _{b+} /58	C/P _{b+} /64

to the target temperature, 300 gyrations were applied with the SGC indenter on top of the mixture.

Using the continuously measured height changes of the mixture, percent vertical strains ($\% \epsilon$) at each number of gyrations (N) were calculated as follows;

$$\% \epsilon (@ N = n) = \frac{H_1 - H_n}{H_1 - h} \times 100 \quad (2)$$

where, H_1 = the height of the mixture at $N = 1$,
 H_n = the height of the mixture at $N = n$, and
 h = the height of the SGC indenter, 36.7 mm

Figure 9 illustrates the permanent deformation of the mixtures subjected to $N = 300$ and the test results were plotted Figure 10 through 12, showing the main effects, i.e., test temperature, asphalt binder content, aggregate gradation, on the permanent deformations of the mixtures. The details of 27 test results are enclosed in Appendix B-I, and The observations made on the test results clearly show that the mixtures exhibit more permanent deformation at higher test temperature and at higher asphalt binder

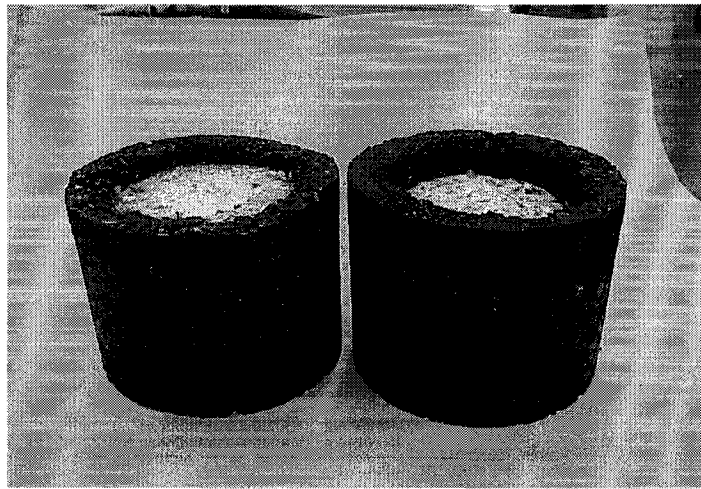


Figure 9. D/P_{bo}/58(left) and D/P_{b+}/58(right) after subjected to 300 gyrations

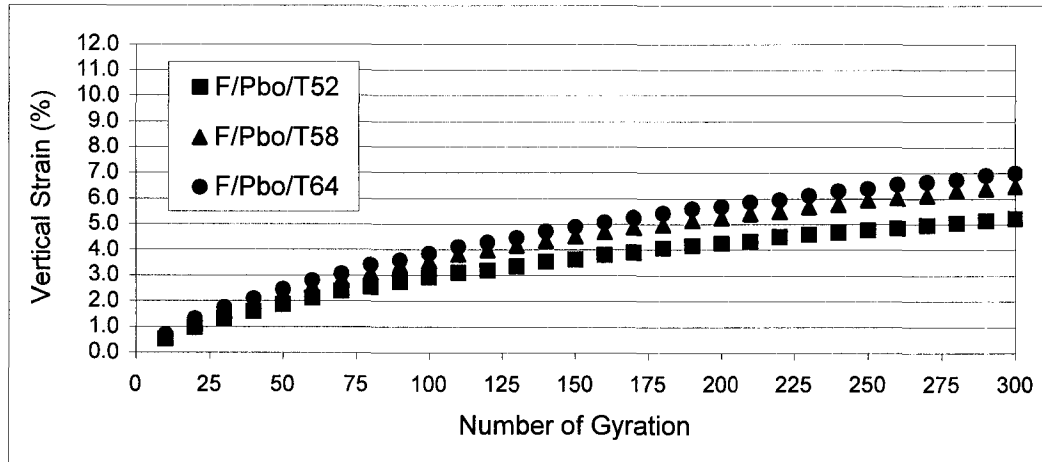


Figure 10. %ε vs. N curves showing temperature effect

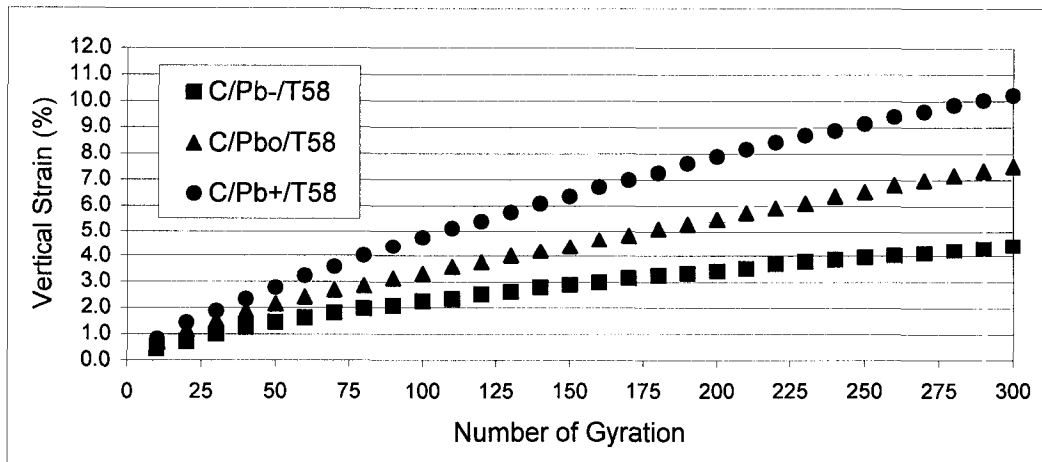


Figure 11. %ε vs. N curves showing asphalt content effect

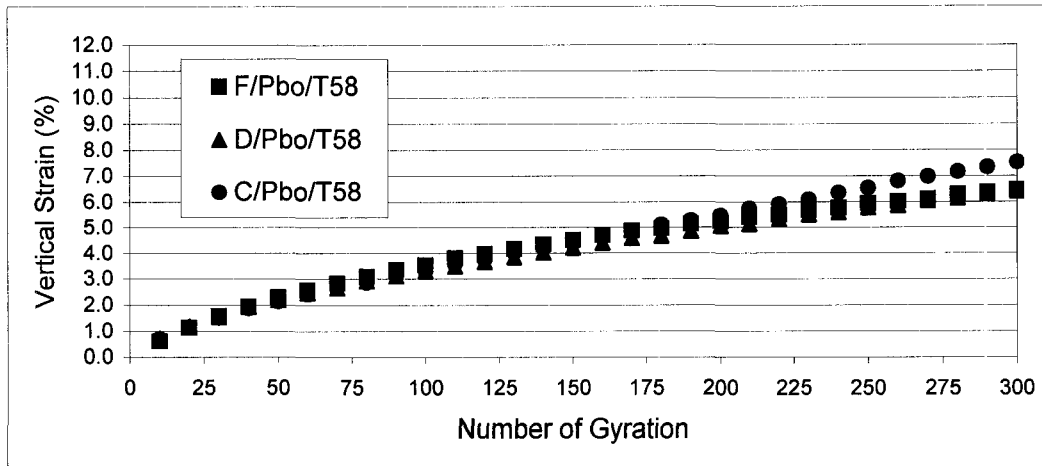


Figure 12. % ϵ vs. N curves showing aggregate gradation effect

content. However, the aggregate gradation does not show any noticeable differences.

Even though there are many possible ways to compare the responses of the mixtures and rank them with respect to the permanent deformation, a simple way is to compare the number of repeated loading (gyrations) causing the same deformation for all mixtures. Table 3 was drawn using the number of gyrations required to cause a 2% strain of each of 27 mixtures tested.

Table 3. Number of gyrations causing 2% vertical strain

Asphalt Binder Content	Aggregate Gradation								
	Fine			Dense			Coarse		
	Testing Temperature ($^{\circ}$ C)								
	52	58	64	52	58	64	52	58	64
$P_{b(opt)} - 0.5\%$	147	93	93	121	88	83	89	71	54
$P_{b(opt)}$	54	42	36	49	45	42	54	46	32
$P_{b(opt)} + 0.5\%$	39	31	27	38	37	28	36	33	25

The numbers in three 3 x 3 matrixes of Table 3 are diminishing from left to right and from top to bottom because the higher the test temperature or the asphalt content, the less gyrations required to induce 2% strain. By taking the mean responses to each main factor, these general trends are visualized in Figure 13. It needs to be noted that, in Figure 13, the coarse-graded mixtures appear to be slightly inferior to fine or dense mixtures. That is because the numbers of gyrations causing 2% strain of the coarse mixtures tested at 64°C are much smaller, even though the results obtained at 52°C and 58°C are not very different from those of fine and dense mixtures. This can be explained in part by the fact that the coarse mixtures have thicker asphalt films coating the aggregate particles, which makes them more susceptible to temperature.

In order to quantitatively examine the main effects and their interactions, a statistical analysis was conducted on the data in Table 3 and the result, the analysis of variance (ANOVA) is shown in Table 4.

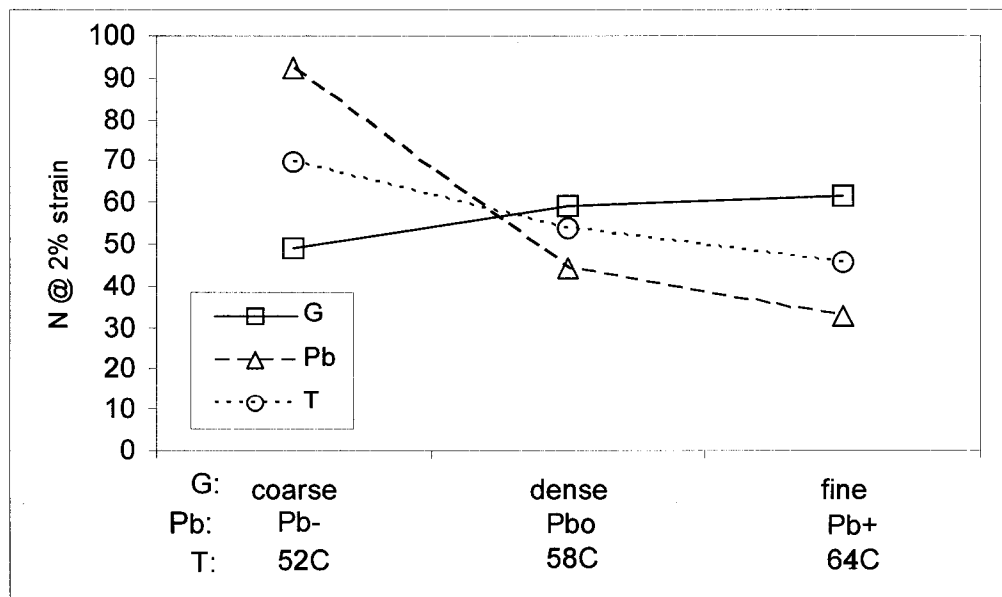


Figure 13. Trends of the responses (N for %ε=2) on the main effects

Table 4. ANOVA for number of gyrations causing 2% vertical strain

Source	DF	Sum of Squares	Mean Square
<i>Gradation (G)</i>	2	807.6	403.8
<i>Asphalt Content (Pb)</i>	2	17976.5	8988.3
<i>Temperature (T)</i>	2	2651.2	1325.6
G × Pb	4	1375.9	344.9
Pb × T	4	1253.0	313.3
T × G	4	238.6	59.6
G × Pb × T	8	237.9	29.7
Total	26	24540.7	

A complete analysis could not be done because there was '0' degree of freedom for the error term due to the lack of replication for each of the treatment combinations during the preliminary study, which makes impossible the calculations of F-test and p-value of each treatment effect, deciding the level of significance. However, there is a way to perform F-test for the level of significance. By assuming the interactions are negligible, the interaction sources can be designated as error and the sum of the mean square (MS) of interactions as MS of error (47). However, performing F-test is inappropriate in the case of Table 4 because the MSs of interactions involving P_b are not quite small. Without further discussion on the statistical analysis, a reasonable inference (relative level of significance, not absolute value) can be made by simply comparing the magnitudes of MSs because the F-test (or p-value) is calculated by dividing the MS of each treatment by MS of error, which is constant for all MSs. As seen in Table 4, the MSs of the main effects are considerably larger, especially that of asphalt content and

test temperature.

In general, the test results discussed above clearly indicated that the sensitivities of HMA mixtures to various effects can be detected by the proposed simple test protocol, which demonstrates the potential use of the proposed RPT to evaluate the susceptibility of HMA mixtures to permanent deformation.

The last task of the preliminary study was to evaluate the proposed RPT by comparing the test results obtained from the RPT with those from currently used fundamental/simulative tests. The Nottingham Asphalt Tester (NAT) is one method and the NAT has been used at Iowa State University to characterize HMA mixtures for various purposes (Figure 14).

Using the NAT, the repeated load axial tests (or dynamic creep test) were performed

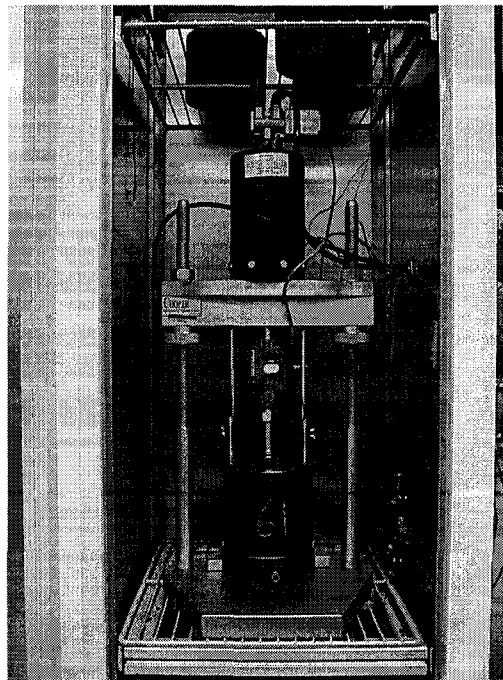


Figure 14. The Nottingham Asphalt Tester, Cooper Research Technology Ltd.

Table 5. Test conditions for the repeated load axial test

Temperature (°C)	Number of pulse	Pulse frequency (Hz)	Test stress (kPa)	Conditioning stress (kPa)	Conditioning period (second)	Test period (minute)
40	3600	0.5	100	10	120	120

on nine mixtures that are identical to those used for the RPT, and test conditions were in accordance with the manufacturer's recommendations and the British Standards as shown in Table 5 (48).

It needs to be noted that a recent study conducted in Sweden, demonstrated that performing the dynamic creep test with the diameter of the platen smaller than the diameter of the sample gave the better correlation with the results of wheel-tracking tests (49, 50, 51). Their explanation is that the outer annulus of the mixture, which is not directly loaded, provides a form of lateral confining pressure to the mixture during the dynamic creep test, and the confining pressure provided is related to the properties of the HMA mixture subjected to testing. A similar approach has been used in developing a mix design in United Kingdom, also (52, 53).

This European method seemed to be quite promising and, hence, was accepted for the preliminary study. A 100 mm diameter loading platen was used for the repeated load axial test and the results of total nine mixtures are plotted in Figure 15. For the purpose of comparison, Table 6 and Figure 16 were drawn, along with the results from the RPT.

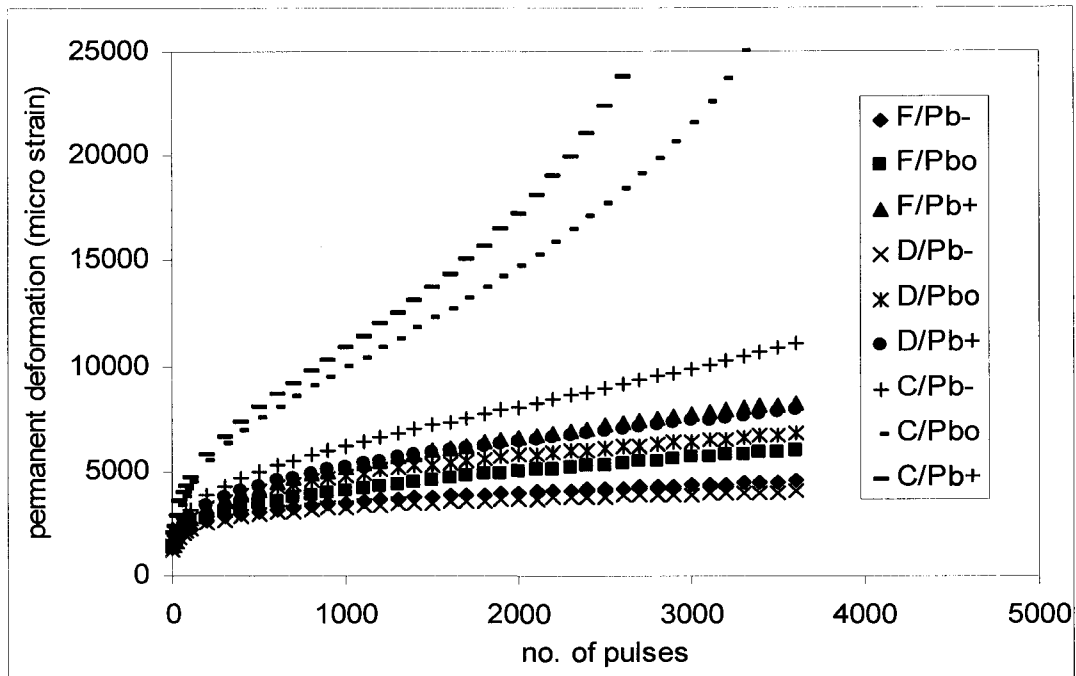


Figure 15. The permanent deformations of nine mixtures from the NAT

Table 6. Comparison of the results from two test methods

Mixture	Micro strain after 3600 pulses (Nottingham Asphalt Tester)		%strain after 300 gyrations @58°C (the proposed RPT)	
	Micro strain	Rank	Percent strain	Rank
F/P _{b-}	4524	2	4.04	2
F/P _{bo}	5997	3	6.47	4
F/P _{b+}	8277	6	7.48	6
D/P _{b-}	4035	1	3.91	1
D/P _{bo}	6777	4	6.40	3
D/P _{b+}	7899	5	6.87	5

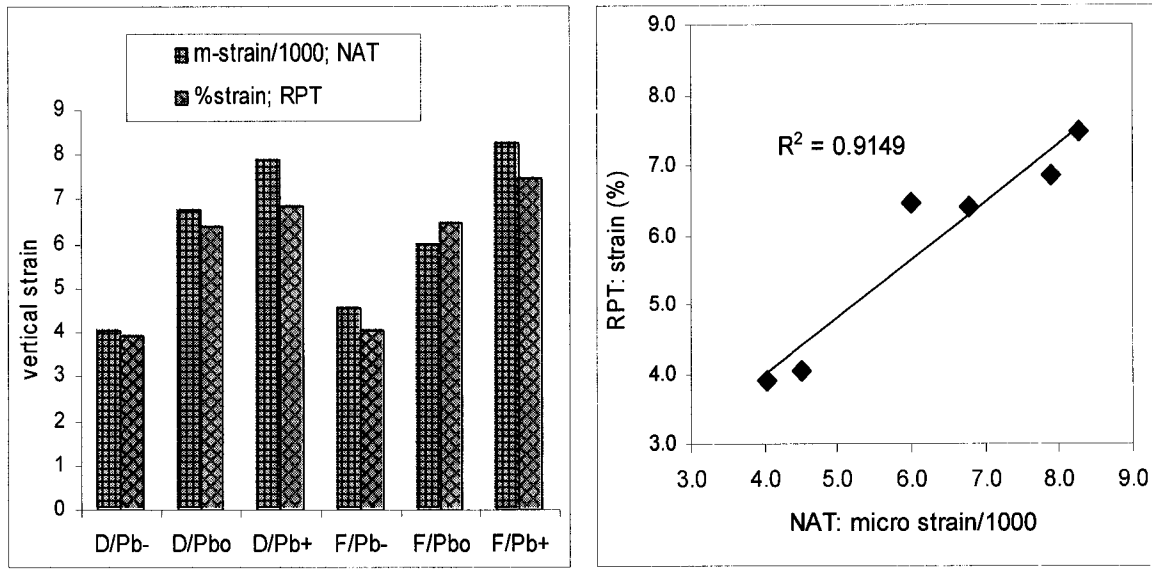


Figure 16. The NAT (micro strain) versus the RPT (%strain)

Two test methods appear to be quite comparable and rank the mixtures almost in the same order, in term of the high temperature performance. The results of the coarse graded mixtures, however, were excluded due to the excessive premature deformation or failure. This led to an interesting discussion on the appropriate degree of confinement for testing HMA mixtures and confirmed the necessity of a confining stress as several researchers pointed out, particularly for coarse/open graded mixtures and stone mastic asphalt (54, 55, 56, 57). There is still a disagreement on this matter, and it will be further discussed in chapter 4.

3.3 Summary

In summary, the major findings through the preliminary study were:

1. The responses of HMA mixtures obtained from the proposed RPT are in good agreement with the general expectation.

2. The proposed test protocol is capable of detecting the sensitivities of HMA mixtures to temperature, asphalt content, and other compositional differences, which indicates the possible use of the RPT for quality control and quality assurance practices.
3. The results demonstrated that the RPT results are compatible with a fundamental test such as the NAT.
4. The proposed RPT has enough potential of being used as an alternative to other simple performance tests to differentiate stable from unstable mixtures and/or rank the mixtures in terms of the permanent deformation susceptibility, during mix design procedure.

4. DESIGN OF EXPERIMENT

After the potential of the RPT using the SGC was investigated through the preliminary study, the test needed to be extended on other representative HMA mixtures being used in asphalt paving construction. It was intended, by doing so, to establish criteria and a practical guide for the RPT to evaluate the performance potential of HMA mixtures.

The design of experiment requires that the sources of variation among the mixtures be identified first. As well recognized, the variations among the mixtures are from aggregate type and gradation, asphalt binder grade (PG), and the design number of gyrations (N_d) because the Superpave mix design allows some variations of aggregate type and gradation, while the optimum asphalt binder content ($P_{b(opt)}$) is selected as the exact amount of asphalt binder providing 4% air voids at N_d , corresponding to the design traffic level.

In central Iowa, surface mixtures typically use a 12.5 mm nominal maximum aggregate size and a PG 58-28 binder. Therefore, it was decided that the major sources of variation in this experiment were 1) the blending proportions of manufactured and natural aggregate, 2) the gradations of blended aggregates, and 3) the design traffic levels (N_d). The experiment was designed for each of three variables to have three levels so that the mixtures tested in this study could embrace a variety of asphalt surface course mixes. In addition to the variables of the mixtures, another interesting variable conceived was the vertical loading pressure of the SGC. Even though 600 kPa (87 psi) is the standard vertical pressure to compact HMA mixtures using the SGC, for the purpose of testing, the pressure can be altered to simulate different tire inflation

pressures, e.g., 689 kPa (100 psi) or 827 kPa (120 psi). In this study, 689 kPa (100 psi) was used, and all twenty seven different types of mixtures shown in Table 7 were tested at two levels of loading pressures (87 psi and 100 psi). Including a replication for each mixture, one hundred eight mixtures in total were tested.

4.1 Material Properties

Two sources of aggregates (manufactured limestone aggregate from Martin Marietta

Table 7. Notations for twenty seven mixtures

Aggregate gradations	Fine aggregate blending proportion	Design traffic level: N_{design}		
		75	100	125
Fine	Man. 100 + Nat. 0	FG/M100+N0/75	FG/M100+N0/100	FG/M100+N0/125
	Man. 75 + Nat. 25	FG/M75+N25/75	FG/M75+N25/100	FG/M75+N25/125
	Man. 50 + Nat. 50	FG/M50+N50/75	FG/M50+N50/100	FG/M50+N50/125
Dense	Man. 100 + Nat. 0	DG/M100+N0/75	DG/M100+N0/100	DG/M100+N0/125
	Man. 75 + Nat. 25	DG/M75+N25/75	DG/M75+N25/100	DG/M75+N25/125
	Man. 50 + Nat. 50	DG/M50+N50/75	DG/M50+N50/100	DG/M50+N50/125
Coarse	Man. 100 + Nat. 0	CG/M100+N0/75	CG/M100+N0/100	CG/M100+N0/125
	Man. 75 + Nat. 25	CG/M75+N25/75	CG/M75+N25/100	CG/M75+N25/125
	Man. 50 + Nat. 50	CG/M50+N50/75	CG/M50+N50/100	CG/M50+N50/125

Aggregates of Ames, Iowa and natural gravel aggregate from Automated Sand and Gravel of Fort Dodge, Iowa) were washed first, to remove dust- and clay-coatings from the aggregate particles. After being oven-dried, the aggregates were sieved and stored into ten standard sieve sizes; 1/2" (12.5 mm), 3/8" (9.5 mm), #4 (4.75 mm), #8 (2.36 mm), #16 (1.18 mm), #30 (0.6 mm), #50 (0.3 mm), #100 (0.15 mm), #200 (0.075 mm), and minus #200 (filler).

In order to select real aggregate gradations, twenty four gradations (Table 8) of recent historical projects conducted in Iowa were reviewed and three representative gradations were selected as shown in Figure 17.

The specific gravities of each of the aggregate blends were measured using the InstroTek Inc., CORELOK, which has been recently introduced to the asphalt industry to determine the specific gravities of HMA mixtures and those of aggregate more efficiently. This device is relatively new, but the superiority of the vacuum sealing method over the conventional water displacement method has already been reported (58). The test results are summarized in Table 9.

Another test performed on aggregates was the fine aggregate angularity shown in Table 10. It needed to be known because the particle shape and surface texture of fine aggregates have a significant effect on resistance to the permanent deformation of HMA mixtures. The test conformed to ASTM C1252, Method A (59). The sand equivalent test was not performed because the aggregates were washed and oven-dried prior to re-blending those to get desired gradations.

Since the coarse aggregate portions of each mix are 100% manufactured aggregate (crushed limestone) which have at least more than two fractured faces, and odd shape aggregates were removed individually during aggregate blending process, consensus

Table 8. Aggregate gradations recently used for asphalt surface course in Iowa

Mix No.	Sieve sizes									
	3/4"	1/2"	3/8"	#4	#8	#16	#30	#50	#100	#200
1BD9-003	100	99	85	54	39	26	16	7.4	3.7	2.7
1BD9-007	100	99	88	56	37	25	16	7.4	3.8	2.9
1BD9-026	100	93	85	54	35	25	15	6.6	4.8	4
4BD8-52	100	93	84	71	47	30	17	8	4.9	4.3
ABD0-301	100	91	83	61	36	22	14	8.3	5.1	3.4
ABD0-5010	100	91	80	60	46	33	21	9.7	5.6	4.4
ABD0-5014	100	99	90	66	49	36	23	13	6.7	4.8
ABD4-2S05	100	96	90	68	48	34	22	10	5.4	3.9
ABD5-2023	100	99	84	64	48	34	23	11	5.9	4.7
ABD8-2001	100	98	94	72	54	45	34	19	8.4	5.1
ABD8-2011	100	93	82	66	50	35	22	11	6.1	4.7
ABD8-3009	100	92	83	72	53	35	22	13	6.9	4.6
ABD8-3014	100	92	82	71	50	34	22	12	6.9	4.6
ABD8-5021	100	94	85	66	54	42	30	16	7.2	5.1
ABD8-5036	100	94	86	66	50	36	24	10	6.5	5.4
ABD9-3001	100	93	84	68	55	41	27	17	10	3.9
ABD9-5019	100	95	87	63	39	26	16	8.2	5.7	4.8
SWI8-18	100	92	86	74	60	41	25	12	6.1	4.1
SWI8-22	100	90	76	51	36	25	16	5.8	4.2	3.7
SWI8-42	100	93	81	63	50	39	29	17	8.3	4.9
SWI9-10	100	96	87	69	50	35	23	12	6.4	4.6
SWI9-38	100	92	84	50	33	26	17	7.4	3.7	3.3
SWI9-44	100	95	90	51	37	26	17	7.7	4	2.9
SWI9-6	100	92	80	63	50	38	25	14	7.5	5.5

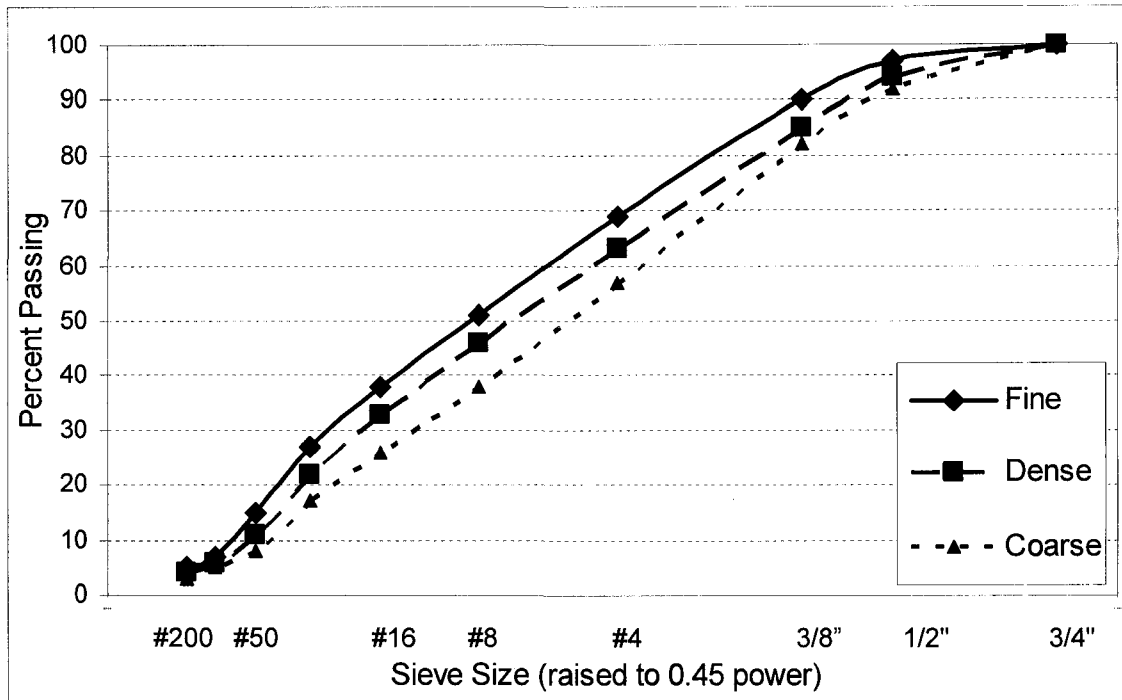


Figure 17. Fine, Dense, and Coarse gradations used in the study

Table 9. The properties of nine aggregate blends

	Fine Gradation			Dense Gradation			Coarse Gradation		
	M100 + N0	M75 + N25	M50 + N50	M100 + N0	M75 + N25	M50 + N50	M100 + N0	M75 + N25	M50 + N50
G_{sa}	2.788	2.772	2.757	2.788	2.774	2.760	2.788	2.775	2.762
G_{sb}	2.639	2.627	2.616	2.639	2.628	2.618	2.639	2.629	2.620
%Abs.	2.03	1.99	1.95	2.03	1.99	1.96	2.03	2.00	1.97
SA	5.929 (m ² /kg)			4.942 (m ² /kg)			3.958 (m ² /kg)		

Table 10. Fine aggregate angularities of three aggregate blends

Aggregate blends	M100 + N0	M75 + N25	M50 + N50
FAA	48.1	46.5	44.6

properties tests for coarse aggregate specified in Superpave system, i.e., coarse aggregate angularity, and flat and elongated particles, were not necessary.

The asphalt binder used in the study was unmodified PG 58-28 binder provided by Koch Materials Company, Dubuque, Iowa. The mixing and compaction temperatures determined using the temperature - viscosity relationship of the asphalt binder by the manufacturer were accepted, and were 150°C and 135°C, respectively. The Superpave binder tests were not necessary as the binder is not a variable in this study.

4.2 Optimum Binder Contents

There have been changes to the original Superpave system based on experience gained during the implementation of the new system and research conducted to enhance the process (60, 61, 62, 63, 64, 65). Two notable changes are,

- 1) The N_{design} table has been simplified from twenty eight to four levels; 50, 75, 100, and 125
- 2) the specimen should be compacted to N_{design} , not N_{max} for the volumetric mix design.

Other changes and the details are well-documented elsewhere (66).

These changes were adopted in this study and the optimum binder contents of nine aggregate blends at three levels of N_d (75, 100, 125) were determined as shown in Table 11. The required numbers of gyrations to achieve 7% air voids or 93% G_{mm} (N^p) in Table 11 were backcalculated as the mixtures should be compacted to those numbers of gyration for the RPT. An air void content of seven percent was selected as a reasonable post-construction density because a recent study conducted at Iowa State University reported that the pooled average of % G_{mm} after field compaction was 93.218 with a

Table 11. Optimum asphalt binder contents ($P_{b(opt)}$) and the number of gyration required to achieve 7% air voids (N')

Mix	Design traffic level: N_{design}					
	75		100		125	
	$P_{b(opt)}$	N'	$P_{b(opt)}$	N'	$P_{b(opt)}$	N'
FG/M100+N0	6.5	31	6.2	40	5.9	48
FG/M75+N25	5.7	29	5.4	38	5.3	49
FG/M50+N50	5.6	28	5.4	35	5.2	41
DG/M100+N0	6.7	34	6.2	41	5.8	50
DG/M75+N25	5.9	31	5.4	39	5.3	47
DG/M50+N50	5.7	28	5.5	34	5.3	41
CG/M100+N0	6.8	34	6.3	44	5.9	53
CG/M75+N25	6.3	33	5.8	41	5.5	48
CG/M50+N50	6.0	31	5.6	38	5.3	46

standard deviation of 1.076, based on the construction data of fifty six HMA paving projects completed in Iowa from 1996 to 1999 (67).

The details of mix designs are attached in Appendix A and Table 12 summarizes the volumetric properties of all twenty seven mixes at their optimum binder contents.

4.3 Tests

The tests in the study were divided into three phases. Phase I was the proposed RPT procedure on the laboratory-prepared mixtures in Table 7 at vertical pressure of 600

Table 12. Volumetrics and other properties of twenty seven mixes at $P_{b(opt)}$

N_d	Mix	P_{be}^a	VMA ^b	VFA ^c	F/B ^d	FT ^e	Compaction curve	
							%G _{mm} @N _{ini}	slope
75	FG/M100+N0	5.715	15.8	74.6	0.88	9.6	87.7	3.449
	FG/M75+N25	4.679	13.7*	70.7	1.07	7.9**	88.2	3.221
	FG/M50+N50	4.704	13.7*	70.8	1.06	7.9**	88.7	3.023
	DG/M100+N0	5.732	15.8	74.7	0.70	11.6	87.0	3.677
	DG/M75+N25	4.983	14.2	71.8	0.80	10.1	87.9	3.318
	DG/M50+N50	4.854	13.9*	71.3	0.82	9.8	88.5	3.094
	CG/M100+N0	5.883	15.9	74.9	0.51*	14.9	86.7	3.858
	CG/M75+N25	5.428	14.9	73.2	0.55*	13.7	87.2	3.660
	CG/M50+N50	5.093	14.4	72.2	0.59*	12.9	87.6	3.454
100	FG/M100+N0	5.337	15.7	74.5	0.94	9.0	87.3	3.414
	FG/M75+N25	4.396	13.7*	70.9	1.14	7.4**	87.9	3.215
	FG/M50+N50	4.470	13.8*	71.1	1.12	7.5**	88.4	2.994
	DG/M100+N0	5.265	15.5	74.1	0.76	10.7	86.9	3.602
	DG/M75+N25	4.493	13.8*	71.0	0.89	9.1	87.7	3.296
	DG/M50+N50	4.602	14.0	71.4	0.87	9.3	88.4	3.048
	CG/M100+N0	5.383	15.7	74.5	0.56*	13.6	86.4	3.790
	CG/M75+N25	4.992	14.8	73.0	0.60	12.6	87.0	3.544
	CG/M50+N50	4.689	14.2	71.9	0.64	11.8	87.6	3.334
125	FG/M100+N0	5.109	15.7	74.5	0.98	8.6	87.2	3.380
	FG/M75+N25	4.266	14.0	71.4	1.17	7.2**	87.9	3.177
	FG/M50+N50	4.269	13.9*	71.1	1.17	7.2**	88.4	2.973
	DG/M100+N0	4.907	15.3	73.9	0.82	9.9	86.8	3.530
	DG/M75+N25	4.325	14.0	71.3	0.93	8.8	87.6	3.268
	DG/M50+N50	4.394	14.1	71.6	0.91	8.9	88.3	3.010
	CG/M100+N0	5.024	15.5	74.2	0.60	12.7	86.3	3.727
	CG/M75+N25	4.671	14.8	72.9	0.64	11.8	87.0	3.424
	CG/M50+N50	4.428	14.2	71.8	0.68	11.2	87.5	3.286

^a P_{be} = effective binder content^b VMA = Voids in Mineral Aggregate^c VFA = Voids Filled with asphalt binder^d F/B = Filler to Bitumen ratio^e FT = Film Thickness

* fails Superpave Spec.

** fails Iowa DOT Spec.

kPa (87 psi) and 689 kPa (100 psi). The procedure was identical to the test protocol described in the previous chapter and 108 mixtures were tested in this phase.

In order to avoid any possible systematic error during this long period of experiment, involving a large number of testing, the testing order was randomized as shown in Table 13. The randomized order was generated by the statistical analysis program, SAS, and, for the efficiency of testing, the experiment was treated as a randomized block design (RBD), rather than the completely randomized design (CRD).

Phase II was testing the laboratory-prepared mixtures using the Nottingham Asphalt Tester (NAT) to evaluate the test results of the RPT. The mixtures subjected to the NAT test were nine mixes of $N_a = 100$ in Table 7. Unlike the preliminary study, a confining stress of 20 kPa was applied and the test conditions used are shown in Table 14.

Table 13. The randomized testing order

Blocks	Experiment Units		
	1	2	3
1	FG / M100+N0 / 125	FG / M100+N0 / 75	FG / M100+N0 / 100
2	CG / M50+N50 / 100	CG / M50+N50 / 75	CG / M50+N50 / 125
3	FG / M75+N25 / 75	FG / M75+N25 / 125	FG / M75+N25 / 100
4	CG / M100+N0 / 125	CG / M100+N0 / 75	CG / M100+N0 / 100
5	CG / M75+N25 / 100	CG / M75+N25 / 75	CG / M75+N25 / 125
6	DG / M50+N50 / 125	DG / M50+N50 / 75	DG / M50+N50 / 100
7	DG / M100+N0 / 100	DG / M100+N0 / 125	DG / M100+N0 / 75
8	DG / M75+N25 / 125	DG / M75+N25 / 75	DG / M75+N25 / 100
9	FG / M50+N50 / 100	FG / M50+N50 / 75	FG / M50+N50 / 125

Table 14. Test conditions for the confined repeated load axial test

Temp. (°C)	Number of pulse	Pulse frequency (Hz)	Test stress (kPa)	Conditioning stress (kPa)	Conditioning period (second)	Test period (hrs)
40	10000	0.5	$\sigma_1 = 300$ $\sigma_3 = 20$	10	120	6

As discussed earlier, there has been no consensus on the appropriateness of the application of confining stress or the level of confinement for the creep test. However, it has been noted that unconfined tests occasionally result in excessive deformation or premature failure of the mixture (particularly for coarse or open graded mixtures), which makes the analysis of the test results difficult, and zero confining pressure ($\sigma_3 = 0$) does not appear to be an appropriate test condition. On the other hand, the application of confinement has a significant positive effect on the deformation, which reduces the magnitude of permanent deformation or may even overestimate the performance of the mixture (55).

Close attention, hence, was paid to the selection of the confining stress and 20 kPa was adopted because, as shown in Figure 18, the dynamic creep test conducted on identical mixtures but different at levels of confinement showed the confining stress has a significant effect on the deformation characteristics of the mixtures, but further increases of σ_3 , more than 17 kPa do not make significant differences. It was preferred to apply the minimum confining stress necessary not to underestimate or overestimate the mixture.

Prior to the NAT testing, each end of the specimen compacted to 7% air voids was

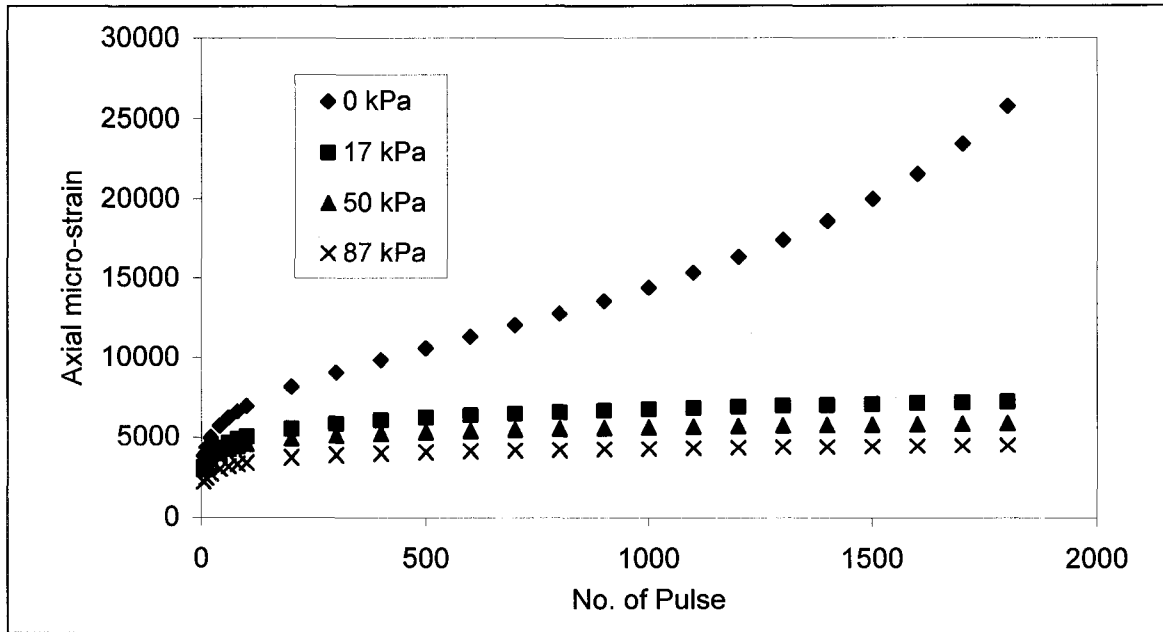


Figure 18. Effect of confining stress on the deformations of identical mixtures

sawn and silicon-Teflon grease was applied on the top and the bottom of the specimen to minimize the end restraints resulting from the friction between the loading platens and the surfaces of the specimen. All mixtures were preconditioned in the temperature controlled cabinet for at least five hours to ensure that the uniform thermal equilibrium was achieved throughout the specimen at the test temperature. The height of each specimen was consistently 100 mm.

In phase III, the RPT was performed again, but on the field samples provided by Iowa Department of Transportation (DOT). The mixtures were plant-mixed samples, collected on asphalt paving project sites during 2002 construction season. Figure 19 and Table 15 show the properties of the field samples as appeared in the Job Mix Formula (JMF) of each mix. Phase III involved the cooperation and support from Iowa DOT bituminous materials section because their knowledge and experience on those mixtures

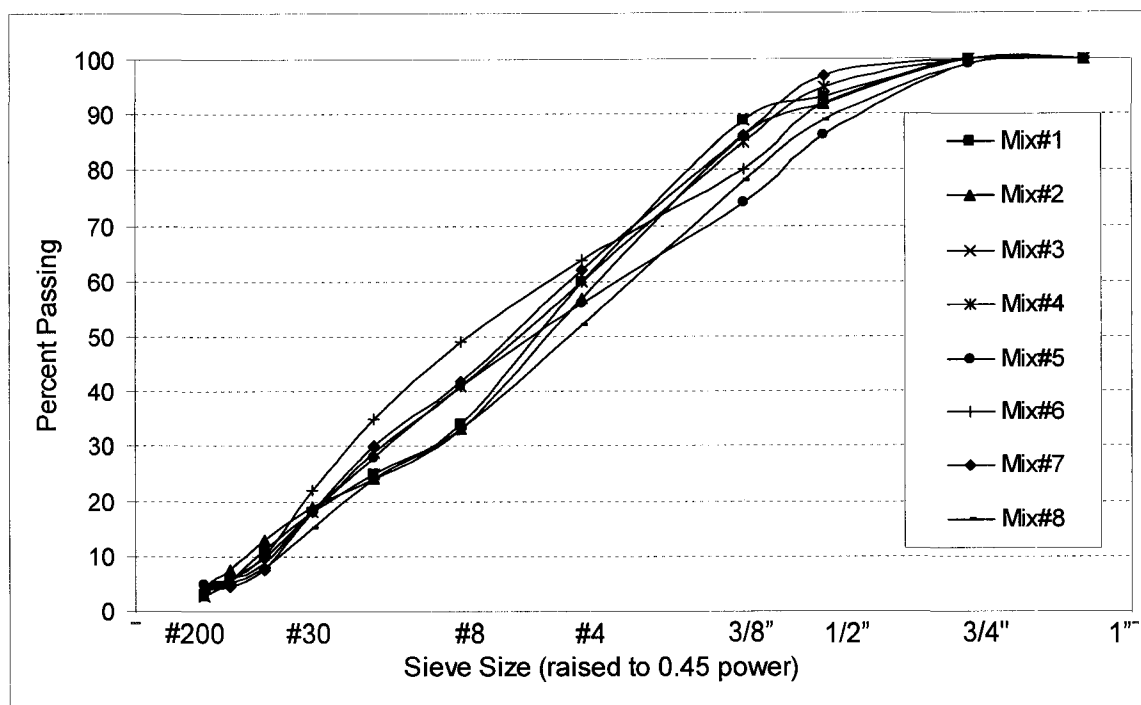


Figure 19. JMF gradations of field samples provided by Iowa DOT

Table 15. The properties of field samples from JMFs

Mix No.	JMF Mix no.	PG	N_d	$P_{b(opt)}$	VMA	VFA	F/B	FT
# 1	3BD2-3013	70-28	109	5.1	15.2	73.7	0.57	12.1
# 2	3BD2-3012	70-28	109	5.6	15.4	74.2	0.90	10.0
# 3	3BD2-3013'	70-28	109	5.1	15.2	73.7	0.57	12.1
# 4	Benton '02 R1	58-28	68	6.4	15.8	81.3	0.78	12.1
# 5	ABD2-5014	64-22	109	5.4	14.2	72.0	1.08	9.2
# 6	SWI2-31	64-22	86	5.4	15.8	74.7	0.91	10.0
# 7	ABD2-2032	58-28	86	5.8	14.1	71.7	0.89	10.2
# 8	ABD2-2006	58-28	76	4.7	12.9	72.7	1.09	9.5

was crucial for analyzing the test results of this phase. The scheme of Phase III was an alternative to the field verification of the proposed RPT without the long-term field observation. Also, the results of this phase can be independently used to establish or calibrate the criteria of the RPT, differentiating good from bad mixtures.

5. ANALYSIS OF TEST RESULTS AND DISCUSSION

This chapter deals with tests conducted in this study (the RPT and the NAT) and the results from each test in detail. First, twenty seven different types of laboratory-fabricated mixtures were subjected to the proposed RPT at two levels of loading pressure (87 psi and 100 psi). Secondly, the NAT testing was conducted on nine types of mixtures used for the RPT testing to evaluate the RPT test results. The last testing was the RPT on the field samples provided by Iowa DOT and it was necessary to calibrate the RPT criteria established based on the test results of laboratory samples.

Prior to the RPT and the NAT testing, there was one further factor that to be examined. That was the repeatability of the proposed RPT. The repeatability of a test method is crucial due to the inherent variations of HMA mixtures. Six samples of DG/M75+N25 (Table 7) mixed with 5.0% asphalt content were subjected to 30 gyrations at 135°C to achieve 7% air voids. After the conditioning period, the samples were re-positioned in the SGC with the indenter on top.

Figure 20 shows the RPT results conducted on six identically prepared mixtures. It shows that at 2% strain, the mean number of gyration is fifty five and the standard deviation of six tests is two, which is quite small enough, indicating a good repeatability of the RPT. It can be also seen that the repeatability became worse as the number of gyrations increased especially beyond 100 gyrations. The scatter of data can be explained by the randomly distributed air voids and different orientations and arrangements of aggregates skeleton of the samples for all that the samples were prepared identically. Therefore it was suggested that the results of interest from the RPT be in the range of less than 100 gyrations.

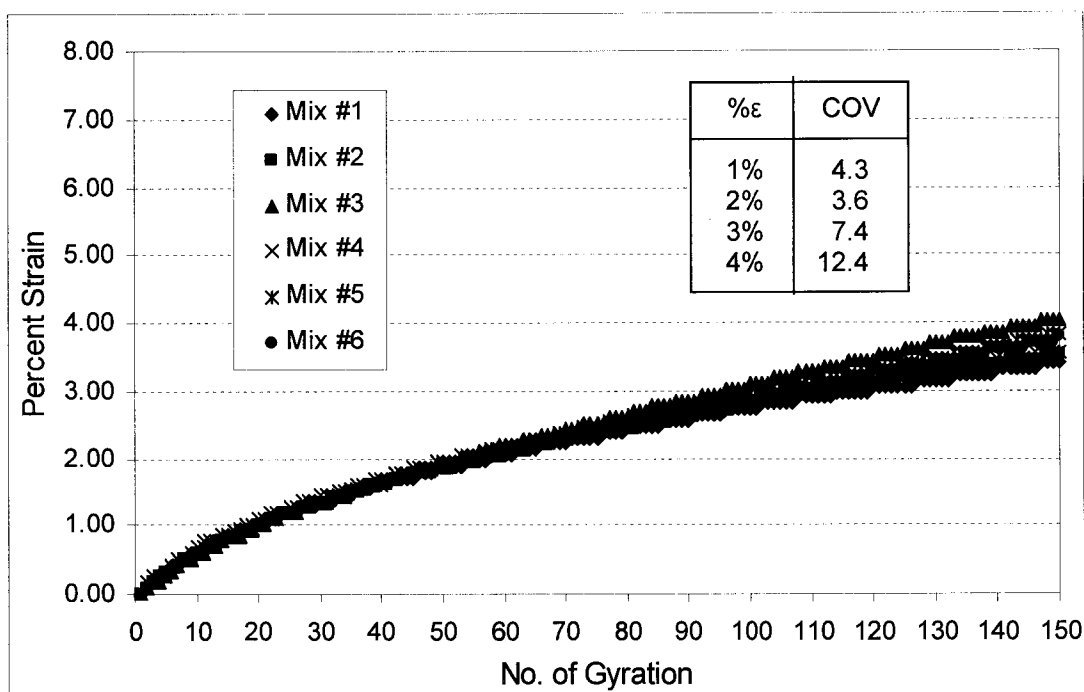


Figure 20. Repeatability of the proposed RPT

5.1 The RPT on Laboratory-Fabricated Samples

As described in the previous chapter, one hundred eight samples were prepared and tested in accordance with the RPT test protocol proposed in this study. Four samples for each of twenty seven mixes in Table 7 were prepared and two samples of each mix were tested at vertical loading pressure of 600 kPa (87 psi) and the other two were tested at 689 kPa (100 psi).

Figure 21, 22, and 23 shows the deformation (percent strain, % ϵ) vs. N curves of each mix tested at 600 kPa (87 psi) and Table 16 summarizes test results at selected numbers of gyrations, i.e., N = 50, 100 and 300. As seen in those figures, % ϵ from the RPT shows the typical relationship between the deformation and loading number, i.e., initially, the strain rate decreases with loading number (primary deformation), and then

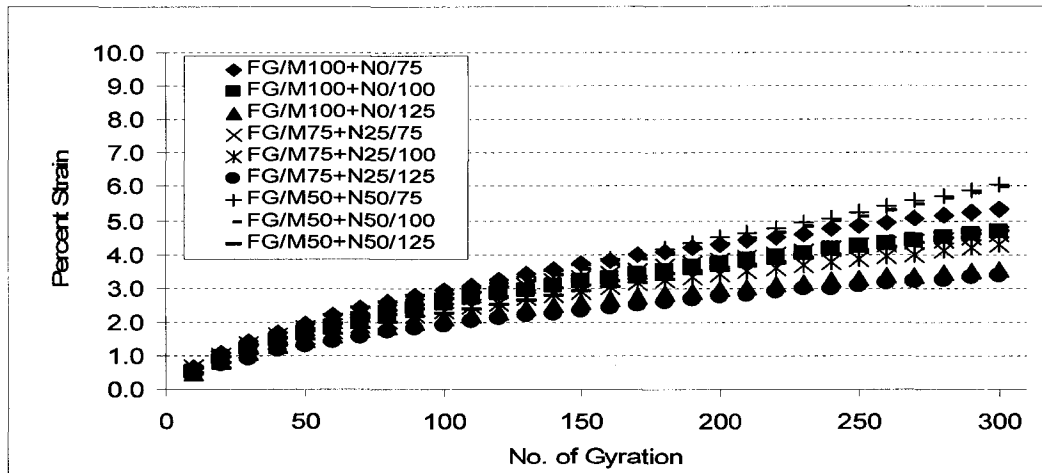
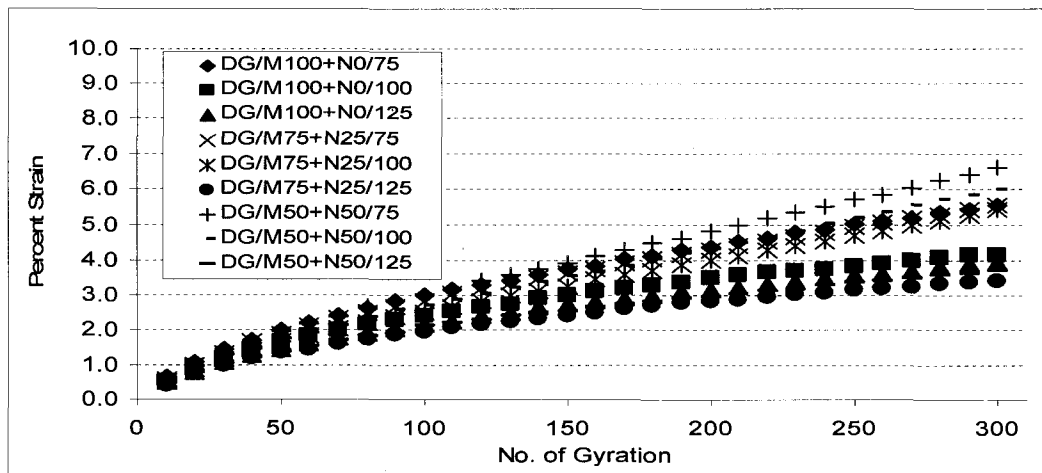
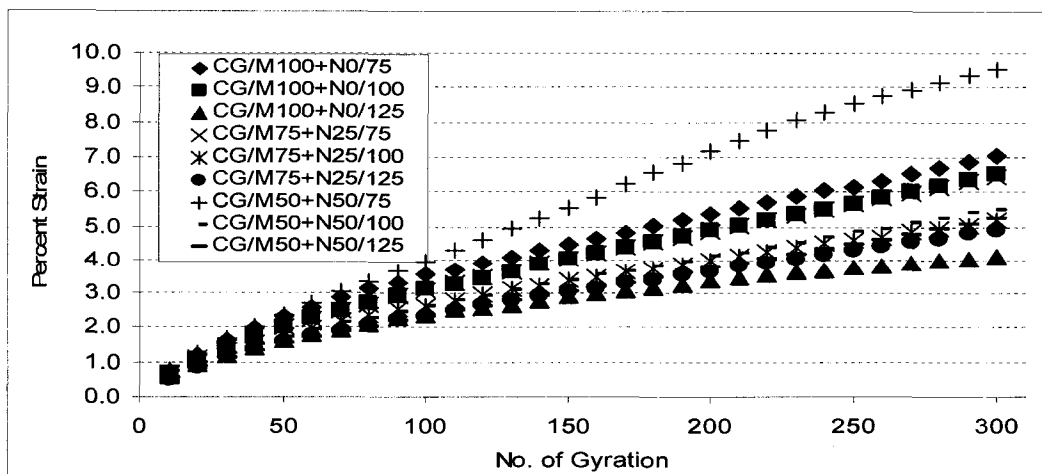
Figure 21. % ϵ vs. N curves of FG mixesFigure 22. % ϵ vs. N curves of DG mixesFigure 23. % ϵ vs. N curves of CG mixes

Table 16. Percent strains (% ϵ) of twenty seven mixes

Mix	p = 87 psi			p = 100 psi		
	N = 50	N = 100	N = 300	N = 50	N = 100	N = 300
FG/M100+N0/75	1.941	2.954	5.317	2.159	3.259	5.926
FG/M100+N0/100	1.694	2.541	4.659	1.829	2.765	5.018
FG/M100+N0/125	1.451	2.134	3.543	1.553	2.286	3.883
FG/M75+N25/75	1.816	2.660	4.603	1.920	2.858	5.121
FG/M75+N25/100	1.570	2.334	4.286	1.744	2.680	5.359
FG/M75+N25/125	1.286	1.886	3.385	1.426	2.117	3.715
FG/M50+N50/75	1.820	2.835	6.052	1.886	2.915	5.744
FG/M50+N50/100	1.525	2.341	4.010	1.598	2.419	4.779
FG/M50+N50/125	1.459	2.231	4.676	1.515	2.338	4.978
DG/M100+N0/75	1.982	2.994	5.567	2.077	3.332	8.049
DG/M100+N0/100	1.656	2.420	4.160	1.894	2.755	5.080
DG/M100+N0/125	1.447	2.170	3.956	1.563	2.388	4.429
DG/M75+N25/75	1.850	2.816	5.548	2.149	3.309	7.048
DG/M75+N25/100	1.648	2.494	5.452	1.796	2.779	5.601
DG/M75+N25/125	1.361	1.957	3.403	1.464	2.238	4.004
DG/M50+N50/75	1.955	2.975	6.631	2.281	3.573	8.222
DG/M50+N50/100	1.748	2.687	6.013	1.910	2.994	6.986
DG/M50+N50/125	1.372	2.100	3.686	1.726	2.545	4.788
CG/M100+N0/75	2.320	3.543	7.043	2.659	4.136	8.652
CG/M100+N0/100	2.019	3.113	6.522	2.237	3.503	7.555
CG/M100+N0/125	1.617	2.341	4.128	1.747	2.642	5.071
CG/M75+N25/75	2.031	3.089	6.432	2.434	3.843	8.753
CG/M75+N25/100	1.777	2.624	5.205	1.970	3.041	6.167
CG/M75+N25/125	1.570	2.334	4.881	1.837	2.820	5.982
CG/M50+N50/75	2.373	3.942	9.536	2.539	4.232	10.283
CG/M50+N50/100	1.701	2.636	5.486	1.830	3.021	7.745
CG/M50+N50/125	1.528	2.335	5.222	1.907	3.008	6.821

the strain rate is almost constant (secondary deformation). Tertiary flow (increasing strain rate) was not observed because of the limited number of gyrations.

Figure 23 reveals that there are some mixes showing significantly larger deformation than others. After reviewing the volumetrics of twenty seven mixes, it was found that four mixes do not meet all the criteria of Superpave mix design. Those mixes are CG/M100+N0/75, CG/M100+N0/100, CG/M75+N25/75, and CG/M50+N50/75, and their filler to bitumen ratios range from 0.5 to 0.59, which are less than the 0.6 minimum value specified in Superpave. When the mixture has a very low filler to bitumen ratio, the binder mastic is relatively soft and the mixture is likely to have high film thickness, increasing the permanent deformation susceptibility of HMA mixtures. The four mixes that do not satisfy the criteria of Superpave were excluded from the analysis of test results because they are not realistic mixtures.

Using the $\% \varepsilon$ at 100 gyrations, a statistical analysis was conducted (Table 17), and it shows the main factors (aggregate gradation, blending proportion of fine aggregate, N-design, and loading pressure) have a significant effect on the test results at $\alpha = 0.05$. The result indicates that the RPT proposed in this study has a good sensitivity to the mixture properties and has a capability of differentiating various HMA mixtures.

The responses of twenty seven mixes obtained from the RPT were generalized by comparing the mean responses for each main factor. As shown in Table 18, fine-graded (FG) mixes have better permanent deformation resistance than dense- and coarse-graded (DG and CG) mixes, which can be explained by more contact points of aggregate interlock and relatively thin asphalt film coating aggregate particles. These facts emphasize the role of asphalt binder mastic on the high temperature performance of HMA mixtures, and that it can be improved by slightly increasing the filler content or

Table 17. ANOVA for percent strains (%ε) from the RPT at N = 100

Source	Type III Sum of Squares	df	Mean Square	F - statistic	p - value
Gradation (G)	1.313	2	0.656	59.746	0.000
Fine aggr. blending proportion (FA)	0.321	2	0.160	14.592	0.000
N-Design (N _d)	8.203	2	4.102	373.355	0.000
Loading pressure (P)	2.180	1	2.180	198.474	0.000
G * FA	0.275	4	0.069	6.261	0.000
G * N _d	0.303	3	0.101	9.183	0.000
FA * N _d	0.111	4	0.028	2.536	0.053
G * FA * N _d	0.085	5	0.017	1.547	0.194
G * P	0.330	2	0.165	15.009	0.000
FA * P	0.016	2	0.078	0.710	0.497
G * FA * P	0.171	4	0.043	3.897	0.008
N _d * P	0.055	2	0.027	2.497	0.093
G * N _d * P	0.022	3	0.007	0.671	0.574
FA * N _d * P	0.073	4	0.018	1.659	0.176
G * FA * N _d * P	0.029	5	0.006	0.528	0.754
Error	0.505	46	0.011		
Total	13.546	91			

decreasing the film thickness, or using the modified binder.

Another notable finding is that M75+N25 mixes are better, or at least not inferior to M100+N0 mixes. Since the fine aggregate angularity of M100+N0 and M75+N25 mixes

Table 18. Mean percent strains for each factor at N = 100

Factors	Mean	Number of sample	Std. Deviation
Gradation			
Fine	2.555	36	0.356
Dense	2.696	36	0.453
Coarse	2.680	20	0.285
Fine aggr. blending proportion			
M100+N0	2.642	28	0.382
M75+N25	2.559	32	0.393
M50+N50	2.712	32	0.379
N-Design			
75	3.040	24	0.271
100	2.686	32	0.220
125	2.326	36	0.288
Loading pressure			
87 psi	2.484	46	0.324
100 psi	2.790	46	0.385

are 48.1 and 46.5, respectively, and that of M50+N50 is 44.6, it seems feasible to use 45.0 as a cut-off value, as specified in Superpave mix design. The responses to the other two main factors, N-design and loading pressure, show good agreement with their expectation; % ϵ increases with decreasing N-design and increasing loading pressure.

It is interesting to note that the correlation coefficient between % ϵ at N = 100 and the compaction characteristics of the mixtures were very poor (0.06 for the slope and 0.37 for the intercept). This confirms the fact found in the literature that compaction characteristics are not good indicators of performance.

Regression analysis was performed on the data, $\% \epsilon$ at $N = 100$, obtained from the RPT with loading pressure of 600 kPa (87 psi). It was hypothesized that $\% \epsilon$ is a function of aggregate properties, N-design and effective binder content, thus the model is

$$\% \epsilon @ N_{100} = 10.4 - 0.0112 \times N_d - 1.033 \times FM - 0.0909 \times FAA + 0.197 \times FT \quad (3)$$

where, N_d = Design number of gyrations (75, 100, 125)

FM = Fineness Modulus

FAA = Fine Aggregate Angularity (ASTM C1252, Method A)

FT = Film Thickness, $P_{be} \times 10 / SA$, in microns, at optimum binder content

As shown in Figure 24, the regression model predicts $\% \epsilon$ of various mixes very close to those observed in this study, and the regression model derived from forty six observations has R-square of 0.90 and predicts (Table 19).

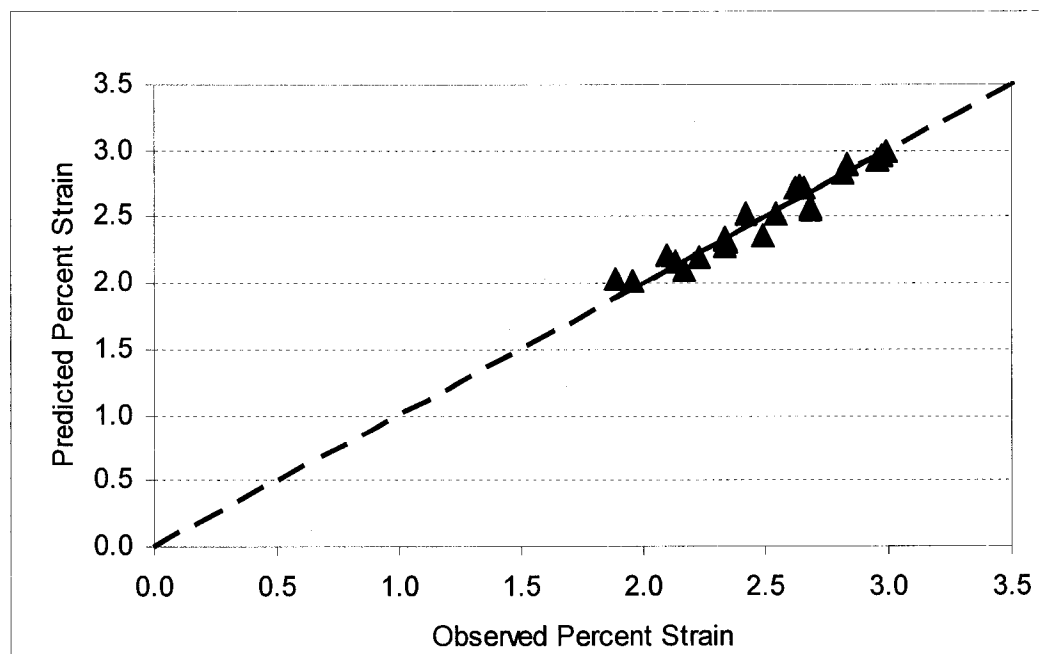


Figure 24. Observed vs. predicted percent strain at N=100

Table 19. Regression results for % ϵ

A. Model Summary					
R	R Square	Adjusted R Square	Std. Error of the Estimate		
0.950	0.903	0.894	0.106		
B. ANOVA					
	Sum of Squares	df	Mean Square	F - statistic	p - value
Regression	4.280	4	1.070	95.980	0.000
Error	0.457	41	0.011		
Total	4.737	45			
C. Coefficients					
	Coefficients	Std. Error	t - statistic	p - value	
Constant	10.400	1.434	7.250	0.000	
FM	-1.033	0.256	-4.032	0.000	
FAA	-0.0909	0.018	-5.008	0.000	
N _d	-0.0112	0.001	-10.329	0.000	
FT	0.197	0.037	5.383	0.000	

Fineness modulus was used to account for aggregate gradation and film thickness for interactions between aggregate skeleton and binder contents. The model can be further expanded to be applicable to all types of mixes if various coarse aggregate properties and several types of asphalt binder will be examined.

5.2 The NAT on Laboratory-Fabricated Samples

For the purpose of evaluating the RPT test results, same mixes subjected to the RPT were tested by the dynamic creep test using the NAT with confining pressure of 20 kPa.

Test conditions are described in Table 14.

Nine mixes of $N_d = 100$ in Table 7 were subjected to ten thousand loading pulses and the results are shown in Figure 25. At the beginning of the test, the mixes experience primary deformation and after about 2,500 pulses, secondary deformation starts.

It was found that the comparison between the RPT and the NAT in terms of ranking nine mixes does not show a good correlation (correlation coefficient = 0.45, Table 20). However, it was because the differences among the NAT testing results are too small to be differentiated or ranked, which is evidenced by the ANOVA showing that none of the factors has a significant effect on the results (Table 21). This less sensitivity of the NAT testing to the factors than the RPT results from the different loading conditions of the two tests. During the RPT test, the mixture experiences continuously applied vertical pressure of 600 kPa with 1.25 degree of gyration angle. Moreover, there is annular

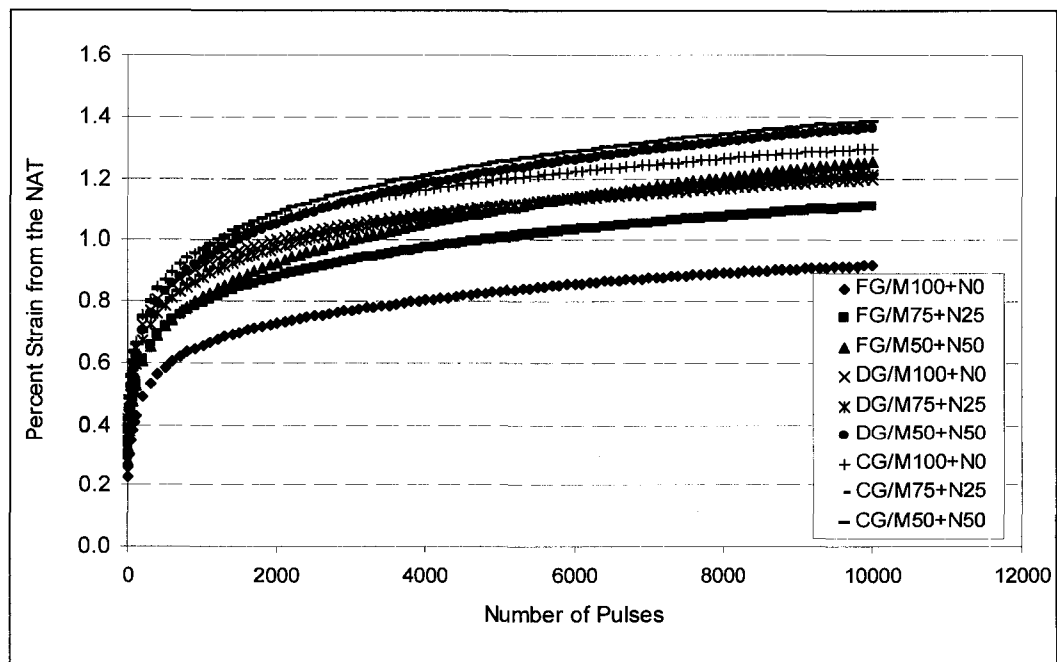


Figure 25. Percent strains of nine ($N_d=100$) mixes from the NAT

Table 20. Comparison of the results (the NAT vs. the RPT)

Mixture ($N_d = 100$)	Percent strain after 10000 pulses (Nottingham Asphalt Tester)		Percent strain after 100 gyrations (the proposed RPT)	
	Percent strain	Rank	Percent strain	Rank
FG/M100+N0	0.918	1	2.541	4
FG/M75+N25	1.110	2	2.334	1
FG/M50+N50	1.254	6	2.683	7
DG/M100+N0	1.197	3	2.420	2
DG/M75+N25	1.213	5	2.494	3
DG/M50+N50	1.363	8	2.687	8
CG/M100+N0	1.297	7	3.113	9
CG/M75+N25	1.211	4	2.624	5
CG/M50+N50	1.384	9	2.636	6

Table 21. ANOVA for percent strains (% ϵ) from the NAT at N = 10000

Source	Type III Sum of Squares	df	Mean Square	F - statistic	p - value
Gradation (G)	0.140	2	0.070	3.086	0.095
Fine aggr. blending proportion (FA)	0.129	2	0.065	2.845	0.110
G * FA	0.049	4	0.012	0.527	0.719
Error	0.204	9	0.023		
Total	0.521	17			

space around the indenter, which allows the mixture to deform with considerable freedom. In contrast, during the confined dynamic creep test using the NAT, 300 kPa loading pulses (one second's loading and one second's rest period) are uniformly applied to the top of the mixture while the mixture is surrounded by the confining pressure of 20 kPa.

The ANOVA in Table 21 suggests that the NAT results need to be more generalized to be compared with the RPT results, and as shown in Table 22, FG mixes are superior to DG or CG mixes, while DG and CG mixes are comparable. Also, M75+N25 mixes show no inferiority to M100+N0 mixes. The same findings were observed with the results from the RPT, as mentioned earlier (Table 18).

Although it is reasonable to make comparisons based on the trends of responses from both tests, further analysis, t-test (Table 23), conducted on the NAT data indicates that there are no differences among the nine mixes; the nine well-designed mixes are

Table 22. Mean percent strains for each factor at N = 10000

Factors	Mean	Number of sample	Std. Deviation
Gradation			
Fine	1.094	6	0.225
Dense	1.258	6	0.104
Coarse	1.297	6	0.121
Fine aggr. blending proportion			
M100+N0	1.137	6	0.194
M75+N25	1.178	6	0.088
M50+N50	1.334	6	0.182

Table 23. p - values of t - test ($\alpha = 0.05$)

	FG/ M75 +N25	FG/ M50 +N50	DG/ M100 +N0	DG/ M75 +N25	DG/ M50 +N50	CG/ M100 +N0	CG/ M75 +N25	CG/ M50 +N50
FG/ M100+N0	0.270	0.414	0.145	0.148	0.161	0.087	0.239	0.107
FG/ M75+N25	-	0.659	0.428	0.429	0.091	0.170	0.347	0.200
FG/ M50+N50	-	-	0.852	0.896	0.724	0.887	0.887	0.671
DG/ M100+N0	-	-	-	0.873	0.143	0.331	0.863	0.408
DG/ M75+N25	-	-	-	-	0.220	0.459	0.979	0.366
DG/ M50+N50	-	-	-	-	-	0.447	0.140	0.900
CG/ M100+N0	-	-	-	-	-	-	0.357	0.643
CG/ M75+N25	-	-	-	-	-	-	-	0.424

expected to perform equally, regardless of the variations in their compositional properties and volumetrics. Therefore it is more appropriate to group the RPT data for each N-design and to assume that the performance potentials of those mixes within each group are of the same rank or equivalent. Table 24 shows the pooled responses of twenty seven mixes to the RPT after 100 gyrations with loading pressure of 600 kPa (87spi).

5.3 The RPT on Plant-Mixed Samples

Iowa Department of Transportation (DOT) provided eight plant-mixed samples for this study and those field samples were collected from seven asphalt paving project sites

Table 24. The pooled average % ϵ from the RPT after 100 gyrations

N-design	Mean	Std. Deviation	Confidence Interval ($\alpha = 0.05$)	
			Lower Limit	Upper Limit
75	2.873	0.129	2.791	2.955
100	2.552	0.137	2.479	2.625
125	2.165	0.181	2.075	2.255

during 2002 construction season. The JMF mix properties are described in Figure 19 and Table 15.

It should be mentioned that the Iowa DOT had been requested to provide a set of mixtures representing a wide range of performance. This was intended to be a “blind” test, where the Iowa State University researchers were not to be told which mixture had shown whatever performance. Unfortunately, the Iowa DOT provided only “random” samples and later suggested that with in-place QC/QA procedures, bad mixtures do not happen. Thus, instead of testing a set of mixtures representing a wide range of performance, the researchers had only a random set of “normal” mixtures to test.

Table 25 summarizes the RPT results on those field samples and shows that the means and standard deviations are larger than those of laboratory mixes. The within-variations of field mixes were expected to be larger as many variations and uncertainties are involved during construction, while laboratory mixes are tightly controlled during fabrication. However, it was somewhat surprising that none of the mixes provided by Iowa DOT had a smaller deformation than laboratory mixes. An appropriate explanation cannot be made here because the properties of field samples

Table 25. The responses of eight field samples to the RPT

Sample No.	Mix No.	N design	N for 7% air voids	%ε at N = 100	
				mean	standard deviation
# 1	3BD2-3013	109	45	5.082	0.135
# 2	3BD2-3012	109	48	3.113	0.008
# 3	3BD2-3013'	109	45	3.988	0.551
# 4	BENTON '02 R1	68	21	5.486	0.497
# 5	ABD2-5014	109	44	3.616	0.416
# 6	SWI2-31	86	32	3.809	0.093
# 7	ABD2-2032	86	36	4.593	0.738
# 8	ABD2-2006	76	29	4.763	0.220

available are only those described on their JMFs and the mixes in production are not same as JMF mixes. The difference between field mixes and laboratory mixes are illustrated in Figure 26. It should be emphasized that sample #1 and #3 are from the same project site, but collected on different dates, therefore those mixes are supposed to have same deformation or very close to each other. As seen in Figure 26, the results of two samples are quite different, which indicates the potential use of the RPT for QC/QA program.

It is important to note that the larger deformations observed on the field samples does not necessarily mean that they are of poor quality or that their performance will be unsatisfactory at this point. It would rather imply that the criteria developed by testing laboratory-fabricated samples needs to be adjusted based on the field observations. It

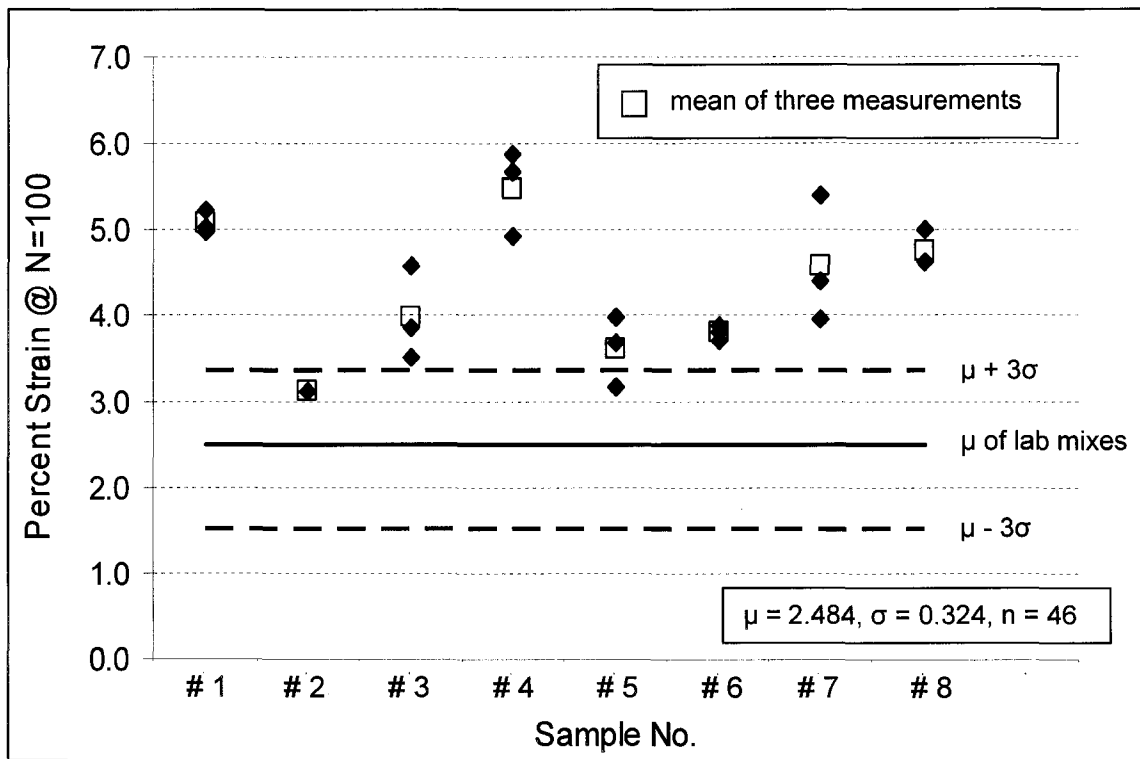


Figure 26. % ϵ (at N=100) of field samples compared with laboratory mixes

would be, however, more convenient to test reference mixes that have been used in full scale road tests or known-performance mixes locally available to establish and validate the criteria.

6. CONCLUSIONS AND RECOMMENDATIONS

This study was initiated to meet the increasing demand for a simple performance test to compliment Superpave mix design (Level I). It has been believed that the current mix design, which entirely depends on the volumetric properties of HMA mixtures, is not quite sufficient to ensure the performance of the mixture. In this study, the lessons from Superpave Level II and Level III mix design have been kept in mind that if the test requires expensive new equipment and complicated procedures, it fails to pass the “practicality” test among the asphalt paving industry, no matter how accurate and rational the test is. Therefore the objective of this study was to develop a performance test for Superpave HMA mixtures that is quick and easy to perform so that it can be routinely used during mix design and during construction, to differentiate stable from unstable mixtures.

The test method proposed in this study, Rapid Performance Test (RPT) utilizes the Superpave Gyrotory Compactor (SGC) as it is, and the only accessory to perform the RPT is the indenter, which can be easily manufactured at a cost of \$100 – \$200. The RPT should be performed at the in-service pavement temperature to which the mixture will be exposed during its design life, not at the conventional laboratory compaction temperature.

The study has been focused on introducing sound rationale of the RPT and mainly examined the potential of the RPT by testing various HMA mixtures being used in Iowa. Also, the proposed RPT was evaluated by comparing with the dynamic creep test using the Nottingham Asphalt Tester (NAT).

6.1 Conclusions

Based on the experiments conducted in this study, several findings have been observed.

1. The responses of HMA mixtures obtained from the RPT are in good agreement with the general expectations and experience.
2. The RPT is capable of detecting the sensitivities of mixtures to temperature, asphalt content, and compositional variations.
3. Test results from the RPT correlate well with those from the repeated load axial test (unconfined dynamic creep test) using the NAT.
4. Stability Indices (SI) appear to be an effective means to determine the performance potential of mixtures, however, they should be further validated before implementation.

In general, it is concluded that the RPT has a good potential of evaluating the performance of Job Mix Formula (JMF) mixes during mix design and examining the acceptability of the modifications often made to the initial JMF during construction. Also, the RPT is a useful tool to control daily productions of HMA.

6.2 Discussion

Although the study has shown that the RPT is an implementable and effective tool for HMA mix design and quality control, there are still a few comments that should be made.

A major drawback of this method might be the lack of analytical justification, which had to be assumed in order to develop a practical test (so called a quick-and-dirty method), not a fundamental test. However, the development of the RPT proposed in this study is based on a sound rationale which can be explained by Prandtl's theory.

In 1921, Prandtl introduced a solution to the problem of the indentation of a rigid solid into a continuous, semi-infinite, homogeneous and isotropic medium, which has formed the basis of bearing capacity theories being used in soil mechanics (68). Also the applications of this theory to pavement structures have been proposed many times by pavement engineers (69, 70, 71). Figure 27 depicts Prandtl's failure mechanism and the superimposed RPT test mode. By placing the indenter on top of the mixture, Zone I (active zone) is developed when the vertical pressure of the SGC is applied and the indenter creates enough room for the lateral and/or upward movements (plastic flow) of

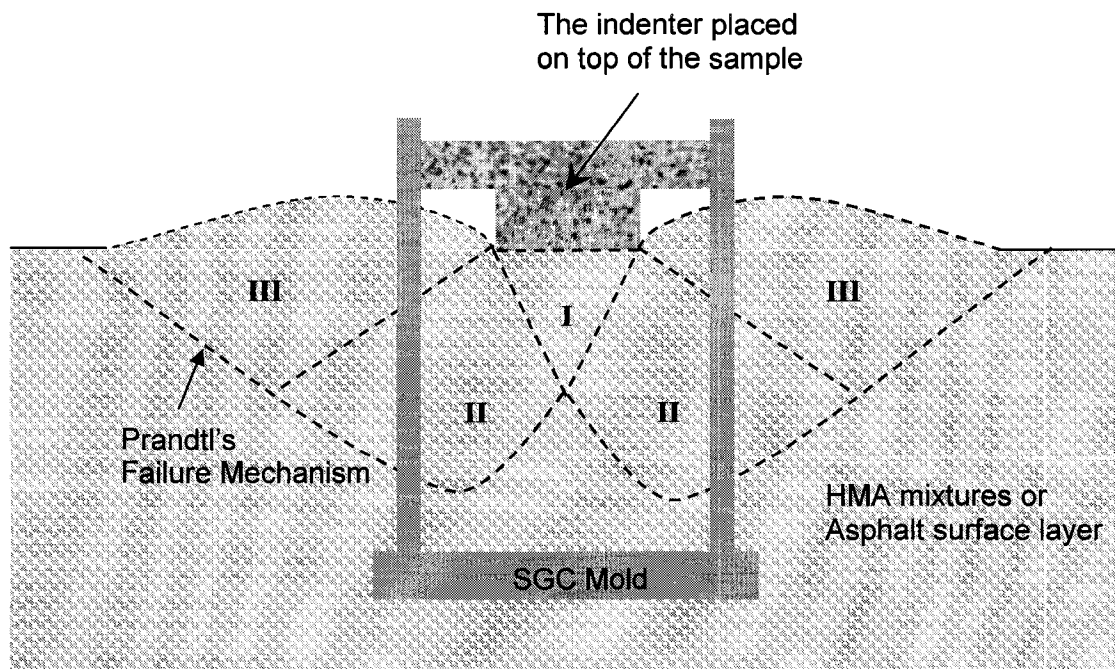


Figure 27. Simplified schematic illustration of the rationale behind the RPT

the mixture, resulting from the shear failure of the mixture. The RPT is a measure of the indentation which is a function of the cohesion (c) and the frictional component (ϕ) of the mixture at in-service temperature, not at the elevated compaction temperature. It should be noted that Prandtl's theory is valid in the cases of eccentric or inclined loads and layered systems and therefore, the application to the RPT is a reasonable inference even though the failure mechanism of the RPT does not satisfies all the idealizations made by Prandtl.

Other things necessary for the further refinements of the RPT are the shape of the indenter and the interpretation of the RPT test results. Possible shapes (cross sections) of the indenter are shown in Figure 28, and the one used in this study is the indenter No.1. It might be a better idea to use No.2 (round edge) or No.3 (hemispherical shape) to avoid the locally concentrated stresses around the edge of No.1 indenter. In addition, the indenter can be made of hard rubbers, like a hockey puck, to more closely simulate tire loadings. With regard to the interpretations of test results, it has been found that comparing the percent strains of the mixtures after 100 gyrations is simple and effective in most cases, but there are cases where the results should be examined more carefully as shown in Figure 29.

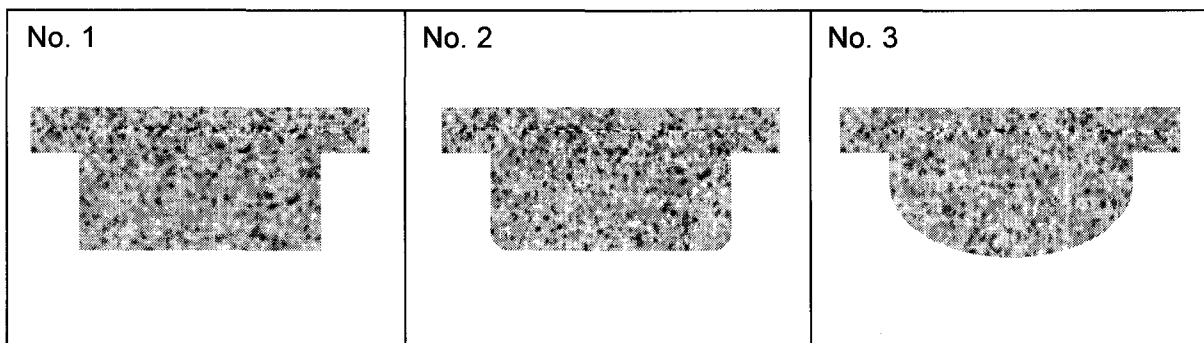


Figure 28. Possible shapes of the indenter

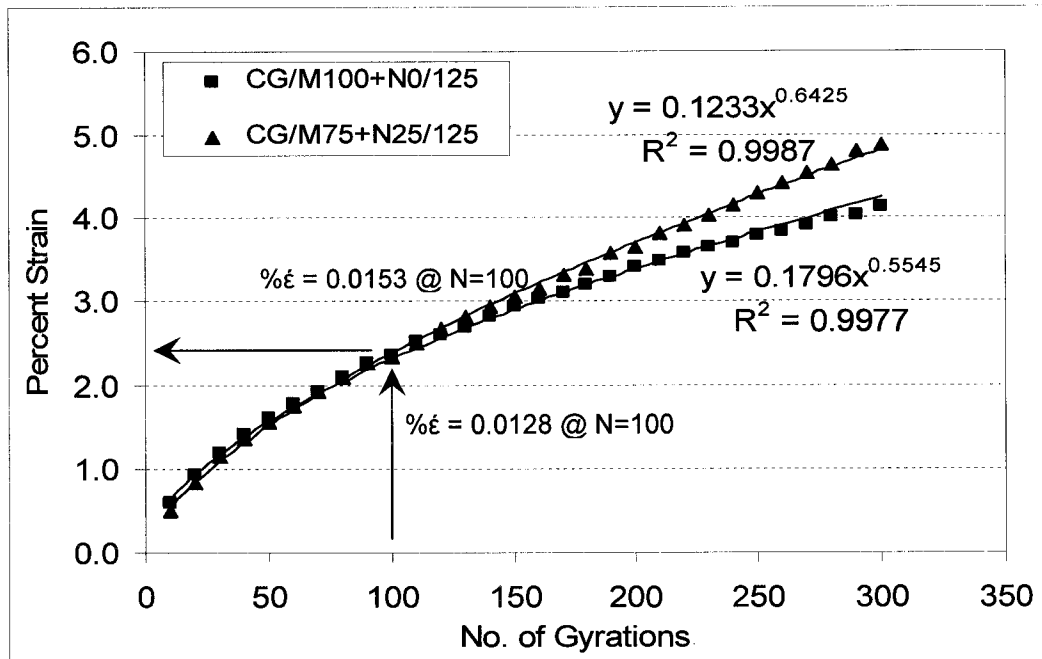


Figure 29. $\% \epsilon$ vs. $\% \dot{\epsilon}$ rate ($\% \dot{\epsilon}$)

Two mixtures showing almost same $\% \epsilon$ at 100 gyrations have different strain rates and different magnitudes of deformation at further gyrations. Therefore it would be better plotting the $\% \epsilon$ vs. N curves using the data recorded by the SGC, which can be easily done using spread sheets. However it should not be forgotten that a long testing period is not a good idea because the SGC does not control the test temperature and the mixture is getting colder during the test. Also, once the annular space around by the indenter becomes filled with the plastically deformed mixture, which happens usually when the deformation reaches approximately 10% strain, the desired failure mechanism of the RPT is no longer valid. Further gyrations beyond that point is introducing just another compaction effort to the mixture and the breakdown of aggregates.

In order to utilize the results of this study more practically, it can be conceived to transform the RPT results into a simple index form which is friendly to agencies and

contractors. In Iowa, quality index (QI) in daily plant report has been used for years, and it is one of the pay factors. QI is determined using the densities of seven cored samples and is a form of *t*-statistic calculated using the mean and standard deviation of seven measurements. Using the data in Table 24 and assuming three measurements of the RPT on newly designed mixture for ensuring its potential performance, Stability Index (SI) is proposed as follows:

For $N_d = 75$ mix (County roadways),

$$SI_{75} = \frac{m - 2.873}{0.077 + (0.253 \times s)} < 2.2 \quad (4)$$

For $N_d = 100$ mix (city roads and state routes),

$$SI_{100} = \frac{m - 2.552}{0.081 + (0.216 \times s)} < 2.1 \quad (5)$$

For $N_d = 125$ mix (Interstates),

$$SI_{125} = \frac{m - 2.165}{0.107 + (0.202 \times s)} < 2.1 \quad (6)$$

where, m = Mean of three % ϵ from the RPT at $N=100$

s = Std. Deviation of three % ϵ from the RPT at $N=100$

It should be mentioned that the constants in the SI equations and the criteria (2.1 or 2.2) are solely based on the results of this study. However, these can be easily replaced by performing the RPT on the known-performance mixes and calibrated by the field observations.

It is, also, possible to simplify SI indices into one index, SI_{RPT} , by introducing the N_{RPT} concept illustrated in Figure 30. For instance, if a mix is designed for $N_d = 100$ and

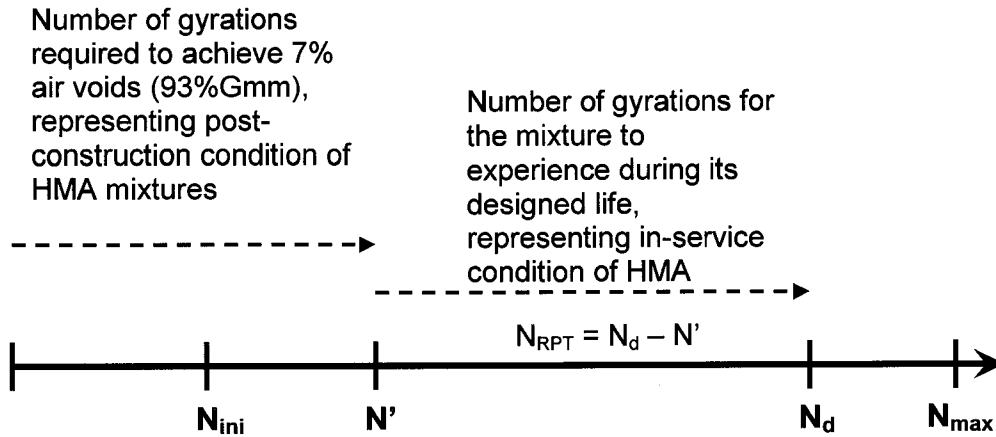


Figure 30. The concepts of N' and N_{RPT}

N' (number of gyrations required to achieve 93% G_{mm}) is 40, the N_{RPT} is 60 (=100 – 40). The idea of N_{RPT} is about the evaluation of relative performance of HMA mixtures designed for different level of traffic. A mix designed for $N_d = 75$ is expected to have a larger deformation than a $N_d = 100$ mix, when the same loading number is applied to them, and yet a $N_d = 75$ mix does satisfy its performance expectation.

The N_{RPT} of all mixes tested in this study were calculated, and the mean and standard deviation were 1.863 and 0.133, respectively. Thus SI_{RPT} is

$$SI_{RPT} = \frac{m - 1.863}{0.078 + (0.123 \times s)} < 2.0 \quad (7)$$

The SI indices allow for HMA mixtures to be evaluated in terms of their performance and make the comparison easier with other candidate mixes during mix design stage. During construction, once the SI has been established using job mix formula (JMF) mix, by conducting the RPT on field samples collected behind the paver, daily production can be controlled, and material adjustments often made can be

justified, instead of entirely relying upon the volumetrics of mixes.

6.3 Recommendations

Even though the findings and conclusions had to be made by testing only locally available materials, due to the limited time and financial support, and the variations of coarse aggregates properties and asphalt binder were not included in the experiments, the methodology is still valid to other types of HMA mixtures composed of different materials from those used in this study. However, future study on the indenter is recommended to refine the RPT and field validations or the RPT testing on known-performance mixtures are strongly suggested to establish appropriate criteria differentiating stable from unstable mixtures.

APPENDIX A.

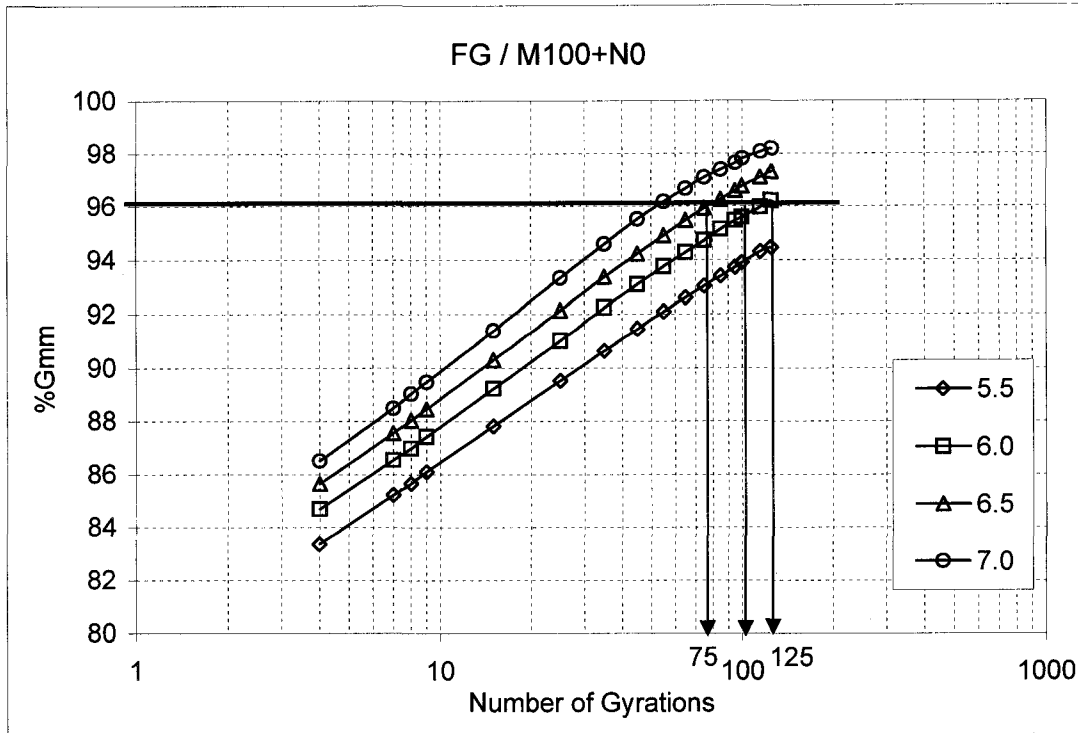
DETERMINATION OF OPTIMUM BINDER CONTENTS

Definitions of the Denotations used in Appendix A.

FG	aggregate gradation; Fine-Graded
DG	aggregate gradation; Dense-Graded
CG	aggregate gradation; Coarse-Graded
M100+N0	blending proportion for fine aggregate ; 100% Manufacture sand + 0% Natural sand
M75+N25	blending proportion for fine aggregate ; 75% Manufacture sand + 25% Natural sand
M50+N50	blending proportion for fine aggregate ; 50% Manufacture sand + 50% Natural sand
N	number of gyrations applied to compact the mixture
N'	number of gyrations required to achieve 7% air voids
N _d	design number of gyrations
P _a	percent air voids by the volume of the compacted mixture (%)
P _b	asphalt content as a percentage of the weight of the mixture (%)
P _{ba}	absorbed asphalt content (%)
P _{be}	effective asphalt content (%)
P _{b(opt)}	optimum asphalt content (%)
%Abs.	percent water absorption of the aggregate (%)
G _{sb}	dry bulk specific gravity of the aggregate
G _{sa}	apparent specific gravity of the aggregate
G _{se}	effective specific gravity of the aggregate
G _b	specific gravity of the asphalt binder
G _{mm}	theoretical maximum specific gravity of the mixture
%G _{mm}	percent theoretical maximum specific gravity of the mixture (%)
VMA	voids in mineral aggregate (%)
VFA	voids filled with asphalt binder (%)
P _{#200}	aggregate passing #200 (0.075mm) sieve = filler (%)
F/B	filler to bitumen ratio
FT	film thickness (micron)
SA	surface area (m ² /kg)

Pb(opt) for FG/M100+N0 Mixes

1. Compaction Curve



N	%Gmm @ Pb						
	5.5	5.941	6.0	6.167	6.5	6.542	7.0
7	85.2		86.5		87.6	87.7	88.5
8	85.7		87.0	87.3	88.0		89.0
9	86.1	87.2	87.4		88.5		89.5
75	93.0		94.7		95.9	96.0	97.1
100	93.9		95.6	96.0	96.8		97.8
125	94.5	96.0	96.2		97.3		98.2
N'	74	48	44	40	32	31	22

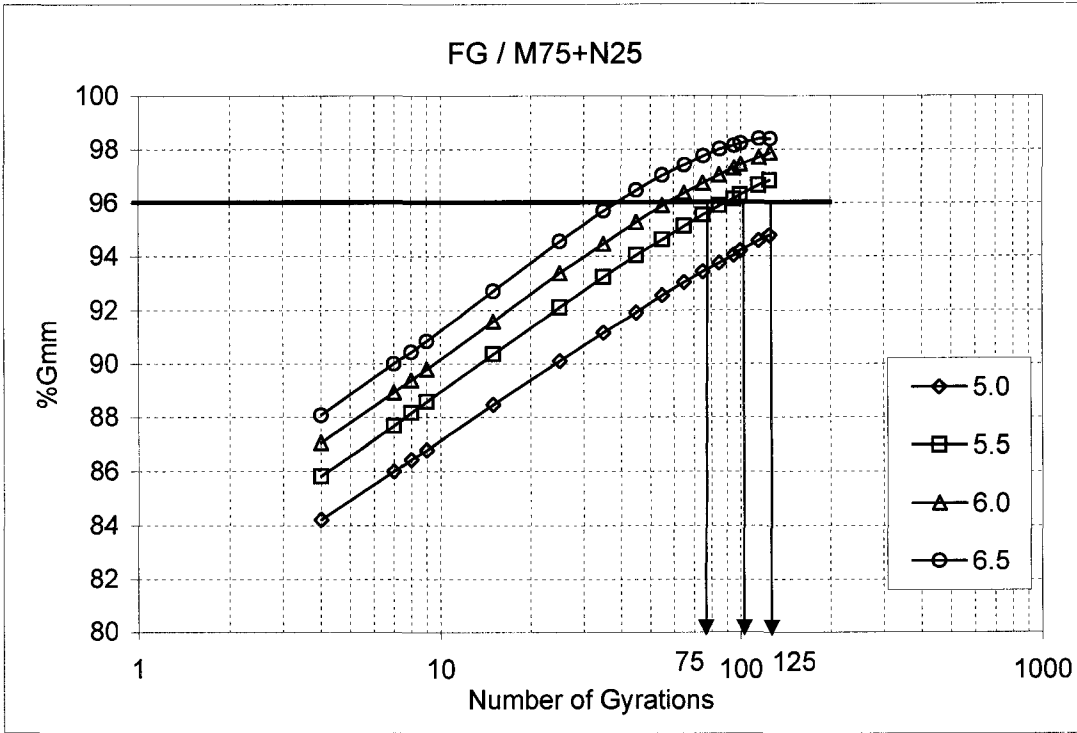
2. Volumetrics

Gsb	Gsa	%Abs.	Gb	SA	P#200	Gse	Pba
2.639	2.788	2.03	1.033	5.929	5	2.700	0.884

Nd	Pb(opt)	Pa @ Nd	VMA	VFA	Pbe	F/B	FT
75	5.941	4.0	15.7	74.5	5.109	1.0	8.6
100	6.167	4.0	15.7	74.5	5.337	0.9	9.0
125	6.542	4.0	15.8	74.6	5.715	0.9	9.6

Pb(opt) for FG/M75+N25 Mixes

1. Compaction Curve



N	%Gmm @ Pb						
	5.0	5.300	5.429	5.5	5.708	6.0	6.5
7	86.0			87.7	88.2	88.9	90.0
8	86.4		87.9	88.2		89.4	90.4
9	86.8	87.9		88.6		89.8	90.8
75	93.4			95.5	96.0	96.7	97.8
100	94.2		96.0	96.3		97.4	98.2
125	94.8	96.0		96.8		97.9	98.4
N'	72	49	38	33	29	23	16

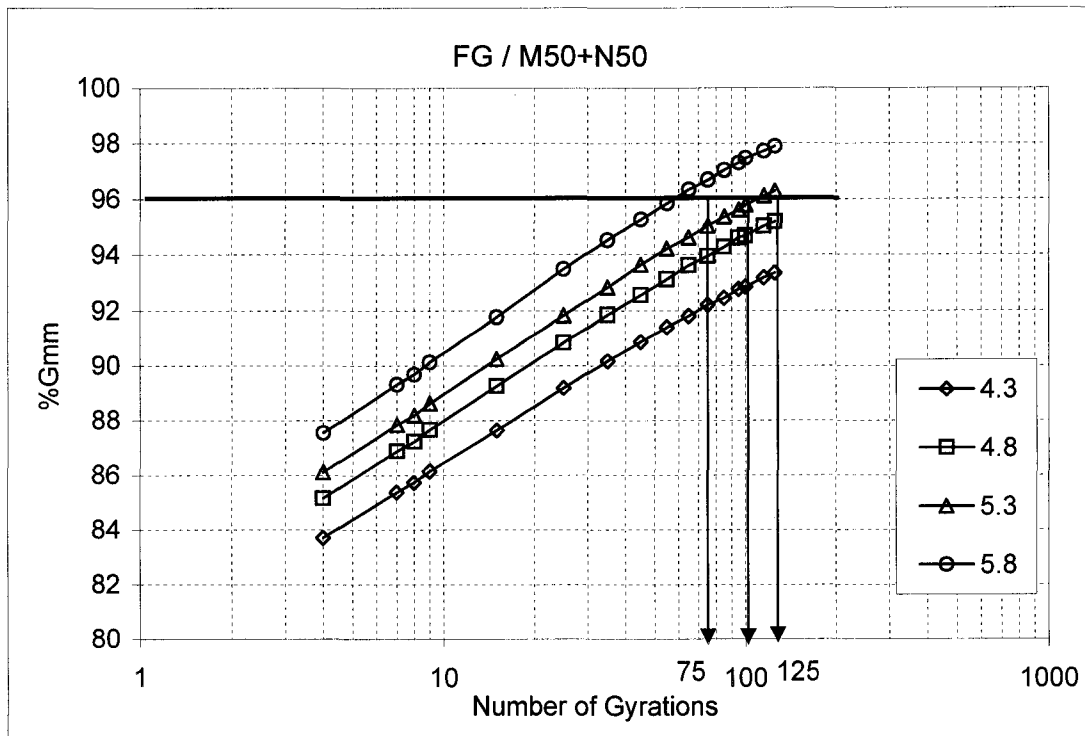
2. Volumetrics

Gsb	Gsa	%Abs.	Gb	SA	P#200	Gse	Pba
2.627	2.772	1.99	1.033	5.929	5	2.702	1.091

Nd	Pb(opt)	Pa @ Nd	VMA	VFA	Pbe	F/B	FT
75	5.300	4.0	14.0	71.4	4.266	1.2	7.2
100	5.429	4.0	13.7	70.9	4.396	1.1	7.4
125	5.708	4.0	13.6	70.7	4.679	1.1	7.9

Pb(opt) for FG/M50+N50 Mixes

1. Compaction Curve



N	%Gmm @ Pb						
	4.3	4.8	5.164	5.3	5.363	5.594	5.8
7	85.4	86.9		87.8		88.7	89.3
8	85.7	87.2		88.2	88.4		89.7
9	86.1	87.7	88.4	88.6			90.1
75	92.2	93.9		95.0		96.0	96.7
100	92.9	94.7		95.8	96.0		97.4
125	93.3	95.2	96.0	96.3			97.9
N'	108	53	41	37	35	28	22

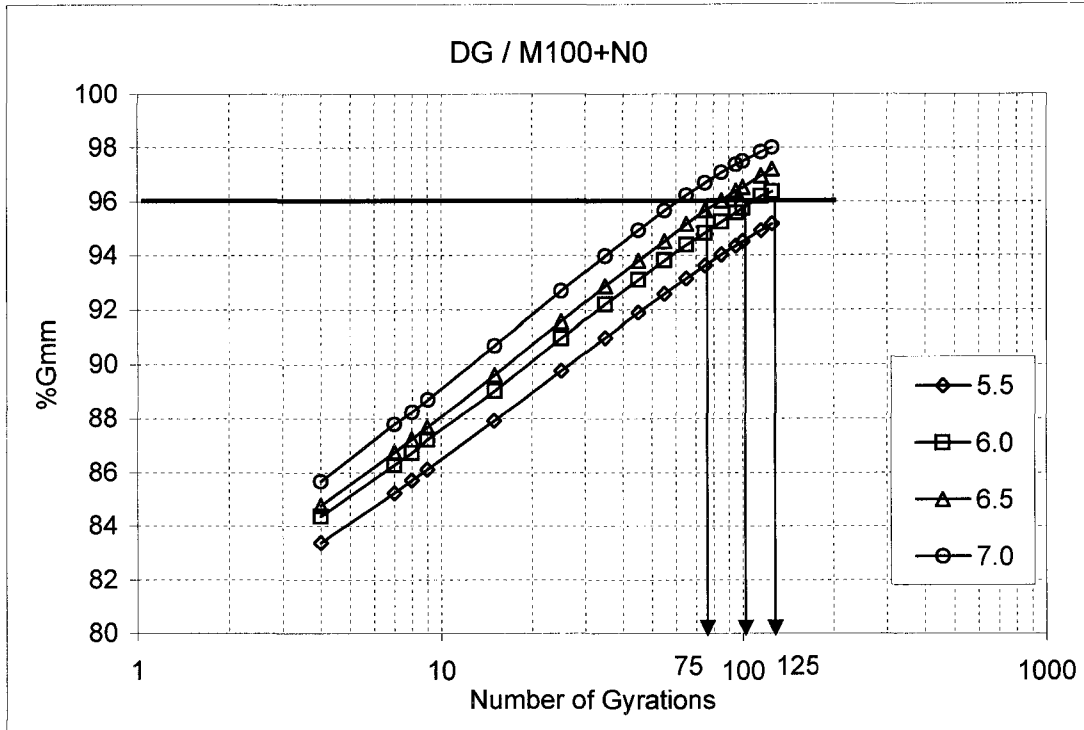
2. Volumetrics

Gsb	Gsa	%Abs.	Gb	SA	P#200	Gse	Pba
2.616	2.757	1.95	1.033	5.929	5	2.680	0.943

Nd	Pb(opt)	Pa @ Nd	VMA	VFA	Pbe	F/B	FT
75	5.164	4.0	13.9	71.1	4.269	1.2	7.2
100	5.363	4.0	13.8	71.1	4.470	1.1	7.5
125	5.594	4.0	13.7	70.8	4.704	1.1	7.9

Pb(opt) for DG/M100+N0 Mixes

1. Compaction Curve



N	%Gmm @ Pb						
	5.5	5.833	6.0	6.188	6.5	6.650	7.0
7	85.2		86.3		86.7	87.0	87.8
8	85.7		86.7	86.9	87.2		88.2
9	86.1	86.8	87.2		87.7		88.7
75	93.6		94.8		95.7	96.0	96.7
100	94.5		95.7	96.0	96.5		97.5
125	95.2	96.0	96.4		97.2		98.0
N'	62	50	44	41	37	34	27

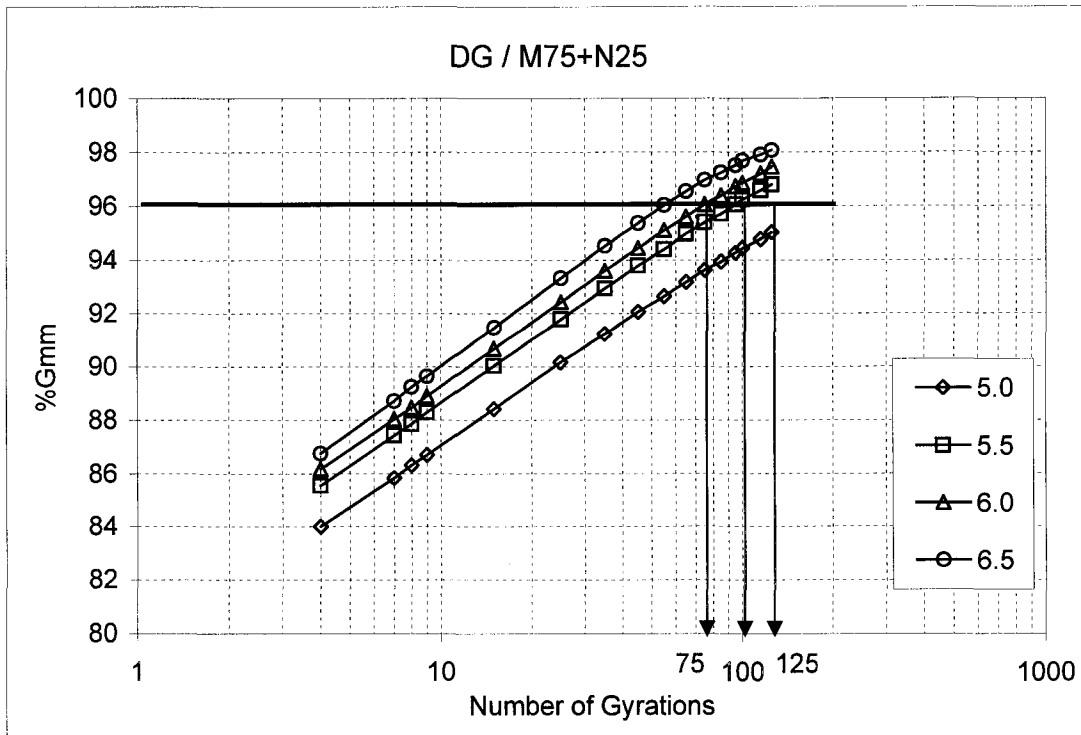
2. Volumetrics

Gsb	Gsa	%Abs.	Gb	SA	P#200	Gse	Pba
2.639	2.788	2.03	1.033	4.942	4	2.707	0.983

Nd	Pb(opt)	Pa @ Nd	VMA	VFA	Pbe	F/B	FT
75	5.833	4.0	15.3	73.9	4.907	0.8	9.9
100	6.188	4.0	15.5	74.1	5.265	0.8	10.7
125	6.650	4.0	15.8	74.7	5.732	0.7	11.6

Pb(opt) for DG/M75+N25 Mixes

1. Compaction Curve



N	%Gmm @ Pb						
	5.0	5.278	5.444	5.5	5.929	6.0	6.5
7	85.8			87.4	87.9	88.0	88.7
8	86.3		87.7	87.9		88.5	89.2
9	86.7	87.6		88.3		88.9	89.6
75	93.6			95.4	96.0	96.1	97.0
100	94.4		96.0	96.2		96.9	97.7
125	95.0	96.0		96.8		97.5	98.1
N'	61	47	39	36	31	30	23

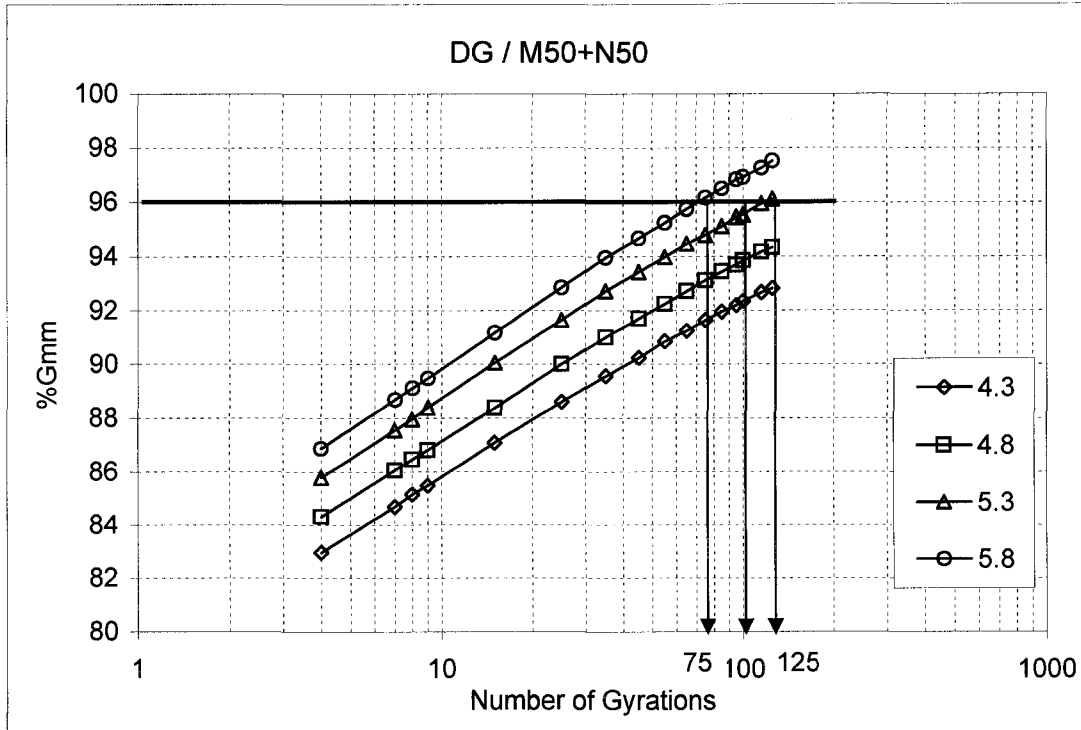
2. Volumetrics

Gsb	Gsa	%Abs.	Gb	SA	P#200	Gse	Pba
2.628	2.774	1.99	1.033	4.942	4	2.697	1.006

Nd	Pb(opt)	Pa @ Nd	VMA	VFA	Pbe	F/B	FT
75	5.278	4.0	14.0	71.3	4.325	0.9	8.8
100	5.444	4.0	13.8	71.0	4.493	0.9	9.1
125	5.929	4.0	14.2	71.8	4.983	0.8	10.1

Pb(opt) for DG/M50+N50 Mixes

1. Compaction Curve



N	%Gmm @ Pb						
	4.3	4.8	5.272	5.3	5.479	5.729	5.8
7	84.7	86.1		87.6		88.5	88.7
8	85.1	86.5		88.0	88.4		89.1
9	85.5	86.8	88.3	88.4			89.5
75	91.6	93.1		94.8		96.0	96.2
100	92.3	93.8		95.5	96.0		96.9
125	92.8	94.3	96.0	96.1			97.5
N'	>125	74	41	39	34	28	26

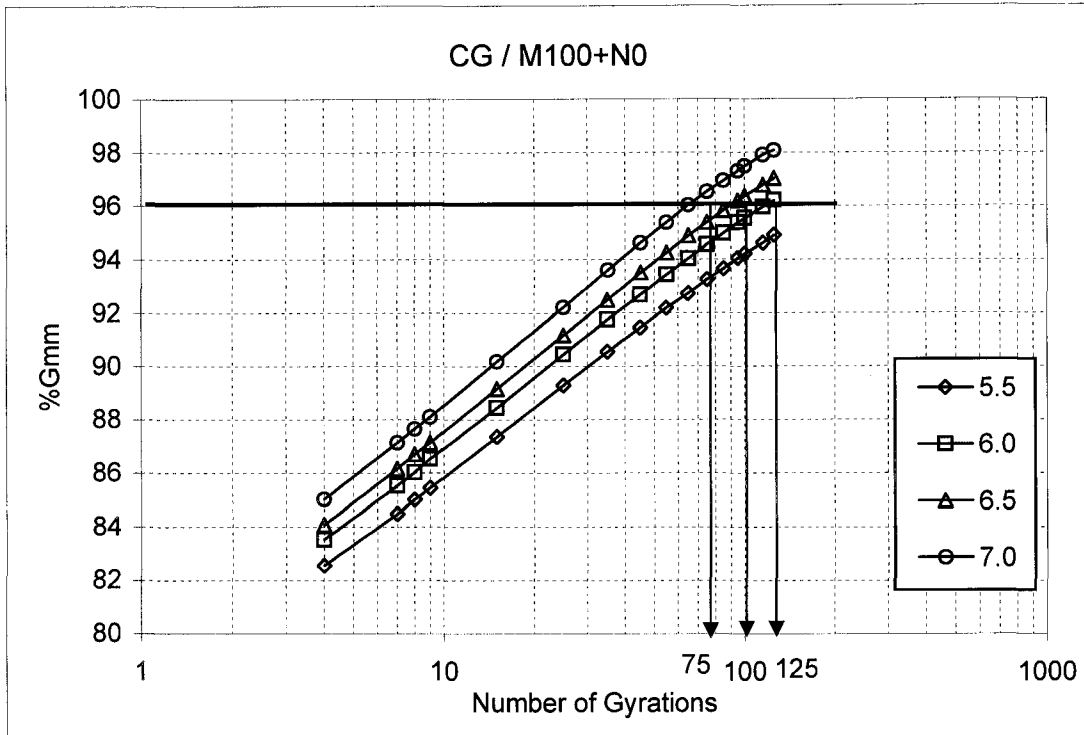
2. Volumetrics

Gsb	Gsa	%Abs.	Gb	SA	P#200	Gse	Pba
2.618	2.76	1.96	1.033	4.942	4	2.681	0.927

Nd	Pb(opt)	Pa @ Nd	VMA	VFA	Pbe	F/B	FT
75	5.272	4.0	14.1	71.6	4.394	0.9	8.9
100	5.479	4.0	14.0	71.4	4.602	0.9	9.3
125	5.729	4.0	13.9	71.3	4.854	0.8	9.8

Pb(opt) for CG/M100+N0 Mixes

1. Compaction Curve



N	%Gmm @ Pb						
	5.5	5.923	6.0	6.278	6.5	6.773	7.0
7	84.5		85.5		86.2	86.7	87.1
8	85.0		86.0	86.4	86.7		87.7
9	85.5	86.3	86.5		87.1		88.1
75	93.2		94.6		95.4	96.0	96.5
100	94.2		95.5	96.0	96.4		97.5
125	94.9	96.0	96.2		97.0		98.1
N'	70	48	49	40	40	31	30

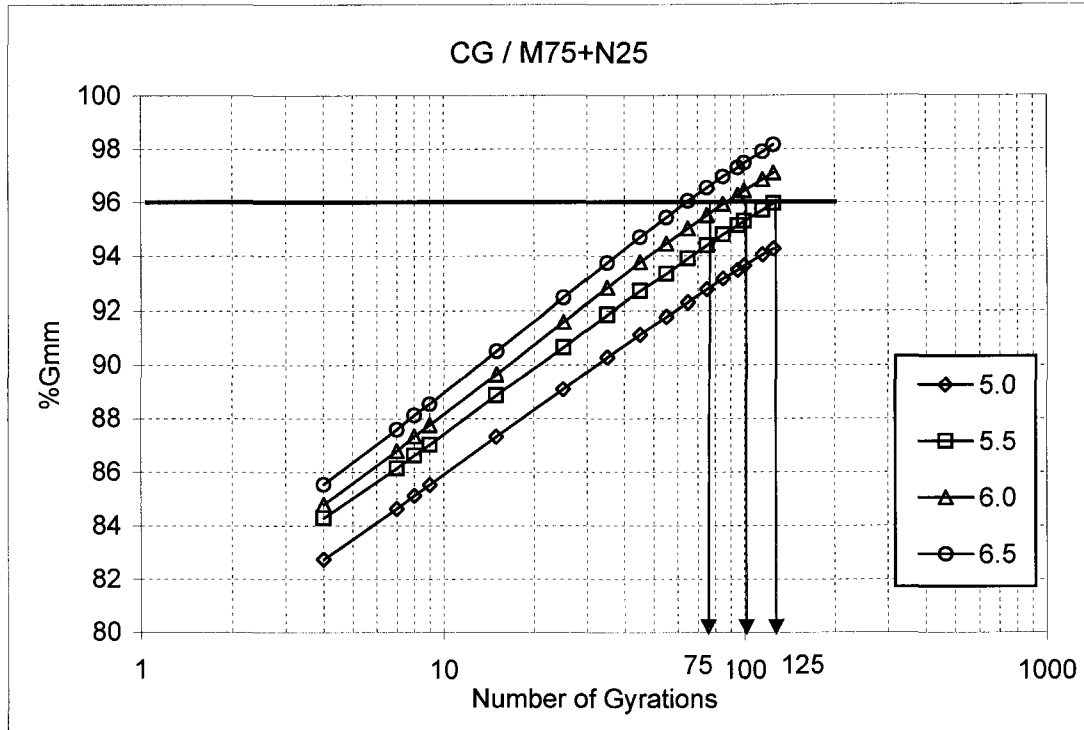
2. Volumetrics

Gsb	Gsa	%Abs.	Gb	SA	P#200	Gse	Pba
2.639	2.788	2.03	1.033	3.958	3	2.705	0.955

Nd	Pb(opt)	Pa @ Nd	VMA	VFA	Pbe	F/B	FT
75	5.923	4.0	15.5	74.2	5.024	0.6	12.7
100	6.278	4.0	15.7	74.5	5.383	0.6	13.6
125	6.773	4.0	15.9	74.9	5.883	0.5	14.9

Pb(opt) for CG/M75+N25 Mixes

1. Compaction Curve



N	%Gmm @ Pb						
	5.0	5.500	5.5	5.818	6.0	6.250	6.5
7	84.6		86.1		86.8	87.2	87.6
8	85.1		86.6	87.0	87.3		88.1
9	85.5	87.0	87.0		87.8		88.5
75	92.8		94.4		95.5	96.0	96.5
100	93.6		95.3	96.0	96.4		97.5
125	94.3	96.0	96.0		97.1		98.2
N'		48	48	41	37	33	29

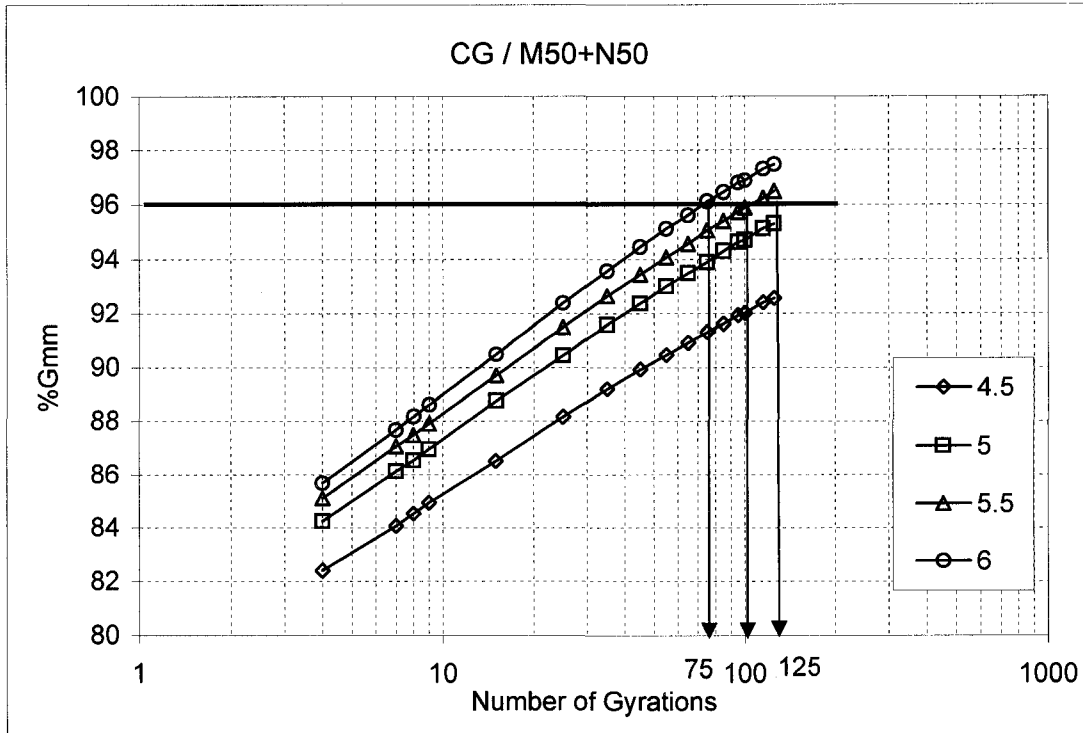
2. Volumetrics

Gsb	Gsa	%Abs.	Gb	SA	P#200	Gse	Pba
2.629	2.775	2.00	1.033	3.958	3	2.689	0.877

Nd	Pb(opt)	Pa @ Nd	VMA	VFA	Pbe	F/B	FT
75	5.500	4.0	14.8	72.9	4.671	0.6	11.8
100	5.818	4.0	14.8	73.0	4.992	0.6	12.6
125	6.250	4.0	14.9	73.2	5.428	0.6	13.7

Pb(opt) for CG/M50+N50 Mixes

1. Compaction Curve



N	%Gmm @ Pb						
	4.5	5.0	5.292	5.5	5.550	5.950	6.0
7	84.1	86.1		87.1		87.6	87.7
8	84.5	86.5		87.5	87.6		88.2
9	84.9	87.0	87.5	87.9			88.6
75	91.3	93.9		95.1		96.0	96.1
100	92.0	94.7		95.9	96.0		96.9
125	92.6	95.3	96.0	96.5			97.5
N'	>125	56	46	39	38	31	30

2. Volumetrics

Gsb	Gsa	%Abs.	Gb	SA	P#200	Gse	Pba
2.620	2.762	1.97	1.033	3.958	3	2.682	0.911

Nd	Pb(opt)	Pa @ Nd	VMA	VFA	Pbe	F/B	FT
75	5.292	4.0	14.2	71.8	4.428	0.7	11.2
100	5.550	4.0	14.2	71.9	4.689	0.6	11.8
125	5.950	4.0	14.4	72.2	5.093	0.6	12.9

APPENDIX B - 1.

DATA SUMMARY: The RPT at p = 87psi

%strains of FG mixes tested during the preliminary study

N	Pb-			Pbo			Pb+		
	52C	58C	64C	52C	58C	64C	52C	58C	64C
5	0.177	0.269	0.266	0.265	0.354	0.349	0.354	0.440	0.436
10	0.355	0.449	0.444	0.531	0.620	0.699	0.620	0.792	0.871
15	0.444	0.539	0.621	0.796	0.886	1.048	0.974	1.143	1.307
20	0.532	0.718	0.710	0.973	1.151	1.310	1.240	1.495	1.568
25	0.621	0.808	0.887	1.149	1.329	1.485	1.417	1.759	1.916
30	0.710	0.987	0.976	1.326	1.594	1.747	1.683	1.935	2.178
35	0.799	1.077	1.154	1.503	1.771	1.921	1.860	2.199	2.439
40	0.887	1.167	1.242	1.592	1.949	2.096	2.037	2.375	2.700
45	0.976	1.257	1.331	1.768	2.126	2.358	2.214	2.639	2.875
50	1.065	1.346	1.420	1.857	2.303	2.445	2.391	2.814	3.136
55	1.154	1.436	1.508	2.034	2.391	2.620	2.569	2.990	3.310
60	1.154	1.526	1.597	2.122	2.569	2.795	2.657	3.166	3.484
65	1.242	1.616	1.686	2.210	2.746	2.969	2.834	3.342	3.659
70	1.331	1.706	1.775	2.387	2.834	3.057	2.923	3.518	3.833
75	1.331	1.795	1.863	2.476	3.012	3.231	3.100	3.606	4.007
80	1.420	1.885	1.952	2.564	3.100	3.406	3.189	3.782	4.181
85	1.420	1.885	2.041	2.653	3.189	3.493	3.277	3.870	4.355
90	1.508	1.975	2.041	2.741	3.366	3.581	3.454	4.046	4.530
95	1.597	2.065	2.130	2.829	3.454	3.755	3.543	4.134	4.617
100	1.597	2.154	2.218	2.918	3.543	3.843	3.632	4.310	4.791
110	1.686	2.244	2.307	3.095	3.809	4.105	3.809	4.485	5.052
120	1.775	2.334	2.484	3.183	3.986	4.279	4.074	4.749	5.314
130	1.863	2.513	2.573	3.360	4.163	4.454	4.252	4.925	5.575
140	1.952	2.603	2.751	3.537	4.340	4.716	4.429	5.189	5.836
150	2.041	2.693	2.839	3.625	4.517	4.891	4.606	5.365	6.010
160	2.130	2.873	2.928	3.802	4.694	5.066	4.694	5.541	6.272
170	2.130	2.962	3.017	3.890	4.872	5.240	4.872	5.717	6.446
180	2.218	3.052	3.106	4.067	4.960	5.415	5.049	5.893	6.620
190	2.307	3.142	3.194	4.156	5.137	5.590	5.137	5.981	6.882
200	2.396	3.232	3.283	4.244	5.226	5.677	5.314	6.157	7.056
210	2.396	3.321	3.372	4.332	5.403	5.852	5.492	6.332	7.230
220	2.484	3.411	3.461	4.509	5.492	5.939	5.580	6.508	7.404
230	2.573	3.501	3.549	4.598	5.669	6.114	5.757	6.596	7.578
240	2.662	3.591	3.638	4.686	5.757	6.288	5.846	6.772	7.753
250	2.662	3.680	3.727	4.775	5.934	6.376	6.023	6.860	7.840
260	2.751	3.770	3.815	4.863	6.023	6.550	6.112	7.036	8.014
270	2.751	3.860	3.904	4.951	6.112	6.638	6.200	7.124	8.188
280	2.839	3.860	3.904	5.040	6.289	6.725	6.377	7.212	8.275
290	2.928	3.950	3.993	5.128	6.377	6.900	6.466	7.388	8.449
300	2.928	4.039	4.082	5.217	6.466	6.987	6.554	7.476	8.624

%strains of DG mixes tested during the preliminary study

N	Pb-			Pbo			Pb+		
	52C	58C	64C	52C	58C	64C	52C	58C	64C
5	0.181	0.273	0.271	0.362	0.364	0.362	0.452	0.362	0.547
10	0.362	0.455	0.451	0.633	0.727	0.723	0.814	0.723	0.912
15	0.542	0.636	0.632	0.905	1.091	0.995	1.086	1.085	1.276
20	0.633	0.818	0.812	1.086	1.455	1.266	1.357	1.356	1.550
25	0.723	0.909	0.903	1.267	1.636	1.447	1.538	1.537	1.823
30	0.814	1.000	1.083	1.448	1.818	1.627	1.719	1.718	2.097
35	0.995	1.091	1.173	1.629	2.000	1.808	1.900	1.989	2.279
40	0.995	1.182	1.264	1.810	2.182	1.989	2.081	2.170	2.461
45	1.085	1.273	1.354	1.900	2.364	2.170	2.262	2.260	2.735
50	1.175	1.364	1.444	2.081	2.545	2.351	2.443	2.441	2.917
55	1.266	1.455	1.625	2.172	2.727	2.441	2.534	2.622	3.099
60	1.356	1.545	1.715	2.353	2.909	2.622	2.715	2.712	3.191
65	1.447	1.636	1.715	2.443	2.909	2.712	2.805	2.893	3.373
70	1.447	1.727	1.805	2.534	3.091	2.893	2.986	2.984	3.555
75	1.537	1.818	1.895	2.715	3.273	2.984	3.077	3.074	3.646
80	1.627	1.818	1.986	2.805	3.273	3.165	3.258	3.255	3.829
85	1.627	1.909	2.076	2.896	3.455	3.255	3.348	3.345	4.011
90	1.718	2.000	2.166	3.077	3.636	3.345	3.439	3.436	4.102
95	1.718	2.091	2.166	3.167	3.636	3.526	3.529	3.526	4.284
100	1.808	2.091	2.256	3.258	3.818	3.617	3.710	3.707	4.376
110	1.899	2.273	2.437	3.439	4.000	3.797	3.891	3.888	4.649
120	1.989	2.364	2.527	3.620	4.182	4.069	4.072	4.069	4.923
130	2.170	2.455	2.708	3.801	4.364	4.250	4.253	4.250	5.105
140	2.260	2.545	2.798	3.982	4.545	4.430	4.434	4.521	5.378
150	2.351	2.727	2.888	4.163	4.727	4.611	4.615	4.702	5.561
160	2.441	2.818	2.978	4.344	4.909	4.792	4.796	4.882	5.834
170	2.532	2.909	3.159	4.525	5.091	4.973	4.977	5.063	6.016
180	2.622	3.000	3.249	4.706	5.273	5.154	5.158	5.154	6.199
190	2.712	3.091	3.339	4.796	5.273	5.335	5.249	5.335	6.381
200	2.712	3.182	3.430	4.977	5.455	5.515	5.430	5.515	6.563
210	2.803	3.273	3.520	5.158	5.636	5.696	5.611	5.606	6.837
220	2.893	3.364	3.610	5.339	5.818	5.787	5.701	5.787	7.019
230	2.984	3.455	3.700	5.430	5.818	5.967	5.882	5.967	7.201
240	3.074	3.455	3.791	5.611	6.000	6.148	6.063	6.058	7.384
250	3.165	3.545	3.971	5.701	6.000	6.329	6.244	6.239	7.566
260	3.255	3.636	4.061	5.882	6.182	6.420	6.335	6.329	7.748
270	3.255	3.727	4.152	5.973	6.182	6.600	6.516	6.510	7.931
280	3.345	3.818	4.242	6.154	6.364	6.781	6.697	6.600	8.113
290	3.436	3.909	4.332	6.244	6.545	6.872	6.787	6.781	8.295
300	3.526	3.909	4.422	6.335	6.545	7.052	6.968	6.872	8.478

%strains of CG mixes tested during the preliminary study

N	Pb-			Pbo			Pb+		
	52C	58C	64C	52C	58C	64C	52C	58C	64C
5	0.271	0.271	0.362	0.356	0.358	0.446	0.448	0.448	0.540
10	0.542	0.452	0.634	0.712	0.716	0.892	0.806	0.806	0.990
15	0.722	0.632	0.906	0.979	0.985	1.160	1.075	1.165	1.350
20	0.812	0.723	1.087	1.246	1.164	1.427	1.344	1.434	1.710
25	0.993	0.903	1.268	1.512	1.343	1.695	1.613	1.703	2.070
30	1.083	0.994	1.359	1.690	1.522	1.963	1.792	1.882	2.430
35	1.173	1.084	1.540	1.957	1.701	2.141	1.971	2.151	2.700
40	1.264	1.265	1.721	2.135	1.880	2.409	2.151	2.330	3.060
45	1.354	1.355	1.812	2.313	1.970	2.587	2.330	2.599	3.330
50	1.444	1.445	1.902	2.491	2.149	2.765	2.509	2.778	3.690
55	1.534	1.536	2.083	2.580	2.238	2.944	2.688	3.047	3.960
60	1.625	1.626	2.174	2.758	2.417	3.211	2.778	3.226	4.230
65	1.715	1.716	2.355	2.936	2.507	3.390	2.957	3.405	4.500
70	1.805	1.807	2.446	3.025	2.686	3.568	3.136	3.584	4.770
75	1.805	1.897	2.536	3.203	2.775	3.747	3.226	3.763	5.041
80	1.895	1.987	2.627	3.292	2.865	3.925	3.405	4.032	5.311
85	1.986	1.987	2.808	3.470	3.044	4.103	3.495	4.211	5.491
90	2.076	2.078	2.899	3.559	3.133	4.193	3.674	4.391	5.761
95	2.166	2.168	2.989	3.737	3.223	4.371	3.763	4.570	6.031
100	2.166	2.258	3.080	3.826	3.312	4.550	3.853	4.749	6.211
110	2.347	2.349	3.351	4.093	3.581	4.906	4.122	5.108	6.661
120	2.437	2.529	3.533	4.270	3.760	5.263	4.301	5.376	7.021
130	2.527	2.620	3.714	4.537	4.029	5.531	4.570	5.735	7.471
140	2.617	2.800	3.986	4.804	4.208	5.798	4.749	6.093	7.921
150	2.798	2.891	4.167	5.071	4.387	6.155	5.018	6.362	8.281
160	2.888	2.981	4.348	5.249	4.655	6.423	5.197	6.720	8.731
170	2.978	3.162	4.529	5.516	4.834	6.780	5.466	6.989	9.091
180	3.069	3.252	4.710	5.694	5.103	7.047	5.645	7.258	9.451
190	3.159	3.342	4.982	5.961	5.282	7.315	5.824	7.616	9.811
200	3.249	3.433	5.163	6.139	5.461	7.672	6.004	7.885	10.171
210	3.339	3.523	5.344	6.406	5.730	7.939	6.183	8.154	10.441
220	3.430	3.704	5.525	6.584	5.909	8.207	6.452	8.423	10.711
230	3.520	3.794	5.797	6.762	6.088	8.475	6.631	8.692	10.981
240	3.610	3.884	5.978	7.028	6.356	8.742	6.810	8.871	11.251
250	3.700	3.975	6.159	7.206	6.535	9.010	6.989	9.140	11.431
260	3.791	4.065	6.341	7.384	6.804	9.188	7.168	9.409	11.701
270	3.881	4.155	6.612	7.562	6.983	9.456	7.348	9.588	11.881
280	3.971	4.246	6.793	7.740	7.162	9.723	7.527	9.857	12.061
290	4.061	4.336	6.975	7.918	7.341	9.902	7.706	10.036	12.241
300	4.152	4.426	7.246	8.096	7.520	10.169	7.885	10.215	12.331

%strains of FG/M100+N0 Mixes

N	Nd = 75			Nd = 100			Nd = 125		
	#1	#2	ave.	#1	#2	ave.	#1	#2	ave.
5	0.340	0.335	0.338	0.255	0.254	0.254	0.258	0.254	0.256
10	0.595	0.671	0.633	0.509	0.507	0.508	0.431	0.508	0.469
15	0.850	0.922	0.886	0.764	0.761	0.762	0.603	0.677	0.640
20	1.020	1.174	1.097	0.934	0.930	0.932	0.775	0.846	0.811
25	1.190	1.341	1.266	1.104	1.099	1.101	0.947	0.931	0.939
30	1.361	1.509	1.435	1.273	1.183	1.228	1.034	1.100	1.067
35	1.531	1.676	1.604	1.358	1.352	1.355	1.120	1.184	1.152
40	1.616	1.760	1.688	1.528	1.437	1.483	1.292	1.269	1.281
45	1.786	1.928	1.857	1.613	1.606	1.609	1.378	1.354	1.366
50	1.871	2.012	1.941	1.698	1.691	1.694	1.464	1.438	1.451
55	2.041	2.179	2.110	1.783	1.775	1.779	1.550	1.523	1.537
60	2.126	2.263	2.195	1.868	1.860	1.864	1.637	1.607	1.622
65	2.211	2.431	2.321	2.037	1.944	1.991	1.723	1.692	1.707
70	2.296	2.515	2.405	2.122	2.029	2.075	1.809	1.777	1.793
75	2.466	2.598	2.532	2.207	2.113	2.160	1.809	1.777	1.793
80	2.551	2.682	2.617	2.292	2.198	2.245	1.895	1.861	1.878
85	2.636	2.766	2.701	2.377	2.282	2.330	1.981	1.946	1.963
90	2.721	2.850	2.786	2.462	2.367	2.414	1.981	2.030	2.006
95	2.806	2.934	2.870	2.547	2.451	2.499	2.067	2.030	2.049
100	2.891	3.018	2.954	2.547	2.536	2.541	2.153	2.115	2.134
110	2.976	3.185	3.081	2.716	2.705	2.711	2.239	2.200	2.220
120	3.146	3.353	3.250	2.886	2.790	2.838	2.326	2.284	2.305
130	3.316	3.521	3.418	2.971	2.959	2.965	2.498	2.369	2.433
140	3.401	3.688	3.545	3.141	3.043	3.092	2.584	2.453	2.519
150	3.571	3.856	3.714	3.226	3.212	3.219	2.670	2.538	2.604
160	3.656	3.940	3.798	3.311	3.297	3.304	2.756	2.623	2.689
170	3.827	4.107	3.967	3.480	3.381	3.431	2.842	2.707	2.775
180	3.912	4.191	4.051	3.565	3.466	3.516	2.929	2.792	2.860
190	3.997	4.359	4.178	3.650	3.635	3.643	2.929	2.876	2.902
200	4.167	4.443	4.305	3.735	3.719	3.727	3.015	2.961	2.988
210	4.252	4.610	4.431	3.905	3.804	3.854	3.101	2.961	3.031
220	4.337	4.694	4.515	3.990	3.888	3.939	3.187	3.046	3.116
230	4.422	4.778	4.600	4.075	3.973	4.024	3.187	3.130	3.159
240	4.592	4.946	4.769	4.160	4.142	4.151	3.273	3.215	3.244
250	4.677	5.029	4.853	4.244	4.227	4.236	3.359	3.215	3.287
260	4.762	5.113	4.938	4.329	4.311	4.320	3.445	3.299	3.372
270	4.847	5.281	5.064	4.414	4.396	4.405	3.445	3.299	3.372
280	4.932	5.365	5.148	4.499	4.480	4.490	3.531	3.384	3.458
290	5.017	5.448	5.233	4.584	4.565	4.574	3.531	3.469	3.500
300	5.102	5.532	5.317	4.669	4.649	4.659	3.618	3.469	3.543

%strains of FG/M75+N25 Mixes

N	Nd = 75			Nd = 100			Nd = 125		
	#1	#2	ave.	#1	#2	ave.	#1	#2	ave.
5	0.339	0.336	0.338	0.256	0.253	0.255	0.258	0.256	0.257
10	0.679	0.589	0.634	0.427	0.507	0.467	0.431	0.427	0.429
15	0.848	0.841	0.845	0.597	0.760	0.679	0.603	0.597	0.600
20	1.018	1.009	1.014	0.768	0.929	0.848	0.689	0.768	0.728
25	1.187	1.177	1.182	0.939	1.014	0.976	0.775	0.853	0.814
30	1.357	1.346	1.351	1.024	1.182	1.103	0.861	0.939	0.900
35	1.527	1.514	1.520	1.195	1.267	1.231	1.034	1.109	1.071
40	1.612	1.598	1.605	1.280	1.351	1.316	1.120	1.195	1.157
45	1.696	1.766	1.731	1.365	1.520	1.443	1.206	1.280	1.243
50	1.781	1.850	1.816	1.536	1.605	1.570	1.206	1.365	1.286
55	1.951	1.934	1.943	1.621	1.689	1.655	1.292	1.451	1.371
60	2.036	2.019	2.027	1.706	1.774	1.740	1.378	1.451	1.414
65	2.120	2.103	2.112	1.792	1.858	1.825	1.464	1.536	1.500
70	2.205	2.271	2.238	1.877	1.943	1.910	1.464	1.621	1.543
75	2.290	2.355	2.322	1.877	2.027	1.952	1.550	1.706	1.628
80	2.375	2.439	2.407	1.962	2.111	2.037	1.637	1.792	1.714
85	2.460	2.523	2.491	2.048	2.196	2.122	1.637	1.792	1.714
90	2.545	2.607	2.576	2.133	2.280	2.207	1.723	1.877	1.800
95	2.545	2.607	2.576	2.218	2.280	2.249	1.809	1.962	1.886
100	2.629	2.691	2.660	2.304	2.365	2.334	1.809	1.962	1.886
110	2.799	2.860	2.829	2.389	2.534	2.461	1.895	2.133	2.014
120	2.884	3.028	2.956	2.474	2.618	2.546	1.981	2.218	2.100
130	3.053	3.112	3.083	2.645	2.787	2.716	2.153	2.304	2.229
140	3.138	3.280	3.209	2.730	2.872	2.801	2.153	2.389	2.271
150	3.223	3.364	3.294	2.816	2.956	2.886	2.239	2.474	2.357
160	3.393	3.448	3.420	2.901	3.125	3.013	2.326	2.560	2.443
170	3.478	3.532	3.505	3.072	3.209	3.141	2.412	2.645	2.528
180	3.562	3.701	3.631	3.157	3.294	3.225	2.498	2.730	2.614
190	3.647	3.785	3.716	3.242	3.463	3.353	2.584	2.816	2.700
200	3.732	3.869	3.800	3.328	3.547	3.437	2.670	2.901	2.786
210	3.817	3.953	3.885	3.413	3.632	3.522	2.670	2.986	2.828
220	3.902	4.037	3.969	3.498	3.716	3.607	2.756	3.072	2.914
230	3.986	4.121	4.054	3.584	3.801	3.692	2.842	3.157	3.000
240	4.071	4.205	4.138	3.669	3.885	3.777	2.842	3.157	3.000
250	4.156	4.289	4.223	3.754	3.970	3.862	2.929	3.242	3.085
260	4.241	4.373	4.307	3.840	4.054	3.947	3.015	3.328	3.171
270	4.326	4.458	4.392	3.840	4.139	3.989	3.015	3.413	3.214
280	4.326	4.542	4.434	3.925	4.307	4.116	3.101	3.413	3.257
290	4.411	4.626	4.518	4.010	4.392	4.201	3.187	3.498	3.343
300	4.495	4.710	4.603	4.096	4.476	4.286	3.187	3.584	3.385

%strains of FG/M50+N50 Mixes

N	Nd = 75			Nd = 100			Nd = 125		
	#1	#2	ave.	#1	#2	ave.	#1	#2	ave.
5	0.254	0.254	0.254	0.341	0.341	0.341	0.258	0.257	0.257
10	0.592	0.593	0.592	0.596	0.596	0.596	0.516	0.428	0.472
15	0.761	0.847	0.804	0.767	0.767	0.767	0.688	0.599	0.644
20	0.930	1.017	0.973	0.937	0.937	0.937	0.775	0.770	0.772
25	1.099	1.186	1.143	1.107	1.107	1.107	0.947	0.941	0.944
30	1.268	1.356	1.312	1.278	1.278	1.278	1.033	1.027	1.030
35	1.437	1.525	1.481	1.448	1.363	1.405	1.205	1.112	1.158
40	1.522	1.610	1.566	1.533	1.533	1.533	1.291	1.283	1.287
45	1.691	1.780	1.735	1.618	1.618	1.618	1.377	1.369	1.373
50	1.775	1.864	1.820	1.789	1.704	1.746	1.463	1.454	1.459
55	1.944	2.034	1.989	1.874	1.874	1.874	1.549	1.540	1.544
60	2.029	2.119	2.074	1.959	1.959	1.959	1.635	1.625	1.630
65	2.113	2.203	2.158	2.129	2.044	2.087	1.721	1.711	1.716
70	2.198	2.288	2.243	2.215	2.129	2.172	1.807	1.796	1.802
75	2.367	2.458	2.412	2.300	2.215	2.257	1.893	1.882	1.888
80	2.451	2.542	2.497	2.385	2.300	2.342	1.979	1.967	1.973
85	2.536	2.627	2.582	2.470	2.385	2.428	2.065	2.053	2.059
90	2.620	2.712	2.666	2.555	2.470	2.513	2.151	2.139	2.145
95	2.705	2.797	2.751	2.641	2.555	2.598	2.151	2.224	2.188
100	2.790	2.881	2.835	2.726	2.641	2.683	2.238	2.224	2.231
110	2.959	3.051	3.005	2.896	2.811	2.853	2.410	2.395	2.402
120	3.128	3.220	3.174	3.066	2.981	3.024	2.496	2.566	2.531
130	3.297	3.390	3.343	3.237	3.152	3.194	2.668	2.652	2.660
140	3.466	3.559	3.513	3.407	3.322	3.365	2.754	2.823	2.788
150	3.635	3.729	3.682	3.578	3.492	3.535	2.840	2.994	2.917
160	3.804	3.898	3.851	3.748	3.578	3.663	3.012	3.080	3.046
170	3.888	4.068	3.978	3.918	3.748	3.833	3.098	3.251	3.174
180	4.057	4.237	4.147	4.089	3.918	4.003	3.184	3.336	3.260
190	4.227	4.407	4.317	4.259	4.089	4.174	3.356	3.507	3.432
200	4.396	4.576	4.486	4.429	4.174	4.302	3.442	3.593	3.518
210	4.480	4.746	4.613	4.600	4.344	4.472	3.528	3.764	3.646
220	4.649	4.915	4.782	4.770	4.514	4.642	3.614	3.849	3.732
230	4.818	5.085	4.952	4.940	4.685	4.813	3.787	4.021	3.904
240	4.903	5.254	5.079	5.111	4.855	4.983	3.873	4.106	3.989
250	5.072	5.424	5.248	5.281	4.940	5.111	3.959	4.277	4.118
260	5.241	5.593	5.417	5.451	5.111	5.281	4.045	4.363	4.204
270	5.410	5.763	5.586	5.622	5.281	5.451	4.131	4.534	4.332
280	5.495	5.932	5.713	5.792	5.451	5.622	4.303	4.619	4.461
290	5.664	6.102	5.883	5.963	5.622	5.792	4.389	4.790	4.590
300	5.833	6.271	6.052	6.133	5.792	5.963	4.475	4.876	4.676

%strains of DG/M100+N0 Mixes

N	Nd = 75			Nd = 100			Nd = 125		
	#1	#2	ave.	#1	#2	ave.	#1	#2	ave.
5	0.338	0.337	0.337	0.342	0.253	0.297	0.256	0.340	0.298
10	0.676	0.673	0.675	0.598	0.506	0.552	0.512	0.509	0.511
15	0.845	0.842	0.844	0.769	0.759	0.764	0.683	0.679	0.681
20	1.099	1.094	1.097	0.940	0.927	0.934	0.768	0.849	0.808
25	1.268	1.263	1.265	1.111	1.012	1.061	0.939	1.019	0.979
30	1.437	1.431	1.434	1.197	1.180	1.189	1.024	1.104	1.064
35	1.606	1.599	1.603	1.368	1.265	1.316	1.109	1.188	1.149
40	1.691	1.684	1.687	1.453	1.433	1.443	1.195	1.358	1.276
45	1.860	1.852	1.856	1.624	1.518	1.571	1.280	1.443	1.361
50	1.944	2.020	1.982	1.709	1.602	1.656	1.365	1.528	1.447
55	2.113	2.104	2.109	1.795	1.686	1.741	1.451	1.613	1.532
60	2.198	2.189	2.193	1.880	1.771	1.825	1.536	1.698	1.617
65	2.282	2.357	2.320	1.966	1.855	1.910	1.621	1.783	1.702
70	2.367	2.441	2.404	2.051	1.939	1.995	1.706	1.868	1.787
75	2.451	2.525	2.488	2.137	2.024	2.080	1.792	1.952	1.872
80	2.620	2.609	2.615	2.222	2.108	2.165	1.792	2.037	1.915
85	2.705	2.694	2.699	2.308	2.192	2.250	1.877	2.037	1.957
90	2.790	2.862	2.826	2.308	2.277	2.292	1.962	2.122	2.042
95	2.874	2.946	2.910	2.393	2.277	2.335	2.048	2.207	2.127
100	2.959	3.030	2.994	2.479	2.361	2.420	2.048	2.292	2.170
110	3.128	3.199	3.163	2.564	2.530	2.547	2.133	2.377	2.255
120	3.297	3.283	3.290	2.735	2.614	2.674	2.304	2.547	2.425
130	3.381	3.451	3.416	2.821	2.698	2.759	2.389	2.632	2.510
140	3.550	3.620	3.585	2.906	2.867	2.886	2.474	2.801	2.638
150	3.719	3.788	3.754	2.991	2.951	2.971	2.560	2.886	2.723
160	3.804	3.872	3.838	3.162	3.035	3.099	2.645	2.971	2.808
170	3.973	4.040	4.007	3.248	3.120	3.184	2.730	3.056	2.893
180	4.057	4.125	4.091	3.333	3.204	3.269	2.816	3.141	2.978
190	4.227	4.293	4.260	3.419	3.288	3.354	2.901	3.311	3.106
200	4.311	4.377	4.344	3.504	3.457	3.481	2.901	3.396	3.148
210	4.480	4.545	4.513	3.590	3.541	3.566	2.986	3.480	3.233
220	4.565	4.630	4.597	3.675	3.626	3.650	3.072	3.565	3.319
230	4.734	4.798	4.766	3.761	3.626	3.693	3.157	3.650	3.404
240	4.818	4.882	4.850	3.761	3.710	3.735	3.242	3.735	3.489
250	4.987	5.051	5.019	3.846	3.794	3.820	3.328	3.820	3.574
260	5.072	5.135	5.103	3.932	3.879	3.905	3.328	3.905	3.616
270	5.156	5.219	5.188	4.017	3.963	3.990	3.413	3.990	3.701
280	5.325	5.387	5.356	4.103	4.047	4.075	3.498	4.160	3.829
290	5.410	5.471	5.441	4.188	4.132	4.160	3.584	4.244	3.914
300	5.579	5.556	5.567	4.188	4.132	4.160	3.584	4.329	3.956

%strains of DG/M75+N25 Mixes

N	Nd = 75			Nd = 100			Nd = 125		
	#1	#2	ave.	#1	#2	ave.	#1	#2	ave.
5	0.336	0.252	0.294	0.339	0.253	0.296	0.255	0.170	0.213
10	0.673	0.504	0.589	0.593	0.506	0.550	0.426	0.425	0.425
15	0.841	0.756	0.799	0.762	0.675	0.719	0.596	0.595	0.595
20	1.009	1.008	1.009	0.931	0.844	0.888	0.766	0.765	0.766
25	1.262	1.176	1.219	1.101	1.013	1.057	0.851	0.850	0.851
30	1.346	1.345	1.345	1.185	1.097	1.141	1.021	0.935	0.978
35	1.514	1.429	1.471	1.355	1.266	1.310	1.021	1.105	1.063
40	1.682	1.597	1.639	1.439	1.350	1.395	1.191	1.190	1.191
45	1.766	1.765	1.765	1.524	1.519	1.522	1.277	1.276	1.276
50	1.850	1.849	1.850	1.693	1.603	1.648	1.362	1.361	1.361
55	2.019	2.017	2.018	1.778	1.688	1.733	1.362	1.446	1.404
60	2.103	2.101	2.102	1.863	1.772	1.817	1.447	1.446	1.446
65	2.187	2.185	2.186	1.948	1.857	1.902	1.532	1.531	1.531
70	2.271	2.353	2.312	2.032	2.025	2.029	1.617	1.616	1.616
75	2.355	2.437	2.396	2.117	2.110	2.113	1.617	1.701	1.659
80	2.439	2.521	2.480	2.202	2.194	2.198	1.702	1.786	1.744
85	2.607	2.605	2.606	2.286	2.278	2.282	1.787	1.786	1.786
90	2.607	2.689	2.648	2.371	2.363	2.367	1.872	1.871	1.872
95	2.691	2.773	2.732	2.456	2.447	2.451	1.872	1.956	1.914
100	2.775	2.857	2.816	2.540	2.447	2.494	1.957	1.956	1.957
110	2.944	3.109	3.026	2.710	2.616	2.663	2.043	2.126	2.084
120	3.112	3.277	3.195	2.879	2.785	2.832	2.128	2.211	2.169
130	3.280	3.445	3.363	3.048	2.954	3.001	2.213	2.296	2.254
140	3.364	3.613	3.489	3.133	3.122	3.128	2.298	2.381	2.339
150	3.532	3.697	3.615	3.302	3.207	3.255	2.383	2.466	2.424
160	3.616	3.866	3.741	3.472	3.376	3.424	2.468	2.551	2.510
170	3.785	4.034	3.909	3.556	3.544	3.550	2.553	2.636	2.595
180	3.869	4.202	4.035	3.726	3.629	3.677	2.638	2.721	2.680
190	4.037	4.286	4.161	3.895	3.797	3.846	2.723	2.806	2.765
200	4.121	4.454	4.287	3.980	3.966	3.973	2.723	2.891	2.807
210	4.205	4.622	4.414	4.149	4.051	4.100	2.809	2.891	2.850
220	4.373	4.706	4.540	4.318	4.219	4.269	2.894	2.976	2.935
230	4.458	4.874	4.666	4.403	4.388	4.396	2.979	3.061	3.020
240	4.542	5.042	4.792	4.572	4.473	4.522	2.979	3.146	3.062
250	4.710	5.126	4.918	4.742	4.641	4.692	3.064	3.231	3.148
260	4.794	5.294	5.044	4.826	4.810	4.818	3.149	3.231	3.190
270	4.878	5.462	5.170	4.996	4.979	4.987	3.149	3.316	3.233
280	4.962	5.546	5.254	5.165	5.063	5.114	3.234	3.401	3.318
290	5.130	5.714	5.422	5.334	5.232	5.283	3.319	3.401	3.360
300	5.214	5.882	5.548	5.504	5.401	5.452	3.319	3.486	3.403

%strains of DG/M50+N50 Mixes

N	Nd = 75			Nd = 100			Nd = 125		
	#1	#2	ave.	#1	#2	ave.	#1	#2	ave.
5	0.341	0.339	0.340	0.256	0.341	0.298	0.257	0.343	0.300
10	0.597	0.678	0.637	0.512	0.597	0.554	0.429	0.514	0.471
15	0.853	0.847	0.850	0.768	0.767	0.768	0.600	0.686	0.643
20	1.023	1.102	1.062	0.939	0.938	0.938	0.772	0.857	0.814
25	1.194	1.271	1.232	1.109	1.108	1.109	0.858	0.943	0.900
30	1.364	1.356	1.360	1.280	1.279	1.279	0.943	1.114	1.029
35	1.535	1.525	1.530	1.365	1.364	1.365	1.115	1.200	1.157
40	1.705	1.695	1.700	1.536	1.449	1.493	1.201	1.285	1.243
45	1.790	1.864	1.827	1.621	1.620	1.620	1.286	1.371	1.329
50	1.961	1.949	1.955	1.792	1.705	1.748	1.286	1.457	1.372
55	2.046	2.034	2.040	1.877	1.790	1.834	1.372	1.542	1.457
60	2.131	2.203	2.167	1.962	1.876	1.919	1.458	1.628	1.543
65	2.302	2.288	2.295	2.133	1.961	2.047	1.544	1.714	1.629
70	2.387	2.373	2.380	2.218	2.046	2.132	1.630	1.799	1.714
75	2.472	2.542	2.507	2.304	2.217	2.260	1.630	1.885	1.757
80	2.643	2.627	2.635	2.389	2.302	2.345	1.715	1.971	1.843
85	2.728	2.712	2.720	2.560	2.387	2.473	1.801	1.971	1.886
90	2.813	2.797	2.805	2.645	2.472	2.559	1.801	2.057	1.929
95	2.899	2.881	2.890	2.730	2.558	2.644	1.887	2.142	2.015
100	2.984	2.966	2.975	2.816	2.558	2.687	1.973	2.228	2.100
110	3.154	3.136	3.145	2.986	2.728	2.857	2.058	2.314	2.186
120	3.410	3.390	3.400	3.157	2.899	3.028	2.144	2.399	2.272
130	3.581	3.559	3.570	3.328	3.069	3.198	2.230	2.571	2.400
140	3.751	3.729	3.740	3.498	3.240	3.369	2.316	2.656	2.486
150	3.922	3.898	3.910	3.669	3.410	3.540	2.316	2.742	2.529
160	4.177	4.068	4.123	3.840	3.495	3.667	2.401	2.913	2.657
170	4.348	4.237	4.293	4.010	3.666	3.838	2.487	2.999	2.743
180	4.518	4.407	4.463	4.181	3.836	4.009	2.573	3.085	2.829
190	4.689	4.492	4.590	4.352	4.007	4.179	2.659	3.171	2.915
200	4.945	4.661	4.803	4.522	4.092	4.307	2.659	3.256	2.957
210	5.115	4.831	4.973	4.693	4.263	4.478	2.744	3.342	3.043
220	5.371	5.000	5.185	4.863	4.433	4.648	2.830	3.428	3.129
230	5.541	5.169	5.355	5.034	4.604	4.819	2.830	3.513	3.172
240	5.712	5.339	5.525	5.290	4.774	5.032	2.916	3.599	3.257
250	5.968	5.508	5.738	5.461	4.945	5.203	3.002	3.685	3.343
260	6.138	5.593	5.866	5.631	5.115	5.373	3.002	3.770	3.386
270	6.394	5.763	6.078	5.802	5.286	5.544	3.087	3.856	3.472
280	6.564	5.932	6.248	5.973	5.456	5.714	3.173	3.942	3.557
290	6.735	6.102	6.418	6.143	5.541	5.842	3.173	4.027	3.600
300	6.991	6.271	6.631	6.314	5.712	6.013	3.259	4.113	3.686

%strains of CG/M100+N0 Mixes

N	Nd = 75			Nd = 100			Nd = 125		
	#1	#2	ave.	#1	#2	ave.	#1	#2	ave.
5	0.422	0.421	0.422	0.424	0.334	0.379	0.342	0.339	0.340
10	0.676	0.758	0.717	0.679	0.668	0.673	0.598	0.594	0.596
15	1.014	1.095	1.054	0.933	0.835	0.884	0.769	0.763	0.766
20	1.182	1.264	1.223	1.103	1.085	1.094	0.939	0.933	0.936
25	1.436	1.516	1.476	1.272	1.252	1.262	1.110	1.018	1.064
30	1.605	1.685	1.645	1.442	1.419	1.430	1.196	1.187	1.192
35	1.774	1.853	1.814	1.612	1.586	1.599	1.366	1.272	1.319
40	1.943	2.022	1.982	1.781	1.753	1.767	1.452	1.357	1.404
45	2.111	2.190	2.151	1.866	1.836	1.851	1.537	1.442	1.490
50	2.280	2.359	2.320	2.036	2.003	2.019	1.623	1.612	1.617
55	2.365	2.527	2.446	2.120	2.087	2.104	1.708	1.696	1.702
60	2.534	2.612	2.573	2.290	2.254	2.272	1.793	1.781	1.787
65	2.618	2.780	2.699	2.375	2.337	2.356	1.879	1.781	1.830
70	2.787	2.949	2.868	2.545	2.421	2.483	1.964	1.866	1.915
75	2.872	3.033	2.952	2.629	2.588	2.608	2.050	1.951	2.000
80	3.041	3.201	3.121	2.714	2.671	2.693	2.135	2.036	2.085
85	3.125	3.286	3.205	2.799	2.755	2.777	2.220	2.120	2.170
90	3.209	3.370	3.290	2.969	2.838	2.903	2.306	2.205	2.255
95	3.294	3.538	3.416	3.053	3.005	3.029	2.306	2.205	2.255
100	3.463	3.623	3.543	3.138	3.088	3.113	2.391	2.290	2.341
110	3.632	3.791	3.711	3.308	3.255	3.282	2.562	2.460	2.511
120	3.801	4.044	3.922	3.478	3.422	3.450	2.647	2.545	2.596
130	3.970	4.212	4.091	3.647	3.673	3.660	2.733	2.629	2.681
140	4.139	4.465	4.302	3.902	3.840	3.871	2.904	2.714	2.809
150	4.307	4.634	4.470	4.071	4.007	4.039	2.989	2.884	2.936
160	4.476	4.802	4.639	4.241	4.174	4.207	3.074	2.969	3.021
170	4.645	4.971	4.808	4.411	4.341	4.376	3.160	3.053	3.107
180	4.814	5.223	5.019	4.580	4.508	4.544	3.245	3.138	3.192
190	4.983	5.392	5.187	4.750	4.674	4.712	3.330	3.223	3.277
200	5.152	5.560	5.356	4.919	4.841	4.880	3.501	3.308	3.405
210	5.321	5.729	5.525	5.089	4.925	5.007	3.587	3.393	3.490
220	5.490	5.897	5.694	5.259	5.092	5.175	3.672	3.478	3.575
230	5.659	6.066	5.862	5.428	5.259	5.344	3.757	3.562	3.660
240	5.828	6.234	6.031	5.598	5.426	5.512	3.843	3.562	3.703
250	5.912	6.403	6.157	5.768	5.593	5.680	3.928	3.647	3.788
260	6.081	6.571	6.326	5.937	5.760	5.848	3.928	3.732	3.830
270	6.250	6.824	6.537	6.107	5.927	6.017	4.014	3.817	3.915
280	6.419	6.992	6.706	6.277	6.093	6.185	4.099	3.902	4.000
290	6.588	7.161	6.874	6.446	6.260	6.353	4.184	3.902	4.043
300	6.757	7.329	7.043	6.616	6.427	6.522	4.270	3.986	4.128

%strains of CG/M75+N25 Mixes

N	Nd = 75			Nd = 100			Nd = 125		
	#1	#2	ave.	#1	#2	ave.	#1	#2	ave.
5	0.338	0.339	0.339	0.423	0.339	0.381	0.256	0.253	0.255
10	0.677	0.677	0.677	0.676	0.593	0.635	0.512	0.506	0.509
15	0.931	0.847	0.889	0.845	0.847	0.846	0.683	0.759	0.721
20	1.100	1.101	1.100	1.014	1.017	1.016	0.854	0.844	0.849
25	1.269	1.270	1.270	1.183	1.186	1.185	0.939	1.013	0.976
30	1.438	1.439	1.439	1.268	1.356	1.312	1.110	1.181	1.146
35	1.607	1.609	1.608	1.437	1.441	1.439	1.196	1.266	1.231
40	1.777	1.778	1.777	1.522	1.610	1.566	1.366	1.350	1.358
45	1.861	1.863	1.862	1.691	1.695	1.693	1.452	1.519	1.485
50	2.030	2.032	2.031	1.775	1.780	1.777	1.537	1.603	1.570
55	2.115	2.117	2.116	1.860	1.864	1.862	1.623	1.688	1.655
60	2.284	2.202	2.243	1.944	2.034	1.989	1.708	1.772	1.740
65	2.369	2.371	2.370	2.113	2.119	2.116	1.793	1.857	1.825
70	2.538	2.456	2.497	2.198	2.203	2.201	1.879	1.941	1.910
75	2.623	2.540	2.581	2.282	2.288	2.285	1.964	2.025	1.995
80	2.707	2.625	2.666	2.367	2.373	2.370	2.050	2.110	2.080
85	2.876	2.794	2.835	2.451	2.458	2.455	2.135	2.194	2.165
90	2.961	2.879	2.920	2.536	2.542	2.539	2.220	2.278	2.249
95	3.046	2.964	3.005	2.536	2.627	2.582	2.306	2.363	2.334
100	3.130	3.048	3.089	2.620	2.627	2.624	2.306	2.363	2.334
110	3.384	3.218	3.301	2.790	2.797	2.793	2.477	2.532	2.504
120	3.553	3.387	3.470	2.959	2.966	2.962	2.647	2.700	2.674
130	3.723	3.556	3.639	3.128	3.136	3.132	2.733	2.869	2.801
140	3.976	3.810	3.893	3.212	3.220	3.216	2.904	2.954	2.929
150	4.146	3.895	4.020	3.381	3.390	3.386	2.989	3.122	3.056
160	4.315	4.064	4.190	3.466	3.475	3.470	3.074	3.207	3.141
170	4.484	4.234	4.359	3.635	3.644	3.639	3.245	3.376	3.310
180	4.653	4.403	4.528	3.719	3.729	3.724	3.330	3.460	3.395
190	4.822	4.572	4.697	3.804	3.898	3.851	3.501	3.629	3.565
200	4.992	4.742	4.867	3.973	3.983	3.978	3.587	3.713	3.650
210	5.161	4.911	5.036	4.057	4.153	4.105	3.757	3.882	3.820
220	5.330	5.080	5.205	4.227	4.237	4.232	3.843	3.966	3.905
230	5.499	5.165	5.332	4.311	4.407	4.359	3.928	4.135	4.032
240	5.668	5.334	5.501	4.480	4.492	4.486	4.099	4.219	4.159
250	5.838	5.504	5.671	4.565	4.661	4.613	4.184	4.388	4.286
260	6.007	5.673	5.840	4.649	4.746	4.697	4.355	4.473	4.414
270	6.176	5.758	5.967	4.818	4.915	4.867	4.441	4.641	4.541
280	6.345	5.927	6.136	4.903	5.000	4.951	4.526	4.726	4.626
290	6.514	6.097	6.305	4.987	5.085	5.036	4.697	4.895	4.796
300	6.684	6.181	6.432	5.156	5.254	5.205	4.782	4.979	4.881

%strains of CG/M50+N50 Mixes

N	Nd = 75			Nd = 100			Nd = 125		
	#1	#2	ave.	#1	#2	ave.	#1	#2	ave.
5	0.426	0.422	0.424	0.256	0.339	0.297	0.255	0.254	0.255
10	0.767	0.759	0.763	0.512	0.593	0.553	0.510	0.508	0.509
15	1.022	1.012	1.017	0.769	0.847	0.808	0.680	0.678	0.679
20	1.278	1.180	1.229	0.939	1.016	0.978	0.850	0.847	0.849
25	1.533	1.433	1.483	1.025	1.101	1.063	1.020	0.932	0.976
30	1.704	1.602	1.653	1.196	1.270	1.233	1.105	1.102	1.104
35	1.959	1.771	1.865	1.366	1.355	1.361	1.276	1.186	1.231
40	2.129	1.939	2.034	1.452	1.524	1.488	1.361	1.271	1.316
45	2.300	2.108	2.204	1.537	1.609	1.573	1.446	1.356	1.401
50	2.470	2.277	2.373	1.708	1.693	1.701	1.616	1.441	1.528
55	2.726	2.445	2.585	1.793	1.863	1.828	1.701	1.525	1.613
60	2.896	2.530	2.713	1.879	1.948	1.913	1.786	1.610	1.698
65	3.066	2.698	2.882	1.964	2.032	1.998	1.871	1.695	1.783
70	3.237	2.867	3.052	2.135	2.117	2.126	1.956	1.780	1.868
75	3.407	2.951	3.179	2.220	2.202	2.211	2.041	1.864	1.953
80	3.578	3.120	3.349	2.306	2.286	2.296	2.126	1.949	2.038
85	3.748	3.288	3.518	2.391	2.371	2.381	2.211	2.034	2.122
90	3.918	3.373	3.645	2.477	2.456	2.466	2.296	2.119	2.207
95	4.089	3.541	3.815	2.562	2.540	2.551	2.381	2.119	2.250
100	4.259	3.626	3.942	2.647	2.625	2.636	2.466	2.203	2.335
110	4.600	3.963	4.281	2.818	2.794	2.806	2.636	2.373	2.504
120	4.940	4.216	4.578	2.989	2.879	2.934	2.806	2.458	2.632
130	5.366	4.469	4.918	3.160	3.048	3.104	2.976	2.627	2.802
140	5.707	4.806	5.257	3.330	3.218	3.274	3.146	2.712	2.929
150	6.048	5.059	5.553	3.501	3.302	3.402	3.231	2.881	3.056
160	6.388	5.312	5.850	3.672	3.472	3.572	3.401	2.966	3.184
170	6.814	5.649	6.232	3.757	3.556	3.657	3.571	3.051	3.311
180	7.155	5.987	6.571	3.928	3.726	3.827	3.741	3.220	3.481
190	7.411	6.239	6.825	4.099	3.810	3.955	3.912	3.305	3.608
200	7.751	6.577	7.164	4.270	3.980	4.125	4.082	3.475	3.778
210	8.007	6.914	7.460	4.355	4.064	4.210	4.252	3.559	3.906
220	8.348	7.167	7.757	4.526	4.234	4.380	4.422	3.644	4.033
230	8.603	7.504	8.054	4.697	4.318	4.508	4.592	3.729	4.160
240	8.773	7.757	8.265	4.868	4.488	4.678	4.762	3.898	4.330
250	9.029	8.010	8.520	5.038	4.657	4.848	4.932	3.983	4.458
260	9.284	8.263	8.774	5.124	4.742	4.933	5.102	4.068	4.585
270	9.455	8.432	8.943	5.295	4.911	5.103	5.272	4.237	4.755
280	9.625	8.685	9.155	5.465	4.996	5.231	5.527	4.322	4.925
290	9.796	8.938	9.367	5.636	5.165	5.401	5.697	4.407	5.052
300	9.966	9.106	9.536	5.722	5.250	5.486	5.867	4.576	5.222

%strains of 3BD2-3013 Mixes

N	#1	#2	#3	ave.
5	0.507	0.502	0.422	0.477
10	0.930	0.921	0.845	0.898
15	1.268	1.255	1.098	1.207
20	1.606	1.590	1.436	1.544
25	1.860	1.925	1.689	1.825
30	2.198	2.176	1.943	2.105
35	2.367	2.427	2.196	2.330
40	2.620	2.678	2.449	2.583
45	2.874	2.845	2.703	2.807
50	3.128	3.096	2.872	3.032
55	3.297	3.264	3.125	3.228
60	3.466	3.515	3.378	3.453
65	3.719	3.682	3.632	3.678
70	3.888	3.933	3.801	3.874
75	4.057	4.100	4.054	4.071
80	4.311	4.268	4.307	4.295
85	4.480	4.519	4.561	4.520
90	4.649	4.686	4.814	4.717
95	4.818	4.854	4.983	4.885
100	4.987	5.021	5.236	5.082
110	5.241	5.356	5.743	5.447
120	5.579	5.774	6.166	5.840
130	5.833	6.109	6.672	6.205
140	6.171	6.444	7.095	6.570
150	6.424	6.862	7.601	6.963
160	6.678	7.197	7.939	7.271
170	6.932	7.531	8.361	7.608
180	7.101	7.866	8.699	7.889
190	7.354	8.201	9.037	8.197
200	7.608	8.536	9.375	8.506
210	7.861	8.870	9.713	8.815
220	8.115	9.121	9.966	9.068
230	8.284	9.372	10.220	9.292
240	8.538	9.623	10.473	9.545
250	8.791	9.874	10.726	9.797
260	8.960	10.126	10.895	9.994
270	9.129	10.293	11.064	10.162
280	9.383	10.544	11.233	10.387
290	9.552	10.711	11.402	10.555
300	9.721	10.879	11.571	10.724

%strains of 3BD2-3012 Mixes

N	#1	#2	#3	ave.
5	0.337	0.419	0.337	0.364
10	0.590	0.671	0.673	0.645
15	0.843	0.923	0.926	0.897
20	1.096	1.091	1.094	1.094
25	1.265	1.342	1.347	1.318
30	1.433	1.510	1.515	1.486
35	1.602	1.678	1.684	1.654
40	1.771	1.762	1.768	1.767
45	1.939	1.930	1.936	1.935
50	2.108	2.013	2.020	2.047
55	2.192	2.181	2.189	2.187
60	2.361	2.265	2.273	2.300
65	2.445	2.349	2.441	2.412
70	2.530	2.517	2.525	2.524
75	2.614	2.601	2.609	2.608
80	2.782	2.685	2.694	2.720
85	2.867	2.768	2.778	2.804
90	2.951	2.852	2.862	2.888
95	3.035	3.020	3.030	3.029
100	3.120	3.104	3.114	3.113
110	3.288	3.272	3.283	3.281
120	3.457	3.440	3.451	3.449
130	3.626	3.607	3.620	3.618
140	3.794	3.775	3.704	3.758
150	3.879	3.943	3.872	3.898
160	4.047	4.111	4.040	4.066
170	4.132	4.279	4.209	4.206
180	4.300	4.446	4.293	4.346
190	4.384	4.530	4.461	4.459
200	4.553	4.698	4.630	4.627
210	4.637	4.866	4.798	4.767
220	4.806	4.950	4.882	4.879
230	4.890	5.117	5.051	5.019
240	4.975	5.285	5.135	5.132
250	5.059	5.369	5.303	5.244
260	5.228	5.537	5.471	5.412
270	5.312	5.621	5.556	5.496
280	5.396	5.789	5.724	5.636
290	5.481	5.872	5.808	5.720
300	5.565	5.956	5.976	5.833

%strains of 3BD2-3013' Mixes

N	#1	#2	#3	ave.
5	0.501	0.334	0.336	0.390
10	0.918	0.669	0.672	0.753
15	1.252	0.920	1.008	1.060
20	1.503	1.171	1.259	1.311
25	1.836	1.338	1.511	1.562
30	2.003	1.505	1.679	1.729
35	2.254	1.672	1.847	1.924
40	2.504	1.839	2.099	2.148
45	2.671	2.007	2.267	2.315
50	2.838	2.174	2.435	2.482
55	3.088	2.341	2.603	2.677
60	3.255	2.508	2.771	2.845
65	3.422	2.592	2.855	2.956
70	3.589	2.759	3.023	3.124
75	3.756	2.926	3.191	3.291
80	3.923	3.010	3.359	3.431
85	4.090	3.177	3.442	3.570
90	4.257	3.261	3.610	3.709
95	4.424	3.344	3.778	3.849
100	4.591	3.512	3.862	3.988
110	4.925	3.679	4.114	4.239
120	5.259	3.930	4.366	4.518
130	5.509	4.097	4.618	4.741
140	5.843	4.348	4.870	5.020
150	6.177	4.599	5.038	5.271
160	6.427	4.766	5.290	5.494
170	6.761	5.017	5.458	5.745
180	7.012	5.268	5.709	5.996
190	7.262	5.435	5.877	6.191
200	7.513	5.686	6.129	6.442
210	7.679	5.936	6.297	6.638
220	7.930	6.104	6.549	6.861
230	8.097	6.355	6.717	7.056
240	8.264	6.522	6.885	7.223
250	8.431	6.689	7.053	7.391
260	8.514	6.940	7.221	7.558
270	8.681	7.107	7.389	7.726
280	8.765	7.274	7.473	7.837
290	8.932	7.441	7.641	8.005
300	9.015	7.609	7.809	8.144

%strains of Benton '02 R1 Mixes

N	#1	#2	#3	ave.
5	0.508	0.425	0.424	0.452
10	0.931	0.850	0.849	0.877
15	1.354	1.276	1.188	1.273
20	1.692	1.616	1.443	1.584
25	2.030	1.956	1.698	1.895
30	2.284	2.211	1.952	2.149
35	2.538	2.551	2.207	2.432
40	2.792	2.806	2.462	2.687
45	3.046	3.061	2.632	2.913
50	3.299	3.316	2.886	3.167
55	3.553	3.571	3.056	3.394
60	3.807	3.827	3.311	3.648
65	4.061	4.167	3.480	3.903
70	4.315	4.422	3.650	4.129
75	4.484	4.592	3.905	4.327
80	4.738	4.847	4.075	4.553
85	4.992	5.102	4.329	4.808
90	5.161	5.357	4.499	5.006
95	5.415	5.612	4.669	5.232
100	5.668	5.867	4.924	5.486
110	6.176	6.378	5.263	5.939
120	6.599	6.888	5.688	6.391
130	7.107	7.313	6.027	6.816
140	7.614	7.738	6.367	7.240
150	8.037	8.163	6.621	7.607
160	8.376	8.588	6.961	7.975
170	8.799	8.929	7.301	8.343
180	9.137	9.269	7.640	8.682
190	9.391	9.524	7.895	8.936
200	9.729	9.864	8.149	9.248
210	9.898	10.119	8.404	9.474
220	10.152	10.289	8.659	9.700
230	10.406	10.544	8.913	9.955
240	10.575	10.714	9.168	10.153
250	10.829	10.884	9.338	10.350
260	10.998	11.054	9.508	10.520
270	11.168	11.224	9.677	10.690
280	11.252	11.395	9.847	10.831
290	11.421	11.480	10.017	10.973
300	11.591	11.565	10.187	11.114

%strains of ABD2 - 5014 Mixes

N	#1	#2	#3	ave.
5	0.333	0.334	0.334	0.334
10	0.666	0.668	0.669	0.668
15	0.999	0.918	0.920	0.946
20	1.249	1.169	1.171	1.196
25	1.499	1.336	1.421	1.419
30	1.749	1.503	1.589	1.613
35	1.915	1.669	1.756	1.780
40	2.082	1.836	2.007	1.975
45	2.331	2.003	2.174	2.170
50	2.498	2.087	2.341	2.309
55	2.664	2.254	2.425	2.448
60	2.831	2.337	2.592	2.587
65	2.998	2.421	2.759	2.726
70	3.164	2.588	2.926	2.893
75	3.331	2.671	3.010	3.004
80	3.414	2.755	3.177	3.115
85	3.580	2.922	3.344	3.282
90	3.747	3.005	3.428	3.393
95	3.830	3.088	3.595	3.505
100	3.997	3.172	3.679	3.616
110	4.246	3.339	4.013	3.866
120	4.496	3.506	4.264	4.089
130	4.746	3.673	4.515	4.311
140	5.079	3.840	4.766	4.562
150	5.329	4.007	5.017	4.784
160	5.495	4.090	5.268	4.951
170	5.745	4.257	5.518	5.174
180	5.995	4.424	5.769	5.396
190	6.245	4.508	6.020	5.591
200	6.411	4.674	6.271	5.786
210	6.661	4.758	6.522	5.980
220	6.911	4.925	6.773	6.203
230	7.077	5.008	7.023	6.370
240	7.327	5.175	7.274	6.592
250	7.494	5.259	7.525	6.759
260	7.660	5.342	7.776	6.926
270	7.910	5.509	8.027	7.149
280	8.077	5.593	8.194	7.288
290	8.160	5.676	8.445	7.427
300	8.326	5.843	8.612	7.594

%strains of SWI2 - 31 Mixes

N	#1	#2	#3	ave.
5	0.345	0.260	0.346	0.317
10	0.690	0.608	0.606	0.635
15	0.949	0.868	0.866	0.894
20	1.208	1.128	1.126	1.154
25	1.467	1.302	1.299	1.356
30	1.639	1.563	1.472	1.558
35	1.812	1.736	1.645	1.731
40	1.984	1.910	1.905	1.933
45	2.157	2.083	1.991	2.077
50	2.243	2.257	2.165	2.222
55	2.416	2.431	2.338	2.395
60	2.588	2.517	2.511	2.539
65	2.675	2.691	2.684	2.683
70	2.847	2.865	2.857	2.856
75	3.020	3.038	3.030	3.029
80	3.106	3.212	3.203	3.174
85	3.279	3.385	3.377	3.347
90	3.451	3.559	3.550	3.520
95	3.538	3.646	3.723	3.635
100	3.710	3.819	3.896	3.809
110	4.055	4.167	4.242	4.155
120	4.314	4.427	4.589	4.443
130	4.659	4.774	5.022	4.818
140	4.918	5.122	5.368	5.136
150	5.263	5.469	5.801	5.511
160	5.608	5.816	6.147	5.857
170	5.953	6.163	6.494	6.203
180	6.299	6.424	6.840	6.521
190	6.644	6.771	7.186	6.867
200	6.903	7.118	7.446	7.155
210	7.248	7.378	7.706	7.444
220	7.506	7.639	7.965	7.704
230	7.852	7.899	8.225	7.992
240	8.110	8.160	8.485	8.252
250	8.283	8.420	8.658	8.454
260	8.542	8.594	8.918	8.684
270	8.714	8.767	9.091	8.858
280	8.887	8.941	9.264	9.031
290	9.060	9.201	9.437	9.233
300	9.232	9.288	9.524	9.348

%strains of ABD2-2032 Mixes

N	#1	#2	#3	ave.
5	0.422	0.422	0.339	0.394
10	0.759	0.760	0.679	0.733
15	1.012	1.098	0.933	1.014
20	1.265	1.351	1.187	1.268
25	1.518	1.689	1.442	1.550
30	1.686	1.943	1.696	1.775
35	1.855	2.196	1.866	1.972
40	2.108	2.365	2.120	2.198
45	2.277	2.703	2.290	2.423
50	2.445	2.872	2.460	2.592
55	2.614	3.125	2.714	2.818
60	2.698	3.378	2.884	2.987
65	2.867	3.632	3.053	3.184
70	3.035	3.885	3.223	3.381
75	3.204	4.139	3.478	3.607
80	3.373	4.392	3.647	3.804
85	3.541	4.645	3.817	4.001
90	3.710	4.899	3.986	4.198
95	3.794	5.152	4.241	4.396
100	3.963	5.405	4.411	4.593
110	4.300	5.828	4.835	4.987
120	4.637	6.334	5.259	5.410
130	4.975	6.757	5.683	5.805
140	5.228	7.179	6.107	6.171
150	5.565	7.601	6.531	6.566
160	5.902	7.939	6.955	6.932
170	6.239	8.277	7.379	7.299
180	6.577	8.615	7.888	7.693
190	6.914	8.868	8.227	8.003
200	7.167	9.122	8.651	8.313
210	7.504	9.375	8.991	8.623
220	7.757	9.628	9.330	8.905
230	8.010	9.797	9.584	9.131
240	8.263	9.966	9.839	9.356
250	8.516	10.220	10.093	9.610
260	8.685	10.389	10.348	9.807
270	8.938	10.473	10.517	9.976
280	9.106	10.642	10.687	10.145
290	9.359	10.811	10.857	10.342
300	9.528	10.895	10.941	10.455

%strains of ABD2-2006 Mixes

N	#1	#2	#3	ave.
5	0.502	0.422	0.421	0.448
10	0.920	0.760	0.841	0.840
15	1.254	1.098	1.093	1.149
20	1.589	1.351	1.346	1.429
25	1.839	1.605	1.598	1.681
30	2.090	1.774	1.850	1.905
35	2.341	2.027	2.103	2.157
40	2.592	2.280	2.355	2.409
45	2.759	2.449	2.523	2.577
50	3.010	2.618	2.775	2.801
55	3.177	2.872	2.944	2.998
60	3.428	3.041	3.112	3.193
65	3.595	3.209	3.364	3.390
70	3.846	3.463	3.532	3.614
75	4.013	3.632	3.701	3.782
80	4.264	3.801	3.953	4.006
85	4.431	4.054	4.121	4.202
90	4.599	4.223	4.289	4.370
95	4.849	4.476	4.458	4.594
100	5.017	4.645	4.626	4.763
110	5.351	5.068	4.962	5.127
120	5.686	5.490	5.299	5.491
130	6.020	5.828	5.635	5.828
140	6.438	6.250	5.971	6.220
150	6.773	6.672	6.308	6.584
160	7.023	7.010	6.644	6.893
170	7.358	7.348	6.897	7.201
180	7.609	7.770	7.233	7.537
190	7.943	8.108	7.485	7.846
200	8.194	8.361	7.822	8.126
210	8.445	8.699	8.074	8.406
220	8.696	8.953	8.410	8.686
230	8.863	9.206	8.663	8.911
240	9.114	9.375	8.831	9.107
250	9.365	9.628	9.167	9.387
260	9.532	9.797	9.420	9.583
270	9.699	10.051	9.588	9.779
280	9.950	10.220	9.840	10.003
290	10.117	10.389	10.008	10.171
300	10.201	10.557	10.177	10.312

APPENDIX B - 2.

DATA SUMMARY: The RPT at $p = 100\text{psi}$

%strains of FG/M100+N0 Mixes

N	Nd = 75			Nd = 100			Nd = 125		
	#1	#2	ave.	#1	#2	ave.	#1	#2	ave.
5	0.332	0.432	0.382	0.252	0.345	0.298	0.256	0.349	0.302
10	0.664	0.691	0.678	0.588	0.603	0.596	0.511	0.524	0.518
15	0.997	1.036	1.016	0.756	0.861	0.809	0.681	0.786	0.734
20	1.163	1.209	1.186	1.008	1.034	1.021	0.852	0.961	0.906
25	1.412	1.382	1.397	1.176	1.206	1.191	1.022	1.048	1.035
30	1.578	1.554	1.566	1.345	1.378	1.361	1.107	1.223	1.165
35	1.744	1.727	1.736	1.513	1.464	1.488	1.193	1.310	1.251
40	1.910	1.900	1.905	1.597	1.637	1.617	1.363	1.397	1.380
45	2.076	1.986	2.031	1.765	1.723	1.744	1.448	1.485	1.466
50	2.159	2.159	2.159	1.849	1.809	1.829	1.533	1.572	1.553
55	2.326	2.245	2.285	1.933	1.895	1.914	1.618	1.659	1.639
60	2.492	2.418	2.455	2.101	2.067	2.084	1.704	1.747	1.725
65	2.575	2.504	2.540	2.185	2.153	2.169	1.789	1.834	1.811
70	2.658	2.591	2.624	2.269	2.239	2.254	1.874	1.921	1.898
75	2.824	2.677	2.750	2.353	2.326	2.339	1.874	2.009	1.941
80	2.907	2.763	2.835	2.437	2.412	2.424	1.959	2.096	2.028
85	2.990	2.936	2.963	2.521	2.498	2.509	2.044	2.183	2.114
90	3.073	3.022	3.048	2.605	2.584	2.595	2.129	2.183	2.156
95	3.156	3.109	3.132	2.689	2.670	2.680	2.129	2.271	2.200
100	3.322	3.195	3.259	2.773	2.756	2.765	2.215	2.358	2.286
110	3.488	3.282	3.385	2.941	2.842	2.892	2.300	2.445	2.373
120	3.654	3.454	3.554	3.109	3.015	3.062	2.385	2.533	2.459
130	3.821	3.627	3.724	3.277	3.101	3.189	2.555	2.707	2.631
140	3.987	3.800	3.893	3.361	3.273	3.317	2.641	2.795	2.718
150	4.070	3.886	3.978	3.529	3.359	3.444	2.726	2.882	2.804
160	4.236	4.059	4.147	3.613	3.531	3.572	2.811	2.969	2.890
170	4.402	4.231	4.317	3.782	3.618	3.700	2.896	3.057	2.976
180	4.485	4.318	4.401	3.866	3.704	3.785	2.981	3.144	3.063
190	4.651	4.491	4.571	3.950	3.790	3.870	3.066	3.231	3.149
200	4.817	4.577	4.697	4.118	3.962	4.040	3.066	3.319	3.193
210	4.900	4.750	4.825	4.202	4.048	4.125	3.152	3.406	3.279
220	5.066	4.836	4.951	4.286	4.134	4.210	3.237	3.493	3.365
230	5.150	5.009	5.079	4.454	4.220	4.337	3.322	3.581	3.451
240	5.233	5.095	5.164	4.538	4.307	4.422	3.407	3.581	3.494
250	5.399	5.268	5.333	4.622	4.393	4.507	3.407	3.668	3.538
260	5.482	5.354	5.418	4.706	4.479	4.592	3.492	3.755	3.624
270	5.648	5.440	5.544	4.790	4.565	4.677	3.578	3.843	3.710
280	5.731	5.613	5.672	4.958	4.651	4.805	3.578	3.930	3.754
290	5.814	5.699	5.757	5.042	4.737	4.890	3.663	3.930	3.796
300	5.980	5.872	5.926	5.126	4.910	5.018	3.748	4.017	3.883

%strains of FG/M75+N25 Mixes

N	Nd = 75			Nd = 100			Nd = 125		
	#1	#2	ave.	#1	#2	ave.	#1	#2	ave.
5	0.335	0.348	0.342	0.338	0.342	0.340	0.257	0.262	0.259
10	0.670	0.610	0.640	0.592	0.599	0.596	0.514	0.524	0.519
15	0.921	0.784	0.853	0.761	0.771	0.766	0.685	0.698	0.692
20	1.173	1.045	1.109	1.015	0.942	0.979	0.856	0.785	0.821
25	1.340	1.220	1.280	1.184	1.113	1.149	0.942	0.960	0.951
30	1.508	1.394	1.451	1.269	1.199	1.234	1.027	1.047	1.037
35	1.675	1.481	1.578	1.438	1.370	1.404	1.199	1.134	1.167
40	1.759	1.655	1.707	1.607	1.455	1.531	1.284	1.222	1.253
45	1.926	1.742	1.834	1.692	1.627	1.659	1.370	1.309	1.339
50	2.010	1.829	1.920	1.777	1.712	1.744	1.455	1.396	1.426
55	2.178	1.916	2.047	1.946	1.798	1.872	1.541	1.483	1.512
60	2.261	2.091	2.176	2.030	1.884	1.957	1.627	1.571	1.599
65	2.345	2.178	2.261	2.115	1.969	2.042	1.712	1.658	1.685
70	2.429	2.265	2.347	2.200	2.055	2.127	1.798	1.745	1.772
75	2.596	2.352	2.474	2.369	2.140	2.255	1.798	1.745	1.772
80	2.680	2.439	2.560	2.453	2.226	2.340	1.884	1.832	1.858
85	2.764	2.526	2.645	2.538	2.312	2.425	1.969	1.920	1.944
90	2.848	2.613	2.730	2.623	2.397	2.510	2.055	1.920	1.987
95	2.931	2.613	2.772	2.707	2.483	2.595	2.055	2.007	2.031
100	3.015	2.700	2.858	2.792	2.568	2.680	2.140	2.094	2.117
110	3.183	2.875	3.029	2.961	2.740	2.850	2.226	2.182	2.204
120	3.266	3.049	3.158	3.130	2.825	2.978	2.397	2.269	2.333
130	3.434	3.136	3.285	3.215	2.997	3.106	2.483	2.356	2.419
140	3.601	3.310	3.456	3.384	3.082	3.233	2.568	2.443	2.506
150	3.685	3.397	3.541	3.553	3.253	3.403	2.654	2.531	2.592
160	3.853	3.484	3.668	3.723	3.339	3.531	2.740	2.618	2.679
170	3.936	3.659	3.797	3.807	3.510	3.659	2.825	2.705	2.765
180	4.104	3.746	3.925	3.976	3.596	3.786	2.911	2.792	2.852
190	4.188	3.833	4.010	4.146	3.682	3.914	2.997	2.880	2.938
200	4.271	3.920	4.096	4.315	3.853	4.084	3.082	2.967	3.025
210	4.355	4.094	4.225	4.399	3.938	4.169	3.168	3.054	3.111
220	4.439	4.181	4.310	4.569	4.110	4.339	3.253	3.054	3.154
230	4.606	4.268	4.437	4.738	4.195	4.466	3.339	3.141	3.240
240	4.690	4.355	4.523	4.822	4.281	4.552	3.425	3.229	3.327
250	4.774	4.443	4.608	4.992	4.452	4.722	3.510	3.316	3.413
260	4.858	4.530	4.694	5.161	4.538	4.849	3.596	3.403	3.500
270	4.941	4.617	4.779	5.245	4.623	4.934	3.596	3.403	3.500
280	5.025	4.791	4.908	5.415	4.795	5.105	3.682	3.490	3.586
290	5.193	4.878	5.035	5.584	4.880	5.232	3.767	3.578	3.672
300	5.276	4.965	5.121	5.753	4.966	5.359	3.853	3.578	3.715

%strains of FG/M50+N50 Mixes

N	Nd = 75			Nd = 100			Nd = 125		
	#1	#2	ave.	#1	#2	ave.	#1	#2	ave.
5	0.345	0.341	0.343	0.260	0.344	0.302	0.260	0.260	0.260
10	0.604	0.596	0.600	0.520	0.602	0.561	0.519	0.433	0.476
15	0.863	0.852	0.857	0.694	0.775	0.734	0.693	0.693	0.693
20	1.035	1.022	1.029	0.867	0.947	0.907	0.866	0.779	0.823
25	1.208	1.193	1.200	1.041	1.119	1.080	1.039	0.952	0.996
30	1.381	1.363	1.372	1.127	1.205	1.166	1.126	1.039	1.082
35	1.553	1.533	1.543	1.214	1.377	1.296	1.212	1.212	1.212
40	1.639	1.618	1.629	1.388	1.463	1.425	1.385	1.299	1.342
45	1.812	1.789	1.800	1.474	1.549	1.512	1.472	1.385	1.429
50	1.898	1.874	1.886	1.561	1.635	1.598	1.558	1.472	1.515
55	1.984	2.044	2.014	1.648	1.807	1.728	1.645	1.558	1.602
60	2.157	2.129	2.143	1.735	1.893	1.814	1.732	1.645	1.688
65	2.243	2.215	2.229	1.821	1.979	1.900	1.818	1.732	1.775
70	2.330	2.385	2.357	1.908	2.065	1.987	1.905	1.818	1.861
75	2.416	2.470	2.443	1.995	2.151	2.073	1.991	1.905	1.948
80	2.502	2.555	2.529	2.082	2.238	2.160	2.078	1.991	2.035
85	2.588	2.641	2.614	2.168	2.238	2.203	2.165	2.078	2.121
90	2.761	2.726	2.743	2.255	2.324	2.289	2.251	2.165	2.208
95	2.761	2.811	2.786	2.342	2.410	2.376	2.338	2.251	2.294
100	2.934	2.896	2.915	2.342	2.496	2.419	2.424	2.251	2.338
110	3.020	3.066	3.043	2.515	2.582	2.548	2.511	2.424	2.468
120	3.192	3.237	3.215	2.602	2.754	2.678	2.684	2.597	2.641
130	3.365	3.407	3.386	2.775	2.840	2.808	2.857	2.684	2.771
140	3.538	3.578	3.558	2.862	3.012	2.937	2.944	2.771	2.857
150	3.710	3.663	3.686	3.036	3.098	3.067	3.117	2.944	3.030
160	3.796	3.833	3.815	3.122	3.184	3.153	3.203	3.030	3.117
170	3.969	4.003	3.986	3.209	3.356	3.283	3.377	3.203	3.290
180	4.142	4.089	4.115	3.296	3.442	3.369	3.463	3.377	3.420
190	4.314	4.259	4.287	3.469	3.528	3.499	3.636	3.463	3.550
200	4.400	4.344	4.372	3.556	3.614	3.585	3.723	3.636	3.680
210	4.573	4.514	4.544	3.643	3.701	3.672	3.896	3.723	3.810
220	4.659	4.600	4.629	3.729	3.873	3.801	3.983	3.896	3.939
230	4.832	4.770	4.801	3.816	3.959	3.887	4.156	3.983	4.069
240	5.004	4.940	4.972	3.903	4.045	3.974	4.242	4.156	4.199
250	5.091	5.026	5.058	3.990	4.131	4.060	4.416	4.242	4.329
260	5.263	5.196	5.230	4.163	4.217	4.190	4.502	4.416	4.459
270	5.349	5.281	5.315	4.250	4.303	4.276	4.675	4.502	4.589
280	5.522	5.451	5.487	4.337	4.475	4.406	4.762	4.675	4.719
290	5.608	5.537	5.572	4.423	4.561	4.492	4.935	4.762	4.848
300	5.781	5.707	5.744	4.510	4.647	4.579	5.022	4.935	4.978

%strains of DG/M100+N0 Mixes

N	Nd = 75			Nd = 100			Nd = 125		
	#1	#2	ave.	#1	#2	ave.	#1	#2	ave.
5	0.346	0.346	0.346	0.343	0.345	0.344	0.260	0.261	0.261
10	0.692	0.693	0.692	0.687	0.691	0.689	0.520	0.522	0.521
15	0.952	0.952	0.952	0.858	0.864	0.861	0.694	0.696	0.695
20	1.125	1.126	1.125	1.116	1.036	1.076	0.867	0.870	0.868
25	1.384	1.385	1.385	1.288	1.209	1.248	1.041	1.043	1.042
30	1.557	1.472	1.514	1.373	1.382	1.378	1.127	1.130	1.129
35	1.644	1.645	1.644	1.545	1.554	1.550	1.301	1.217	1.259
40	1.817	1.818	1.817	1.631	1.641	1.636	1.388	1.391	1.389
45	1.990	1.991	1.990	1.803	1.727	1.765	1.474	1.478	1.476
50	2.076	2.078	2.077	1.888	1.900	1.894	1.561	1.565	1.563
55	2.249	2.251	2.250	1.974	1.986	1.980	1.648	1.652	1.650
60	2.336	2.338	2.337	2.146	2.073	2.109	1.735	1.739	1.737
65	2.509	2.511	2.510	2.232	2.159	2.195	1.821	1.826	1.824
70	2.595	2.597	2.596	2.318	2.245	2.281	1.908	1.913	1.911
75	2.682	2.771	2.726	2.403	2.332	2.368	1.995	2.000	1.997
80	2.855	2.857	2.856	2.489	2.418	2.454	2.082	2.087	2.084
85	2.941	2.944	2.942	2.575	2.504	2.540	2.168	2.174	2.171
90	3.028	3.117	3.072	2.661	2.591	2.626	2.255	2.261	2.258
95	3.114	3.203	3.159	2.747	2.677	2.712	2.342	2.261	2.301
100	3.287	3.377	3.332	2.747	2.763	2.755	2.428	2.348	2.388
110	3.460	3.550	3.505	2.918	2.850	2.884	2.515	2.522	2.518
120	3.633	3.810	3.721	3.090	3.022	3.056	2.689	2.609	2.649
130	3.893	4.069	3.981	3.176	3.195	3.186	2.775	2.696	2.736
140	4.066	4.242	4.154	3.348	3.282	3.315	2.862	2.870	2.866
150	4.325	4.502	4.414	3.433	3.454	3.444	3.036	2.957	2.996
160	4.498	4.762	4.630	3.519	3.541	3.530	3.122	3.043	3.083
170	4.758	5.022	4.890	3.691	3.713	3.702	3.209	3.217	3.213
180	4.931	5.281	5.106	3.777	3.800	3.788	3.382	3.304	3.343
190	5.190	5.541	5.366	3.863	3.886	3.874	3.469	3.391	3.430
200	5.363	5.801	5.582	4.034	4.059	4.047	3.556	3.478	3.517
210	5.623	6.061	5.842	4.120	4.145	4.133	3.643	3.565	3.604
220	5.796	6.320	6.058	4.206	4.318	4.262	3.729	3.652	3.691
230	6.055	6.580	6.318	4.292	4.404	4.348	3.903	3.739	3.821
240	6.228	6.926	6.577	4.378	4.491	4.434	3.990	3.826	3.908
250	6.488	7.186	6.837	4.464	4.663	4.563	4.076	3.913	3.995
260	6.661	7.446	7.053	4.635	4.750	4.692	4.163	4.000	4.082
270	6.920	7.706	7.313	4.721	4.836	4.778	4.250	4.087	4.168
280	7.180	7.965	7.573	4.807	5.009	4.908	4.337	4.174	4.255
290	7.353	8.225	7.789	4.893	5.095	4.994	4.423	4.261	4.342
300	7.612	8.485	8.049	4.979	5.181	5.080	4.510	4.348	4.429

%strains of DG/M75+N25 Mixes

N	Nd = 75			Nd = 100			Nd = 125		
	#1	#2	ave.	#1	#2	ave.	#1	#2	ave.
5	0.344	0.344	0.344	0.256	0.342	0.299	0.258	0.259	0.258
10	0.688	0.687	0.688	0.513	0.599	0.556	0.516	0.517	0.517
15	0.946	0.945	0.945	0.769	0.855	0.812	0.688	0.690	0.689
20	1.118	1.203	1.160	0.940	1.027	0.983	0.860	0.862	0.861
25	1.376	1.375	1.375	1.111	1.198	1.154	0.946	0.948	0.947
30	1.548	1.546	1.547	1.282	1.369	1.325	1.118	1.121	1.119
35	1.720	1.718	1.719	1.368	1.540	1.454	1.204	1.207	1.205
40	1.892	1.890	1.891	1.453	1.625	1.539	1.290	1.293	1.291
45	1.978	1.976	1.977	1.624	1.796	1.710	1.376	1.379	1.378
50	2.150	2.148	2.149	1.709	1.882	1.796	1.462	1.466	1.464
55	2.322	2.234	2.278	1.795	1.967	1.881	1.548	1.552	1.550
60	2.408	2.405	2.407	1.966	2.139	2.052	1.634	1.638	1.636
65	2.580	2.491	2.535	2.051	2.224	2.138	1.720	1.724	1.722
70	2.666	2.663	2.664	2.137	2.310	2.223	1.806	1.810	1.808
75	2.837	2.749	2.793	2.222	2.395	2.309	1.892	1.897	1.894
80	2.923	2.835	2.879	2.308	2.566	2.437	1.978	1.983	1.980
85	3.009	3.007	3.008	2.393	2.652	2.523	2.064	2.069	2.066
90	3.181	3.093	3.137	2.479	2.737	2.608	2.064	2.069	2.066
95	3.267	3.179	3.223	2.564	2.823	2.694	2.150	2.155	2.152
100	3.353	3.265	3.309	2.650	2.908	2.779	2.236	2.241	2.238
110	3.611	3.436	3.524	2.821	3.080	2.950	2.322	2.328	2.325
120	3.783	3.694	3.739	2.906	3.251	3.078	2.408	2.500	2.454
130	4.041	3.866	3.954	3.077	3.422	3.249	2.494	2.586	2.540
140	4.213	4.038	4.126	3.248	3.593	3.420	2.666	2.672	2.669
150	4.385	4.210	4.297	3.333	3.764	3.549	2.752	2.845	2.798
160	4.643	4.381	4.512	3.504	3.935	3.720	2.837	2.931	2.884
170	4.815	4.553	4.684	3.590	4.021	3.805	2.923	3.017	2.970
180	4.987	4.725	4.856	3.761	4.192	3.976	3.009	3.103	3.056
190	5.159	4.897	5.028	3.846	4.363	4.104	3.095	3.190	3.143
200	5.417	5.069	5.243	4.017	4.534	4.275	3.181	3.276	3.229
210	5.589	5.241	5.415	4.103	4.705	4.404	3.267	3.362	3.315
220	5.761	5.412	5.587	4.274	4.790	4.532	3.353	3.448	3.401
230	5.933	5.584	5.759	4.359	4.962	4.660	3.439	3.534	3.487
240	6.191	5.756	5.973	4.530	5.133	4.831	3.439	3.621	3.530
250	6.363	5.928	6.145	4.615	5.218	4.917	3.525	3.707	3.616
260	6.535	6.100	6.317	4.701	5.389	5.045	3.611	3.793	3.702
270	6.707	6.271	6.489	4.872	5.560	5.216	3.697	3.879	3.788
280	6.965	6.443	6.704	4.957	5.731	5.344	3.783	3.966	3.874
290	7.137	6.615	6.876	5.128	5.902	5.515	3.869	4.052	3.961
300	7.309	6.787	7.048	5.214	5.988	5.601	3.869	4.138	4.004

%strains of DG/M50+N50 Mixes

N	Nd = 75			Nd = 100			Nd = 125		
	#1	#2	ave.	#1	#2	ave.	#1	#2	ave.
5	0.430	0.431	0.430	0.348	0.346	0.347	0.258	0.347	0.302
10	0.773	0.690	0.732	0.609	0.606	0.608	0.515	0.607	0.561
15	1.031	1.035	1.033	0.783	0.866	0.825	0.773	0.781	0.777
20	1.289	1.208	1.248	0.957	1.039	0.998	0.944	0.954	0.949
25	1.460	1.381	1.420	1.131	1.212	1.172	1.116	1.127	1.122
30	1.718	1.639	1.679	1.305	1.385	1.345	1.288	1.301	1.294
35	1.890	1.726	1.808	1.480	1.558	1.519	1.373	1.388	1.381
40	2.062	1.898	1.980	1.567	1.732	1.649	1.545	1.474	1.510
45	2.148	2.071	2.109	1.741	1.818	1.779	1.631	1.561	1.596
50	2.320	2.243	2.281	1.828	1.991	1.910	1.717	1.735	1.726
55	2.491	2.330	2.411	1.915	2.078	1.996	1.803	1.821	1.812
60	2.577	2.502	2.540	2.002	2.251	2.126	1.974	1.908	1.941
65	2.749	2.588	2.669	2.176	2.338	2.257	2.060	1.995	2.027
70	2.921	2.761	2.841	2.263	2.511	2.387	2.146	2.082	2.114
75	3.007	2.847	2.927	2.350	2.597	2.474	2.232	2.168	2.200
80	3.179	3.020	3.099	2.437	2.771	2.604	2.318	2.255	2.286
85	3.265	3.106	3.185	2.524	2.857	2.691	2.403	2.255	2.329
90	3.436	3.192	3.314	2.611	2.944	2.777	2.489	2.342	2.415
95	3.522	3.365	3.444	2.698	3.030	2.864	2.489	2.428	2.459
100	3.694	3.451	3.573	2.785	3.203	2.994	2.575	2.515	2.545
110	3.866	3.710	3.788	2.959	3.377	3.168	2.747	2.602	2.674
120	4.124	3.883	4.003	3.133	3.636	3.385	2.918	2.775	2.847
130	4.381	4.142	4.261	3.307	3.896	3.602	3.004	2.862	2.933
140	4.639	4.400	4.520	3.481	4.069	3.775	3.176	2.949	3.062
150	4.897	4.573	4.735	3.655	4.329	3.992	3.262	3.122	3.192
160	5.069	4.832	4.950	3.742	4.502	4.122	3.433	3.209	3.321
170	5.326	5.004	5.165	3.916	4.762	4.339	3.519	3.296	3.408
180	5.584	5.263	5.424	4.091	5.022	4.556	3.691	3.469	3.580
190	5.842	5.522	5.682	4.265	5.195	4.730	3.777	3.556	3.666
200	6.014	5.695	5.854	4.439	5.455	4.947	3.863	3.643	3.753
210	6.271	5.953	6.112	4.526	5.714	5.120	4.034	3.729	3.882
220	6.529	6.212	6.371	4.700	5.974	5.337	4.120	3.816	3.968
230	6.787	6.385	6.586	4.874	6.234	5.554	4.206	3.903	4.054
240	7.045	6.644	6.844	5.048	6.407	5.727	4.292	3.990	4.141
250	7.302	6.903	7.102	5.222	6.667	5.944	4.464	4.163	4.313
260	7.560	7.075	7.318	5.396	6.926	6.161	4.549	4.250	4.400
270	7.818	7.334	7.576	5.570	7.186	6.378	4.635	4.337	4.486
280	8.076	7.506	7.791	5.744	7.359	6.552	4.721	4.423	4.572
290	8.333	7.765	8.049	5.918	7.619	6.769	4.893	4.510	4.701
300	8.505	7.938	8.222	6.092	7.879	6.986	4.979	4.597	4.788

%strains of CG/M100+N0 Mixes

N	Nd = 75			Nd = 100			Nd = 125		
	#1	#2	ave.	#1	#2	ave.	#1	#2	ave.
5	0.419	0.425	0.422	0.419	0.425	0.422	0.337	0.259	0.298
10	0.839	0.850	0.844	0.754	0.680	0.717	0.589	0.604	0.597
15	1.174	1.105	1.139	1.006	1.020	1.013	0.842	0.777	0.809
20	1.426	1.444	1.435	1.174	1.189	1.181	1.010	0.949	0.980
25	1.678	1.614	1.646	1.425	1.444	1.435	1.178	1.122	1.150
30	1.846	1.869	1.857	1.593	1.614	1.603	1.263	1.294	1.278
35	2.097	2.039	2.068	1.760	1.784	1.772	1.431	1.381	1.406
40	2.265	2.294	2.280	1.928	1.954	1.941	1.515	1.553	1.534
45	2.517	2.464	2.490	2.096	2.124	2.110	1.684	1.639	1.661
50	2.685	2.634	2.659	2.179	2.294	2.237	1.768	1.726	1.747
55	2.852	2.804	2.828	2.347	2.464	2.405	1.852	1.812	1.832
60	3.020	2.974	2.997	2.515	2.549	2.532	1.936	1.984	1.960
65	3.188	3.059	3.123	2.598	2.719	2.659	2.020	2.071	2.045
70	3.356	3.229	3.292	2.766	2.889	2.827	2.104	2.157	2.131
75	3.440	3.398	3.419	2.850	2.974	2.912	2.273	2.243	2.258
80	3.607	3.483	3.545	3.018	3.144	3.081	2.357	2.330	2.343
85	3.775	3.653	3.714	3.101	3.229	3.165	2.357	2.416	2.386
90	3.943	3.823	3.883	3.185	3.398	3.292	2.441	2.502	2.472
95	4.027	3.908	3.968	3.353	3.483	3.418	2.525	2.588	2.557
100	4.195	4.078	4.136	3.437	3.568	3.503	2.609	2.675	2.642
110	4.446	4.333	4.390	3.604	3.823	3.714	2.778	2.761	2.769
120	4.698	4.588	4.643	3.856	4.078	3.967	2.946	2.934	2.940
130	4.950	4.843	4.896	4.023	4.333	4.178	3.030	3.106	3.068
140	5.201	5.013	5.107	4.275	4.503	4.389	3.199	3.192	3.196
150	5.369	5.268	5.318	4.443	4.758	4.600	3.283	3.365	3.324
160	5.621	5.523	5.572	4.610	4.928	4.769	3.451	3.451	3.451
170	5.872	5.777	5.825	4.862	5.183	5.022	3.620	3.624	3.622
180	6.124	5.947	6.036	5.029	5.353	5.191	3.704	3.710	3.707
190	6.292	6.202	6.247	5.197	5.607	5.402	3.788	3.883	3.835
200	6.544	6.457	6.500	5.365	5.777	5.571	3.956	3.969	3.963
210	6.795	6.627	6.711	5.616	5.947	5.782	4.040	4.142	4.091
220	7.047	6.882	6.964	5.784	6.202	5.993	4.209	4.228	4.218
230	7.215	7.137	7.176	5.951	6.372	6.162	4.293	4.314	4.303
240	7.466	7.307	7.387	6.119	6.627	6.373	4.377	4.487	4.432
250	7.718	7.562	7.640	6.370	6.797	6.584	4.461	4.573	4.517
260	7.886	7.732	7.809	6.538	7.052	6.795	4.630	4.659	4.644
270	8.138	7.901	8.020	6.706	7.222	6.964	4.714	4.832	4.773
280	8.389	8.156	8.273	6.873	7.477	7.175	4.798	4.918	4.858
290	8.641	8.326	8.484	7.041	7.647	7.344	4.882	5.004	4.943
300	8.809	8.496	8.652	7.293	7.816	7.555	5.051	5.091	5.071

%strains of CG/M75+N25 Mixes

N	Nd = 75			Nd = 100			Nd = 125		
	#1	#2	ave.	#1	#2	ave.	#1	#2	ave.
5	0.426	0.428	0.427	0.428	0.343	0.385	0.340	0.343	0.342
10	0.766	0.771	0.769	0.685	0.686	0.685	0.596	0.600	0.598
15	1.021	1.028	1.025	0.942	0.943	0.942	0.766	0.772	0.769
20	1.277	1.285	1.281	1.113	1.114	1.113	0.936	0.943	0.940
25	1.532	1.457	1.494	1.284	1.285	1.285	1.106	1.115	1.111
30	1.787	1.714	1.751	1.455	1.457	1.456	1.277	1.286	1.282
35	1.957	1.885	1.921	1.627	1.628	1.627	1.362	1.458	1.410
40	2.128	2.057	2.092	1.712	1.714	1.713	1.532	1.544	1.538
45	2.298	2.228	2.263	1.884	1.885	1.884	1.617	1.715	1.666
50	2.468	2.399	2.434	1.969	1.971	1.970	1.787	1.887	1.837
55	2.638	2.571	2.604	2.140	2.142	2.141	1.872	1.973	1.922
60	2.809	2.656	2.732	2.226	2.228	2.227	1.957	2.058	2.008
65	2.979	2.828	2.903	2.312	2.314	2.313	2.043	2.230	2.136
70	3.064	2.999	3.031	2.483	2.399	2.441	2.128	2.316	2.222
75	3.234	3.171	3.202	2.568	2.571	2.570	2.298	2.401	2.350
80	3.404	3.256	3.330	2.654	2.656	2.655	2.383	2.487	2.435
85	3.489	3.428	3.458	2.740	2.742	2.741	2.468	2.573	2.520
90	3.660	3.513	3.586	2.825	2.828	2.827	2.553	2.744	2.649
95	3.830	3.685	3.757	2.911	2.913	2.912	2.638	2.830	2.734
100	3.915	3.770	3.843	2.997	3.085	3.041	2.723	2.916	2.820
110	4.170	4.027	4.099	3.168	3.256	3.212	2.809	3.087	2.948
120	4.426	4.284	4.355	3.339	3.428	3.383	2.979	3.259	3.119
130	4.681	4.542	4.611	3.510	3.599	3.555	3.149	3.431	3.290
140	4.936	4.884	4.910	3.682	3.770	3.726	3.319	3.602	3.461
150	5.191	5.141	5.166	3.853	3.942	3.897	3.404	3.774	3.589
160	5.447	5.398	5.423	4.024	4.113	4.069	3.574	3.945	3.760
170	5.702	5.656	5.679	4.195	4.284	4.240	3.745	4.117	3.931
180	5.872	5.913	5.892	4.281	4.456	4.368	3.830	4.288	4.059
190	6.128	6.170	6.149	4.452	4.542	4.497	4.000	4.460	4.230
200	6.383	6.427	6.405	4.623	4.713	4.668	4.085	4.631	4.358
210	6.638	6.684	6.661	4.795	4.884	4.839	4.255	4.803	4.529
220	6.894	6.941	6.917	4.880	5.056	4.968	4.426	4.974	4.700
230	7.149	7.198	7.173	5.051	5.227	5.139	4.511	5.146	4.828
240	7.319	7.455	7.387	5.223	5.313	5.268	4.681	5.317	4.999
250	7.574	7.712	7.643	5.394	5.484	5.439	4.851	5.489	5.170
260	7.830	7.969	7.899	5.479	5.656	5.567	4.936	5.660	5.298
270	8.000	8.226	8.113	5.651	5.741	5.696	5.106	5.832	5.469
280	8.255	8.398	8.326	5.822	5.913	5.867	5.277	6.003	5.640
290	8.511	8.655	8.583	5.993	6.084	6.039	5.447	6.175	5.811
300	8.681	8.826	8.753	6.079	6.255	6.167	5.617	6.346	5.982

%strains of CG/M50+N50 Mixes

N	Nd = 75			Nd = 100			Nd = 125		
	#1	#2	ave.	#1	#2	ave.	#1	#2	ave.
5	0.421	0.426	0.423	0.339	0.256	0.298	0.338	0.340	0.339
10	0.758	0.766	0.762	0.593	0.513	0.553	0.592	0.595	0.593
15	1.094	1.021	1.058	0.847	0.769	0.808	0.761	0.850	0.805
20	1.347	1.277	1.312	1.017	0.940	0.979	1.014	1.020	1.017
25	1.599	1.532	1.566	1.186	1.111	1.149	1.183	1.189	1.186
30	1.768	1.702	1.735	1.356	1.282	1.319	1.352	1.359	1.356
35	2.020	1.957	1.989	1.525	1.453	1.489	1.437	1.529	1.483
40	2.189	2.128	2.158	1.610	1.538	1.574	1.606	1.699	1.653
45	2.357	2.298	2.327	1.780	1.709	1.745	1.775	1.784	1.780
50	2.609	2.468	2.539	1.864	1.795	1.830	1.860	1.954	1.907
55	2.778	2.638	2.708	2.034	1.966	2.000	2.029	2.039	2.034
60	2.946	2.809	2.877	2.119	2.051	2.085	2.113	2.124	2.119
65	3.114	2.979	3.047	2.203	2.222	2.213	2.282	2.294	2.288
70	3.283	3.149	3.216	2.373	2.308	2.340	2.367	2.379	2.373
75	3.451	3.319	3.385	2.458	2.393	2.425	2.451	2.464	2.458
80	3.620	3.489	3.554	2.542	2.564	2.553	2.620	2.634	2.627
85	3.788	3.660	3.724	2.712	2.650	2.681	2.705	2.719	2.712
90	3.956	3.830	3.893	2.797	2.735	2.766	2.790	2.804	2.797
95	4.125	4.000	4.062	2.881	2.906	2.894	2.959	2.889	2.924
100	4.293	4.170	4.232	3.051	2.991	3.021	3.043	2.974	3.008
110	4.630	4.511	4.570	3.220	3.162	3.191	3.212	3.144	3.178
120	4.966	4.851	4.909	3.475	3.419	3.447	3.466	3.398	3.432
130	5.303	5.106	5.205	3.644	3.675	3.660	3.635	3.568	3.602
140	5.640	5.532	5.586	3.898	3.846	3.872	3.888	3.738	3.813
150	6.061	5.872	5.966	4.068	4.103	4.085	4.057	3.908	3.983
160	6.397	6.213	6.305	4.322	4.274	4.298	4.311	4.078	4.195
170	6.818	6.553	6.686	4.576	4.530	4.553	4.480	4.248	4.364
180	7.155	6.894	7.024	4.746	4.786	4.766	4.734	4.418	4.576
190	7.576	7.234	7.405	5.000	4.957	4.979	4.903	4.588	4.745
200	7.912	7.574	7.743	5.254	5.214	5.234	5.156	4.758	4.957
210	8.249	7.915	8.082	5.508	5.470	5.489	5.325	4.928	5.127
220	8.586	8.170	8.378	5.678	5.726	5.702	5.579	5.098	5.338
230	8.838	8.511	8.675	5.932	5.983	5.958	5.748	5.268	5.508
240	9.175	8.766	8.971	6.186	6.325	6.256	6.002	5.438	5.720
250	9.428	9.021	9.224	6.441	6.581	6.511	6.171	5.607	5.889
260	9.680	9.277	9.478	6.695	6.838	6.766	6.424	5.777	6.101
270	9.848	9.532	9.690	6.949	7.094	7.022	6.593	5.947	6.270
280	10.101	9.702	9.902	7.203	7.350	7.277	6.847	6.032	6.440
290	10.269	9.957	10.113	7.458	7.607	7.532	7.016	6.202	6.609
300	10.438	10.128	10.283	7.627	7.863	7.745	7.270	6.372	6.821

APPENDIX C.

DATA SUMMARY: The Nottingham Asphalt Tester (NAT)

μ-strains of the mixes tested during the preliminary study

# of pulse	FG			DG			CG		
	Pb-	Pbo	Pb+	Pb-	Pbo	Pb+	Pb-	Pbo	Pb+
100	2285	2367	2739	2199	2758	2767	3154	4437	4625
200	2604	2772	3268	2498	3249	3334	3814	5505	5775
300	2799	3045	3640	2684	3586	3733	4276	6280	6630
400	2953	3265	3948	2818	3841	4043	4645	6918	7350
500	3076	3439	4207	2919	4054	4301	4965	7491	7994
600	3177	3600	4444	3012	4239	4523	5251	8024	8593
700	3264	3744	4653	3095	4402	4723	5508	8527	9173
800	3351	3874	4847	3160	4550	4905	5752	9006	9731
900	3420	3992	5027	3218	4684	5068	5981	9482	10283
1000	3488	4106	5203	3271	4808	5225	6193	9951	10833
1100	3553	4214	5364	3321	4923	5370	6401	10410	11385
1200	3612	4315	5524	3365	5032	5512	6601	10865	11951
1300	3665	4413	5676	3413	5137	5643	6793	11324	12527
1400	3719	4501	5818	3452	5235	5768	6984	11786	13120
1500	3765	4591	5957	3487	5335	5888	7171	12257	13725
1600	3818	4676	6092	3524	5426	6012	7353	12735	14352
1700	3861	4756	6226	3566	5509	6122	7537	13214	15004
1800	3907	4837	6355	3596	5597	6234	7715	13707	15688
1900	3950	4909	6476	3629	5679	6340	7895	14209	16424
2000	3989	4987	6599	3662	5753	6444	8072	14725	17206
2100	4031	5059	6715	3691	5832	6548	8251	15267	18050
2200	4072	5128	6835	3719	5903	6647	8428	15835	18968
2300	4105	5197	6944	3742	5974	6744	8607	16429	19962
2400	4143	5266	7058	3767	6044	6841	8789	17051	21068
2500	4176	5334	7169	3792	6114	6933	8967	17702	22324
2600	4212	5400	7276	3815	6181	7027	9147	18378	23793
2700	4245	5463	7382	3839	6247	7113	9330	19096	25564
2800	4279	5527	7484	3860	6306	7201	9510	19854	27725
2900	4310	5591	7587	3887	6371	7291	9693	20672	30623
3000	4343	5649	7690	3912	6432	7377	9877	21581	35189

%strains of FG Mixes (Nd=100)

# of pulse	M100+N0			M75+N25			M50+N50		
	#1	#2	ave.	#1	#2	ave.	#1	#2	ave.
5	0.161	0.292	0.227	0.289	0.298	0.294	0.309	0.253	0.281
10	0.185	0.330	0.257	0.333	0.338	0.335	0.355	0.294	0.324
20	0.218	0.378	0.298	0.385	0.389	0.387	0.410	0.342	0.376
40	0.263	0.434	0.348	0.443	0.447	0.445	0.476	0.397	0.436
60	0.293	0.470	0.381	0.481	0.485	0.483	0.517	0.432	0.475
80	0.316	0.496	0.406	0.509	0.513	0.511	0.549	0.458	0.503
100	0.336	0.517	0.426	0.530	0.536	0.533	0.575	0.478	0.527
200	0.398	0.586	0.492	0.602	0.613	0.608	0.662	0.544	0.603
300	0.438	0.628	0.533	0.647	0.661	0.654	0.719	0.583	0.651
400	0.465	0.659	0.562	0.681	0.698	0.689	0.761	0.612	0.687
500	0.488	0.682	0.585	0.708	0.726	0.717	0.796	0.635	0.716
600	0.506	0.702	0.604	0.726	0.751	0.738	0.825	0.656	0.740
700	0.522	0.718	0.620	0.741	0.772	0.756	0.850	0.674	0.762
800	0.535	0.732	0.634	0.753	0.790	0.772	0.873	0.689	0.781
900	0.547	0.745	0.646	0.763	0.806	0.785	0.894	0.703	0.798
1000	0.558	0.756	0.657	0.772	0.821	0.796	0.913	0.715	0.814
1500	0.600	0.799	0.699	0.809	0.879	0.844	0.992	0.763	0.878
2000	0.628	0.829	0.729	0.838	0.922	0.880	1.052	0.799	0.925
2500	0.651	0.853	0.752	0.862	0.956	0.909	1.102	0.829	0.965
3000	0.670	0.871	0.771	0.882	0.985	0.934	1.145	0.853	0.999
3500	0.685	0.888	0.787	0.901	1.009	0.955	1.183	0.874	1.028
4000	0.700	0.908	0.804	0.917	1.030	0.974	1.218	0.892	1.055
4500	0.713	0.925	0.819	0.932	1.049	0.991	1.248	0.907	1.077
5000	0.726	0.939	0.832	0.945	1.066	1.005	1.277	0.922	1.099
5500	0.738	0.952	0.845	0.958	1.081	1.020	1.304	0.935	1.119
6000	0.750	0.964	0.857	0.970	1.095	1.032	1.329	0.948	1.138
6500	0.760	0.974	0.867	0.981	1.108	1.045	1.352	0.959	1.155
7000	0.769	0.983	0.876	0.990	1.120	1.055	1.373	0.970	1.172
7500	0.778	0.991	0.885	1.000	1.132	1.066	1.395	0.980	1.188
8000	0.786	0.999	0.892	1.009	1.142	1.075	1.416	0.989	1.202
8500	0.793	1.005	0.899	1.017	1.152	1.085	1.434	0.998	1.216
9000	0.799	1.012	0.906	1.025	1.162	1.093	1.453	1.006	1.229
9500	0.806	1.018	0.912	1.033	1.171	1.102	1.470	1.013	1.242
10000	0.812	1.024	0.918	1.040	1.179	1.110	1.486	1.021	1.254

%strains of DG Mixes (Nd=100)

# of pulse	M100+N0			M75+N25			M50+N50		
	#1	#2	ave.	#1	#2	ave.	#1	#2	ave.
5	0.388	0.349	0.369	0.337	0.298	0.317	0.317	0.348	0.332
10	0.442	0.399	0.421	0.388	0.346	0.367	0.370	0.400	0.385
20	0.506	0.456	0.481	0.450	0.403	0.426	0.434	0.464	0.449
40	0.578	0.519	0.549	0.520	0.468	0.494	0.507	0.536	0.521
60	0.622	0.559	0.590	0.564	0.508	0.536	0.539	0.581	0.560
80	0.655	0.588	0.621	0.597	0.538	0.567	0.568	0.615	0.592
100	0.680	0.611	0.646	0.624	0.561	0.592	0.593	0.642	0.618
200	0.762	0.686	0.724	0.709	0.636	0.673	0.677	0.731	0.704
300	0.811	0.731	0.771	0.762	0.681	0.722	0.729	0.786	0.757
400	0.846	0.764	0.805	0.800	0.714	0.757	0.766	0.827	0.797
500	0.874	0.791	0.832	0.831	0.739	0.785	0.797	0.860	0.828
600	0.896	0.812	0.854	0.856	0.761	0.809	0.822	0.887	0.855
700	0.915	0.831	0.873	0.878	0.780	0.829	0.845	0.912	0.878
800	0.932	0.846	0.889	0.896	0.797	0.847	0.865	0.932	0.898
900	0.947	0.861	0.904	0.913	0.812	0.863	0.882	0.951	0.917
1000	0.960	0.873	0.917	0.929	0.826	0.877	0.899	0.968	0.933
1500	1.010	0.921	0.965	0.988	0.879	0.933	0.964	1.036	1.000
2000	1.046	0.956	1.001	1.031	0.918	0.974	1.012	1.087	1.050
2500	1.073	0.982	1.028	1.066	0.947	1.006	1.051	1.129	1.090
3000	1.096	1.004	1.050	1.094	0.972	1.033	1.085	1.164	1.124
3500	1.114	1.022	1.068	1.118	0.994	1.056	1.113	1.196	1.155
4000	1.131	1.038	1.084	1.138	1.012	1.075	1.138	1.222	1.180
4500	1.145	1.052	1.098	1.157	1.029	1.093	1.161	1.245	1.203
5000	1.157	1.065	1.111	1.174	1.043	1.108	1.181	1.267	1.224
5500	1.168	1.075	1.122	1.189	1.056	1.123	1.200	1.287	1.243
6000	1.178	1.086	1.132	1.203	1.069	1.136	1.217	1.303	1.260
6500	1.187	1.095	1.141	1.216	1.080	1.148	1.233	1.319	1.276
7000	1.195	1.103	1.149	1.228	1.091	1.160	1.248	1.334	1.291
7500	1.206	1.111	1.158	1.239	1.101	1.170	1.262	1.348	1.305
8000	1.216	1.117	1.167	1.250	1.110	1.180	1.274	1.361	1.318
8500	1.226	1.124	1.175	1.259	1.118	1.189	1.286	1.374	1.330
9000	1.236	1.131	1.183	1.268	1.126	1.197	1.298	1.385	1.342
9500	1.244	1.137	1.190	1.277	1.133	1.205	1.309	1.397	1.353
10000	1.252	1.142	1.197	1.286	1.141	1.213	1.319	1.407	1.363

%strains of CG Mixes (Nd=100)

# of pulse	M100+N0			M75+N25			M50+N50		
	#1	#2	ave.	#1	#2	ave.	#1	#2	ave.
5	0.360	0.383	0.371	0.345	0.331	0.338	0.324	0.393	0.358
10	0.413	0.436	0.424	0.396	0.378	0.387	0.374	0.452	0.413
20	0.476	0.501	0.489	0.457	0.434	0.446	0.432	0.523	0.478
40	0.548	0.575	0.561	0.524	0.505	0.514	0.499	0.603	0.551
60	0.591	0.622	0.607	0.566	0.548	0.557	0.540	0.653	0.597
80	0.625	0.656	0.640	0.595	0.583	0.589	0.571	0.690	0.630
100	0.651	0.684	0.667	0.620	0.610	0.615	0.594	0.720	0.657
200	0.734	0.773	0.753	0.697	0.693	0.695	0.672	0.815	0.744
300	0.786	0.827	0.806	0.743	0.744	0.744	0.721	0.873	0.797
400	0.822	0.866	0.844	0.777	0.781	0.779	0.757	0.915	0.836
500	0.850	0.897	0.874	0.803	0.811	0.807	0.786	0.950	0.868
600	0.874	0.923	0.898	0.825	0.836	0.831	0.811	0.979	0.895
700	0.894	0.944	0.919	0.843	0.857	0.850	0.832	1.003	0.917
800	0.911	0.963	0.937	0.859	0.876	0.867	0.851	1.025	0.938
900	0.927	0.980	0.953	0.873	0.893	0.883	0.867	1.044	0.956
1000	0.940	0.995	0.968	0.885	0.907	0.896	0.882	1.063	0.972
1500	0.994	1.055	1.024	0.935	0.965	0.950	0.941	1.134	1.038
2000	1.032	1.098	1.065	0.971	1.007	0.989	0.984	1.187	1.086
2500	1.063	1.132	1.097	0.998	1.041	1.019	1.020	1.229	1.124
3000	1.086	1.160	1.123	1.020	1.068	1.044	1.050	1.264	1.157
3500	1.105	1.183	1.144	1.039	1.091	1.065	1.075	1.294	1.185
4000	1.122	1.204	1.163	1.055	1.112	1.083	1.098	1.321	1.209
4500	1.138	1.223	1.180	1.070	1.130	1.100	1.119	1.345	1.232
5000	1.151	1.239	1.195	1.082	1.147	1.114	1.136	1.368	1.252
5500	1.164	1.255	1.209	1.094	1.162	1.128	1.152	1.387	1.269
6000	1.175	1.268	1.221	1.103	1.176	1.140	1.167	1.406	1.286
6500	1.185	1.281	1.233	1.113	1.188	1.151	1.181	1.422	1.301
7000	1.195	1.292	1.243	1.122	1.200	1.161	1.194	1.438	1.316
7500	1.203	1.304	1.253	1.130	1.210	1.170	1.206	1.452	1.329
8000	1.212	1.316	1.264	1.137	1.221	1.179	1.217	1.466	1.342
8500	1.220	1.326	1.273	1.145	1.231	1.188	1.228	1.478	1.353
9000	1.227	1.336	1.281	1.152	1.240	1.196	1.238	1.491	1.364
9500	1.234	1.344	1.289	1.158	1.249	1.204	1.247	1.502	1.375
10000	1.241	1.352	1.297	1.165	1.257	1.211	1.256	1.513	1.384

REFERENCES

1. S.F Brown and C.A. Bell, "The Validity of Design Procedures for the Permanent Deformation of Asphalt Pavements", Proceedings of the Fourth International Conference on the Structural Design of Asphalt Pavements, 1977.
2. J.B. Sousa, J. Craus, and C.L. Monismith, "Summary Report on Permanent Deformation in Asphalt Concrete", SHRP-A/IR-91-104, Strategic Highway Research Program, National Research Council, Washington, D.C., 1991.
3. D.R. Middleton, E.L. Roberts, and T. Chria-Chavala, "Measurement and Analysis of Truck Tire Pressures on Texas Highways", Transportation Research Record 1070, Transportation Research Board, National Research Council, Washington, D.C., 1986.
4. O. Kim and C.A. Bell, "Measurement and Analysis of Truck Tire Pressures in Oregon", Transportation Research Record 1207, Transportation Research Board, National Research Council, Washington, D.C., 1988.
5. S.W. Hudson and S.B. Seeds, "Evaluation of Increased Pavement Loading and Tire Pressures", Transportation Research Record 1207, Transportation Research Board, National Research Council, Washington, D.C., 1988.
6. E.R. Brown and S.A. Cross, "A National Study of Rutting in Hot Mix Asphalt (HMA) Pavements", Journal of the Association of Asphalt Paving Technologists, Volume 61, 1992.
7. "Performance of Coarse-Graded Mixes at Westrack – Premature Rutting", Final Report, FHWA-RD-99-134, U.S. Department of Transportation, Federal Highway Administration, 1998.
8. E.R. Brown, P.S. Kandhal, and Jingna Zhang, "Performance Testing For Hot Mix Asphalt", NCAT Report No. 01-05, National Center for Asphalt Technology, 2001.
9. M.W. Witczak, K. Kaloush, T. Pellinen, M. El-Basyouny, and H. Von Quintus, "Simple Performance Test for Superpave Mix Design", NCHRP Report 465, National Cooperative Highway Research Program, Transportation Research Board, National Research Council, Washington, D.C., 2002.
10. K.E. Kaloush and M.W. Witczak, "Tertiary Flow Characteristics of Asphalt Mixtures

- Pavements”, *Journal of the Association of Asphalt Paving Technologists*, Volume 71, 2002.
11. D.E. Newcomb, “Performance Related Specifications Developments”, *HMAT, Hot Mix Asphalt Technology*, Volume 6, No. 3, National Asphalt Pavement Association, 2001.
 12. J.A. Epps, A. Hand, S. Seeds, T. Schulz, S. Alavi, C. Ashmore, C.L. Monismith, J.A. Deacon, J.T. Harvey, and R. Leahy, “Recommended Performance-Related Specification for Hot-Mix Asphalt Construction: Results of the WesTrack Project”, NCHRP Report 455, National Cooperative Highway Research Program, Transportation Research Board, National Research Council, Washington, D.C., 2002.
 13. R.C. McGennis, R.M. Anderson, T.W. Kennedy, and M. Solaimanian, “Background of Superpave Asphalt Mixture Design and Analysis”, FHWA-SA-95-003, U.S. Department of Transportation, Federal Highway Administration, 1995.
 14. R.J. Cominsky, G.A. Huber, T.W. Kennedy, and M. Anderson, “The Superpave Mix Design Manual for New Construction and Overlays”, SHRP-A-407, Strategic Highway Research Program, National Research Council, Washington, D.C., 1994.
 15. R. Cominsky, R.B. Leahy, and E.T. Harrigan, “Level One Mix Design: Materials Selection, Compaction, and Conditioning”, SHRP-A-408, Strategic Highway Research Program, National Research Council, Washington, D.C., 1994.
 16. T.W. Kennedy, G.A. Huber, E.T. Harrigan, R.J. Cominsky, C.S. Hughes, H.V. Quintus, and J.S. Moulthrop, “Superior Performing Asphalt Pavements (Superpave): The Products of the SHRP Asphalt Research Program”, SHRP-A-410, Strategic Highway Research Program, National Research Council, Washington, D.C., 1994.
 17. V.A. Endersby and B.A. Vallergera, “Laboratory Compaction Methods and Their Effects on Mechanical Stability Tests for Asphaltic Pavements”, *Journal of the Association of Asphalt Paving Technologists*, Volume 21, 1952.
 18. L. Ortolani, and H.A. Sandberg Jr., “The Gyrotory-Shear Method of Molding Asphaltic Concrete Test Specimens; Its Development and Correlation with Field Compaction Methods. A Texas Highway Department Standard Procedure”,

- Journal of the Association of Asphalt Paving Technologists, Volume 21, 1952.
19. J.L. McRae, "Compaction of Bituminous Concrete", Journal of the Association of Asphalt Paving Technologists, Volume 26, 1957.
 20. J.L. McRae, and C.R. Foster, "Theory and Application of A Gyratory Testing Machine for Hot-Mix Bituminous Pavement", American Society of Testing and Materials, Special Technical Publication No. 252, 1959.
 21. T.W. Lambe and R.V. Whitman, "Soil Mechanics, SI version", New York: John Wiley & Sons, 1979.
 22. Standard Test Method for Compaction and Shear Properties of Bituminous Mixtures by Means of the U.S. Corps of Engineers Gyratory Testing Machine (GTM), American Society of Testing and Materials, ASTM D3387.
 23. H.L. Von Quintus, J.A. Scherocman, C.S. Hughes, and T.W. Kennedy, "Asphalt-Aggregate Mixture Analysis System", NCHRP Report 338, National Cooperative Highway Research Program, Transportation Research Board, National Research Council, Washington, D.C., 1991.
 24. J.B. Sousa, J. Harvey, L. Painter, J.A. Deacon, and C.L. Monismith, "Evaluation of Laboratory Procedures for Compacting Asphalt-Aggregate Mixtures", SHRP-A-UWP-91-523, Strategic Highway Research Program, National Research Council, Washington, D.C., 1991.
 25. J.W. Button, D.W. Little, V. Jagadam, and O.J. Pendleton, "Correlation of Selected Laboratory Compaction Methods with Field Compaction", Texas Transportation Institute, Texas A&M University, College Station, 1992.
 26. A. Kumar and W.H. Goetz, "The Gyratory Testing Machine As a Design Tool And an Instrument For Bituminous Mixture Evaluation", Journal of the Association of Asphalt Paving Technologists, Volume 43, 1974.
 27. J. Bonnot, "Asphalt Aggregate Mixtures", Transportation Research Record 1096, Transportation Research Board, National Research Council, Washington, D.C., 1986.
 28. S. Sigurjonsson and B.E. Ruth, "Use of Gyratory Testing Machine to Evaluate Shear Resistance of Asphalt Paving Mixture", Transportation Research Record 1259, Transportation Research Board, National Research Council, Washington, D.C., 1990.

29. J.G. Cabrera, "Assessment of the Workability of Bituminous Mixtures", *Highways and Transportation*, Vol. 38, No. 11, 1991.
30. M.R. Anderson, R.D. Bosley, and P.A. Creamer, "Quality Management of HMA Construction Using Superpave Equipment: A Case Study", *Transportation Research Record 1513*, Transportation Research Board, National Research Council, Washington, D.C., 1995.
31. T.P. Harman, J. D'Angelo, and J.R. Bukowski, "Evaluation of Superpave Gyratory Compactor in the Field Management of Asphalt Mixes: four Simulation Studies", *Transportation Research Record 1513*, Transportation Research Board, National Research Council, Washington, D.C., 1995.
32. H.U. Bahia, T.P. Friemel, P.A. Peterson, J.S. Russell, and B. Poehnelt, "Optimization of Constructibility and Resistance to Traffic: A New Design Approach for HMA Using the Superpave Compactor", *Journal of the Association of Asphalt Paving Technologists*, Volume 67, 1998.
33. R.B. Mallick, "Use of Superpave Gyratory Compaction To Characterize Hot-Mix Asphalt", *Transportation Research Record 1681*, Transportation Research Board, National Research Council, Washington, D.C., 1999.
34. E.R. Brown and M.S. Buckman, "Superpave Gyratory Compaction Guidelines", *NCHRP 9-9: Evaluation of the Superpave Gyratory Compaction procedure*, National Cooperative Highway Research Program, Transportation Research Board, National Research Council, Washington, D.C., 1998.
35. P.S. Kandhal, and R.B. Mallick, "Evaluation of Asphalt Pavement Analyzer for HMA Mix Design", *NCAT Report No. 99-4*, National Center for Asphalt Technology, 1999.
36. K.D. Stuart, W.S. Mogawar, and P. Romero, "Validation of Asphalt Binder and Mixture Tests that Measure Rutting Susceptibility Using the Accelerated Loading Facility", *FHWA Report RD-99-204*, Federal Highway Administration, McLean, VA, 1999.
37. M. Butcher, "Determining Gyratory Compaction Characteristics Using Servopac Gyratory compactor", *Transportation Research Record 1630*, Transportation Research Board, National Research Council, Washington, D.C., 1998.
38. M. Guler, H.U. Bahia, P.J. Bosscher, and M.E. Plesha, "Device for Measureing Shear

- Resistance of Hot-Mix Asphalt in Gyratory Compactor”, Transportation Research Record 1723, Transportation Research Board, National Research Council, Washington, D.C., 2000.
39. R.M. Anderson, “Relationship Between Superpave Gyratory Compaction Properties and the Rutting Potential of Asphalt Mixtures”, Journal of the Association of Asphalt Paving Technologists, Volume 71, 2002.
 40. E.R. Brown and M.S. Buchanan, “Literature Review: Verification of Gyration Levels in the Superpave N_{design} Table”, NCHRP Web Document 34 (Project D 9-9 [1]): Contractor’s Final Report, National Cooperative Highway Research Program, Transportation Research Board, National Research Council, Washington, D.C., 2001.
 41. K.D. Stuart, W.S. Mogawar, and P. Romero, “Validation of Asphalt Binder and Mixture Tests that Measure Rutting Susceptibility Using the Accelerated Loading Facility”, FHWA Report RD-99-204, Federal Highway Administration, McLean, VA, 1999.
 42. B.J. Coree and K Vanderhorst, “SUPERPAVE® Compaction”, Crossroads 2000, Transportation Conference Proceedings, Iowa State University, Center for Transportation Research and Education, 1998.
 43. W.G. Cochran and G.M. Cox, “Experimental Designs”, 2nd ed. New York: John Wiley & Sons, 1960.
 44. J.A. John and M.H. Quenouille, “Experiments: Design and Analysis”, 2nd ed. London: Charles Griffin & Company Ltd., 1977.
 45. P.S. Kandhal and L.A. Cooley Jr., “The Restricted Zone in The Superpave Aggregate Gradation Specification”, NCHRP Report 46, National Cooperative Highway Research Program, Transportation Research Board, National Research Council, Washington, D.C., 2001.
 46. L.A. Cooley Jr., J. Zhang, P.S. Kandhal, A.J. Hand, and A.E. Martin, “Significance of Restricted Zone in Superpave Aggregate Gradation Specification” Transportation Research Circular, No. E-C043, Transportation Research Board, Washington, D.C., 2002.
 47. R.L. Ott., “An Introduction to Statistical Methods and Data Analysis”, 4th ed. California: Wadsworth Pub. Co., 1993.

48. British Standards Institution, "Method for determining resistance to permanent deformation of bituminous mixtures subject to unconfined dynamic loading", DD226, BSI, London, 1996.
49. N. Ulmgren, "Dynamic Creep Test (Validation of modified (Swedish) method by comparison with wheel tracking test), NCC Indusrti, FoU-centrum, Report 96-4A, 1996.
50. N. Ulmgren, "Functional testing of asphalt mixes for permanent deformation by dynamic creep test modification of method and round robin test, NCC Indusrti, FoU-centrum, Report 97-3A, 1997.
51. J.T.G. Richardson, R.C. Elliott, J. Mercer, and J. Williams. "Laboratory Performance -Based Testing of Asphalt Mixtures in the United Kingdom", Journal of the Association of Asphalt Paving Technologists, Volume 69, 2000.
52. S.F. Brown, J.N. Preston, and K.E. Cooper, "Application of New Concepts in Asphalt Mix Design", Journal of the Association of Asphalt Paving Technologists, Volume 60, 1991.
53. K.E. Cooper, S.F. Brown, J.N. Preston, and F.M.L. Akeroyd, "Development of a Practical Method for Design of Hot-Mix Asphalt", Transportation Research Record 1317, Transportation Research Board, National Research Council, Washington, D.C., 1991.
54. S.F. Brown and K.E. Cooper, "The Mechanical Properties of Bituminous Materials for Road Base and Basecourses", Journal of the Association of Asphalt Paving Technologists, Volume 53, 1984.
55. C.L. Monismith and A.A. Tayabali, "Permanent Deformation (Rutting) Considerations in Asphalt Concrete Pavement Sections", Journal of the Association of Asphalt Paving Technologists, Volume 57, 1988.
56. S.F. Brown and J.M. Gibb, "Validation Experiment for Permanent Deformation Testing of Bituminous Mixtures", Journal of the Association of Asphalt Paving Technologists, Volume 65, 1996.
57. E.R. Brown and K.Y. Foo, "Comparison of Unconfined- and Confined-Creep Tests for Hot Mix Asphalt", Journal of Materials in Civil Engineering, Volume 6, No. 2, May, 1994.
58. M.S. Buchanan, "An Evaluation of Selected Methods for Measuring the Bulk Specific

- Gravity of Compacted Hot Mix Asphalt (HMA) Mixes”, *Journal of the Association of Asphalt Paving Technologists*, Volume 69, 2000.
59. Standard Test Method for Uncompacted Void Content of Fine Aggregate, American Society of Testing and Materials, ASTM C1252.
60. E.R. Brown, D.I. Hanson, and R.B. Mallick, “Evaluation of Superpave Gyratory Compaction of Hot-Mix Asphalt”, *Transportation Research Record 1543*, Transportation Research Board, National Research Council, Washington, D.C., 1996.
61. G. Gowda, K. Hall, R. Elliott, and A. Meadors, “Critical Evaluation of Superpave Volumetric Mix Design Using Arkansas Surface Course Mixes”, *Journal of the Association of Asphalt Paving Technologists*, Volume 66, 1997.
62. R.B. McGennis, D. Perdomo, T.W. Kennedy, and V.L. Anderson, “Ruggedness Evaluation of AASHTO TP4 The Superpave Gyratory Compactor”, *Journal of the Association of Asphalt Paving Technologists*, Volume 66, 1997.
63. E.R. Brown and R.B. Mallick, “An Initial Evaluation for N_{design} Superpave Gyratory Compactor”, *Journal of the Association of Asphalt Paving Technologists*, Volume 67, 1998.
64. W.R. Vavrik and S.H. Carpenter, “Calculating Air Voids at Specified Number of Gyration in Superpave Gyratory Compactor”, *Transportation Research Record 1630*, Transportation Research Board, National Research Council, Washington, D.C., 1998.
65. E.R. Brown and M.S. Buchanan, “Consolidation of the N_{design} Compaction Matrix and Evaluation of Gyratory Compaction Requirements”, *Journal of the Association of Asphalt Paving Technologists*, Volume 68, 1999.
66. Superpave 2000 – Improved Standards for a New Millennium, C-SHRP Technical Brief #17, Canadian Strategic Highway Research Program, 1999.
67. I-S. Oh, “Statistical Analysis of Construction Tolerances in Asphalt Pavements”, Master thesis, Iowa State University, 2001.
68. A.R. Rodriguez, H.D. Castillo, and G.F. Sowers, “Soil Mechanics in Highway Engineering”, Federal Republic of Germany: Trans Tech Pub., 1988.
69. N.W. McLeod, “Application of Triaxial Testing to the Design of Bituminous Pavements”, American Society of Testing and Materials, Special Technical

Publication No. 106, 1951.

70. N.W. McLeod, "An Ultimate Strength Approach to Flexible Pavement Design",
Journal of the Association of Asphalt Paving Technologists, Volume 23, 1954.
71. I.F. Collins, "Geomechanical Analysis of Unbound Pavements Based On Shakedown
Theory", Journal of Geotechnical and Geoenvironmental Engineering, Vol. 126,
No. 1, January, 2000.

ACKNOWLEDGMENTS

The author wishes to express sincere gratitude to his major professor, Dr. Brian J. Coree for his unconditional care for the past four years. Special thanks are rendered to Mike Heitzman, John Hinrichsen and Dan Seward of the Iowa Department of Transportation for their cooperation.